Article:
Chatterjee, M., Özdemir, S., Fritz, C. et al. (82 more authors) (2024) Plasma extracellular vesicle tau and TDP-43 as diagnostic biomarkers in FTD and ALS. Nature Medicine, 30. pp. 1771-1783. ISSN 1078-8956

https://doi.org/10.1038/s41591-024-02937-4

nature medicine

Article

https://doi.org/10.1038/s41591-024-02937-4

Plasma extracellular vesicle tau and TDP-43 as diagnostic biomarkers in FTD and ALS

Received: 10 July 2023

Accepted: 21 March 2024

Published online: 18 June 2024

Check for updates

A list of authors and their affiliations appears at the end of the paper

Minimally invasive biomarkers are urgently needed to detect molecular pathology in frontotemporal dementia (FTD) and amyotrophic lateral sclerosis (ALS). Here, we show that plasma extracellular vesicles (EVs) contain quantifiable amounts of TDP-43 and full-length tau, which allow the quantification of 3-repeat (3R) and 4-repeat (4R) tau isoforms. Plasma EV TDP-43 levels and EV 3R/4R tau ratios were determined in a cohort of 704 patients, including 37 genetically and 31 neuropathologically proven cases. Diagnostic groups comprised patients with TDP-43 proteinopathy ALS, 4R tauopathy progressive supranuclear palsy, behavior variant FTD (bvFTD) as a group with either tau or TDP-43 pathology, and healthy controls. EV tau ratios were low in progressive supranuclear palsy and high in bvFTD with tau pathology. EV TDP-43 levels were high in ALS and in bvFTD with TDP-43 pathology. Both markers discriminated between the diagnostic groups with area under the curve values >0.9, and between TDP-43 and tau pathology in bvFTD. Both markers strongly correlated with neurodegeneration, and clinical and neuropsychological markers of disease severity. Findings were replicated in an independent validation cohort of 292 patients including 34 genetically confirmed cases. Taken together, the combination of EV TDP-43 levels and EV 3R/4R tau ratios may aid the molecular diagnosis of FTD, FTD spectrum disorders and ALS, providing a potential biomarker to monitor disease progression and target engagement in clinical trials.

FTD encompasses different neurodegenerative disorders, including bvFTD, semantic variant primary progressive aphasia (svPPA) and nonfluent variant primary progressive aphasia. FTD, progressive supranuclear palsy (PSP), corticobasal degeneration (CBD) and ALS are part of a disease continuum with overlapping symptoms, genetics and molecular pathology[1]. Although ALS, FTD–ALS and roughly half of bvFTD cases are characterized by intracellular protein inclusions of TAR DNA-binding protein (TDP-43)[2], PSP, CBD and approximately 40% of bvFTD cases have been linked to tau pathology at autopsy (frontotemporal lobar degeneration, FTLD-tau)[3]. Together, FTLD-tau and FTLD-TDP-43 account for nearly 90% of bvFTD cases. The microtubule-binding protein exists in six different isoforms caused by alternative splicing[4]. Based on the presence of three or four repetitive protein domains, so-called repeats, 3-repeat or 4-repeat isoforms are distinguished (3R, 4R tau). FTLD-tau can be characterized by the predominance of 3R tau aggregates (Pick's disease) or 4R tau pathology PSP, CBD, argyrophilic grain disease or globular glial tauopathy (GGT)[5].

So far, disease-modifying therapies are not available for FTD and ALS spectrum disorders. This is partially caused by the lack of biomarkers detecting the molecular pathology, which is a prerequisite for patient stratification in sporadic bvFTD. Currently, diagnosis of molecular pathology is only possible postmortem, with the exception of genetic cases in which a pathogenic mutation allows ante-mortem deduction of the associated molecular pathology.

e-mail: anja.schneider@dzne.de

A diagnostic biomarker may further help in cases of diagnostic uncertainty and could facilitate early diagnosis, which is important because disease-modifying, novel therapies are expected to be more successful in the early disease stages when irreversible neuron loss is less progressed. Delayed and incorrect diagnoses have been reported for a substantial proportion of patients with ALS[6], PSP[7] and bvFTD[8]. Therefore, pathology-specific biomarkers are urgently needed.

Plasma glial fibrillary acidic protein/neurofilament light chain (NfL) ratios have been suggested to distinguish FTLD-tau from TDP-43 (ref. 9). Other studies have investigated TDP-43, phosphorylated or aggregated TDP-43 in blood or cerebrospinal fluid (CSF)[10–14], CSF p-tau181/tau ratio[15] or CSF peptides encoded by cryptic exons as markers of TDP-43 pathology[16], albeit with conflicting results. CSF tau isoforms have been proposed as diagnostic markers for 3R or 4R predominant tauopathies[17], but detection is hampered by tau fragmentation in extracellular fluids[18] resulting in extremely low concentrations of full-length tau. We recently published a CSF assay employing immunoprecipitation followed by mass spectrometry that could overcome this obstacle[19]. However, because of the invasiveness of lumbar puncture, we turned to blood, more specifically to plasma EVs.

EVs contribute to intercellular communication or serve to clear toxic cellular content[20]. They can transport pathological tau[21–24] and TDP-43 (ref. 25) species between cells and induce aggregate formation in target cells. Importantly, the presence of TDP-43 in EVs could reflect its disease-associated mislocalization from the nucleus to the cytosol, because extranuclear localization of TDP-43 is a prerequisite for its sorting into EVs.

Here, we show that plasma EVs contain substantial amounts of unfragmented tau. This allows the measurement of 3R and 4R tau isoform ratios, which has not been possible from blood, so far. We quantified the plasma EV 3R/4R tau ratio and TDP-43 in a large neurodegenerative disease cohort (DESCRIBE cohort) to test the hypothesis that a combination of both markers may distinguish FTLD-tau from FTLD-TDP-43 pathology. As diagnostic groups we selected bvFTD, which is largely associated with either FTLD-tau or FTLD-TDP-43 pathology, PSP based on its association with 4R tau pathology, Alzheimer disease (AD) as a secondary tauopathy with equally balanced 3R and 4R tau pathology, and svPPA and ALS as disorders with almost exclusive TDP-43 pathology, in addition to healthy controls (HC). Our cohort included 68 genetically and/or neuropathologically proven cases. Findings were validated in a second, independent cohort (Sant Pau cohort), comprising 287 participants with ALS, ALS–FTD, bvFTD, PSP and HC, including 34 genetically confirmed cases (Extended Data Fig. 1).

Intriguingly, we find that the combination of plasma EV 3R/4R tau ratio together with plasma EV TDP-43 allows the distinction of FTLD-tau from FTLD-TDP-43 in FTD and the detection of ALS-TDP-43 in ALS. Furthermore, the plasma EV 3R/4R tau ratio can serve as a biomarker to distinguish 4R tauopathy PSP from other FTD spectrum disorders and from HC.

Results

Detection of full-length tau in CSF and plasma EVs

We prepared medium-sized CSF and plasma EVs (mEVs) after sequential centrifugation from the 10,000*g* centrifugation pellet[26]. Small EVs (sEVs) were isolated from the 10,000*g* supernatant by size-exclusion chromatography as previously described[26] (Supplementary Data and Supplementary Fig. 1c,d). Mass spectrometry revealed full-length tau in CSF and plasma EVs, allowing the distinction of 3R and 4R isoforms (Supplementary Data and Supplementary Fig. 2). Because venous puncture is less invasive than lumbar puncture, we decided to assess 3R and 4R tau isoform concentrations in plasma EVs, using sandwich immunoassays (Methods, Supplementary Fig. 3a–e and Supplementary Table 1).

To test whether plasma EV tau stems from brain or peripheral nerve cells[27], thrombocytes[28] or lymphocytes[29], we immunoisolated anti-L1 cell adhesion molecule-positive EVs (L1CAM EVs) from plasma EV preparations. L1CAM EVs are considered brain–neuron derived, although this notion is controversial[30]. As shown in Supplementary Fig. 4, the vast majority of plasma EV tau resided in L1CAM EVs.

Plasma EV 3R/4R tau ratio is low in PSP and high in bvFTD

We performed a pilot study on plasma EV 3R and 4R tau content in a subcohort of the DZNE multicenter DESCRIBE cohort (subcohort 1) (Extended Data Table 1 and Extended Data Fig. 1).

The plasma EV 3R/4R tau ratio did not correlate with age, sex and disease duration (Supplementary Table 2). HC, AD and svPPA groups showed plasma sEV 3/4R tau ratios of ~1, consistent with the balanced ratios of 3R and 4R tau described in physiological conditions and in AD tau aggregates[31] (HC median 1.16, interquartile range (IQR) [0.99–1.28]; AD median 0.91, IQR [0.57–1.25]; svPPA median 1.00, IQR [0.98–1.11]) (Fig. 1a). sEV 3R/4R tau ratios were lower in the 4R tauopathy PSP (median 0.18, IQR [0.13–0.29]; $P < 0.0001$ for all comparisons), and higher in bvFTD compared with all other groups (bvFTD median 2.59, IQR [2.02–3.87], $P < 0.001$ versus HC; $P < 0.0001$ versus all other groups). Individual bvFTD values overlapped partially with HC, svPPA and groups. Receiver operating characteristic (ROC) curve analysis revealed high diagnostic accuracies for the distinction of PSP (Fig. 1b–e) and bvFTD (Fig. 1f–h) from all other groups (AUC PSP versus HC 0.96, 95% confidence interval (CI) [0.83–0.98]; PSP versus AD 0.99, CI [0.90–1.00]; PSP versus svPPA 0.96, CI [0.90–0.98]; PSP versus bvFTD 0.99, CI [0.94–1.00]; bvFTD versus HC 0.93, CI [0.88–1.00]; bvFTD versus AD 0.90, CI [0.90–1.00]; bvFTD versus svPPA 0.95, CI [0.90–0.98]) (Supplementary Table 3).

Plasma sEV 3R/4R tau ratios correlated positively ($r = 0.68$, $P < 0.0001$) with plasma NfL levels in bvFTD, and negatively in the 4R tauopathy PSP (Fig. 1i,j (sEV $r = -0.48$, $P = 0.001$)). High plasma EV 3R/4R tau ratios in bvFTD corresponded to more severe clinical and cognitive impairment, as did low ratios in PSP, consistent with 4R tau predominance in PSP (Fig. 1k–n, Supplementary Fig. 5 and Supplementary Tables 4 and 5).

We next tested for a potential correlation of 3R/4R tau ratios between CSF and plasma sEV (Supplementary Fig. 6). However, low sample numbers and the need for larger CSF sample volumes prevent a clear conclusion on whether CSF and plasma sEV 3R and 4R tau correlate with each other (Supplementary Table 6).

We validated our findings in additionally available samples of the DZNE DESCRIBE cohort (subcohort 2: 56 HC, 165 ALS, 179 bvFTD and 163 PSP samples). Patient demographics are given in Extended Data Table 2. ALS was chosen as a TDP-43 control group because the vast majority of ALS cases are associated with TDP-43 pathology[32]. Plasma sEV 3R/4R tau ratios were lowest in PSP (median sEV: 3R/4R tau 0.45, IQR [0.34–0.60]) and differed from all other diagnostic groups (median sEV: HC 0.99, IQR [0.91–1.03], PSP versus HC $P < 0.0001$; ALS 0.95, IQR [0.88–1.01], PSP versus ALS $P < 0.0001$; bvFTD 1.10, IQR [0.99–1.76], PSP versus bvFTD $P < 0.0001$) (Fig. 2a). ROC analysis (Fig. 2b–d), revealed high accuracy for the distinction of PSP from HC (AUC 0.98, CI [0.96–1.00]), ALS (AUC 0.96, CI [0.94–0.99]) and bvFTD (AUC 0.98, CI [0.73–1.00]) (Supplementary Table 3 (sEV) and Supplementary Fig. 7a–d and Supplementary Table 3 (mEV)).

Increased EV 3R/4R tau ratios were detected in bvFTD. Approximately 50% (54.19%) of bvFTD values were above the control group median, suggesting tau pathology in these cases (median sEV 3R/4R tau in bvFTD 2.28, IQR [1.13–2.4]; median mEV 3R/4R tau in bvFTD 1.84, IQR [1.19–2.13]; bvFTD versus all other diagnostic groups $P < 0.0001$ (median sEV); bvFTD versus all other diagnostic groups $P < 0.0001$ (median mEV)). Plasma EV 3R/4R tau ratios distinguished bvFTD from HC, ALS and PSP with high diagnostic accuracy (sEVs AUC 0.89–0.98 (Fig. 2d–f) and mEVs AUC 0.86–0.97 (Supplementary Fig. 7d,f); Supplementary Table 3). As in subcohort 1, EV tau ratios were not correlated with age, sex and disease duration (Supplementary Table 7).

https://doi.org/10.1038/s41591-024-02937-4

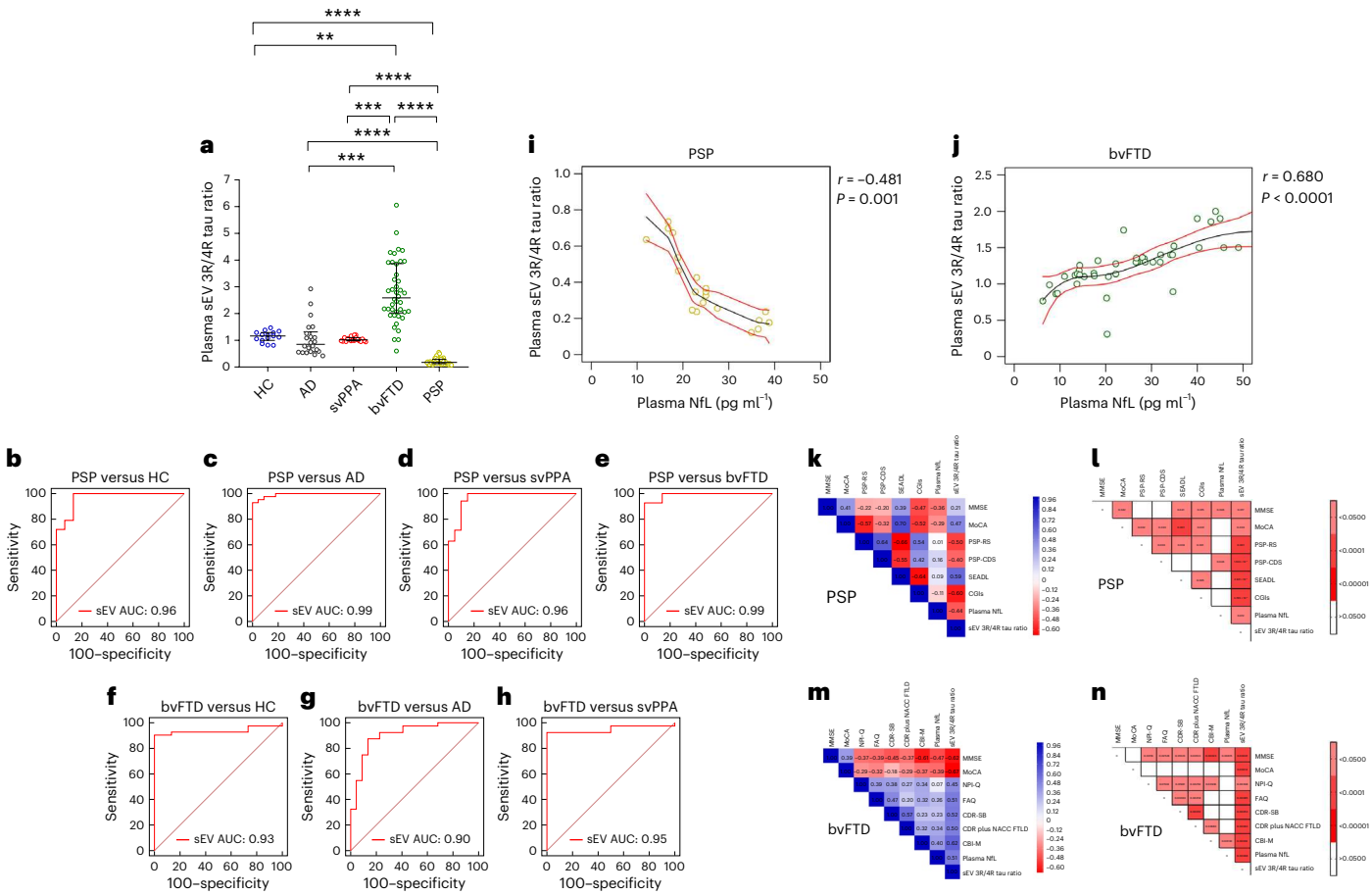

Fig. 1 | 3R/4R tau ratio in plasma sEV in DESCRIBE subcohort 1. a, The long horizontal line represents the median and the short horizontal lines represent the IQR. Kruskal–Wallis test with Dunn's correction for multiple comparisons. (HC versus bvFTD $P = 0.0003$, HC versus PSP $P = 0.0000044$, AD versus bvFTD $P = 0.0003$, AD versus PSP $P = 0.0000052$, svPPA versus bvFTD $P = 0.0007$, svPPA versus PSP $P = 0.0000057$, bvFTD versus PSP $P = 0.0000019$; $^{*}P < 0.05$, $^{**}P < 0.001$, $^{***}P < 0.0001$, $^{****}P < 0.00001$. Biologically independent samples: HC $n = 15$, AD $n = 23$, svPPA $n = 17$, bvFTD $n = 42$, PSP $n = 44$. **b**–**h**, ROC curve for sEV 3R/4R tau ratio in PSP versus HC (**b**), PSP versus AD (**c**), PSP versus svPPA (**d**), PSP versus bvFTD (**e**), bvFTD versus HC (**f**), bvFTD versus AD (**g**) and bvFTD versus svPPA (**h**). **i**,**j**, Two-tailed Spearman correlation analysis of associations and monotonic regression splines between sEV 3R/4R ratio and plasma NfL levels within PSP (**i**) and bvFTD (**j**) ($P = 0.00009$) diagnostic groups. **k**–**n**, Correlation matrix depicting results of two-tailed Spearman correlations, visualized by plotting strength of correlation (r) as a heat map along with P values (right): PSP (**k**,**l**) and bvFTD (**m**,**n**). PSP: MoCA[34], PSP-RS[35], PSP-CDS[36], SEADL[37], CGI-s[38]; PSP-SS[35], MDS-UPDRS Part III[39], SAS[40] and the PSP-QoL[41] (Supplementary Fig. 7a,b and Supplementary Table 5). bvFTD: MMSE[33], MoCa, FAQ[42], CDR-SB[43], CDR plus NACC FTLD, previously termed CDR-SB FTD[44], NPI-Q[45] and CBI-M[46].

Plasma EV 3R/4R tau ratios correlate with disease severity

Similar to subcohort 1, plasma EV 3R/4R tau ratios correlated with plasma NfL in bvFTD ($r = 0.28$, $P < 0.0001$ (sEV) and $r = 0.36$, $P = 0.002$ (mEV)) and inversely in PSP ($r = -0.33$, $P < 0.0001$ (sEV) and $r = -0.24$, $P = 0.005$ (mEV)) (Extended Data Fig. 2a,b and Supplementary Fig. 7g,h).

Plasma EV 3R/4R tau ratios correlated with clinical, neurological and cognitive measures of disease severity in the PSP group, with low plasma ratios indicative of increased severity (PSP: Mini Mental State Examination (MMSE)[33], Montreal Cognitive Assessment (MoCA)[34], PSP rating scale (PSP-RS)[35], PSP clinical deficits scale (PSP-CDS)[36], Schwab and England disability scale (SEADL)[37], Clinical Global Impression Severity Scale (CGI-s)[38] (Fig. 2g,h and Supplementary Table 8 (sEV) and Supplementary Fig. 8i,j and Supplementary Table 8 (mEV)), PSP staging system (PSP-SS)[35], MDS-Unified Parkinson's Disability Rating Scale part III (MDS-UPDRS III)[39], Starkstein Apathy Scale (SAS)[40] and PSP quality of life scale (PSP-QoL)[41] (Supplementary Fig. 8a,b and Supplementary Table 8).

In bvFTD, high plasma sEV 3R/4R tau ratios were associated with impaired cognition, compromised functional activities, increased symptom severity and a higher burden of behavior symptoms (MMSE, MoCA, Functional Activities Questionnaire (FAQ)[42], Clinical Dementia Rating-Sum of Boxes (CDR-SB)[43], Clinical Dementia Rating (CDR) plus National Alzheimer's Coordinating Center (NACC) Behavior and Language Domains Frontotemporal Lobar Degeneration (NACC FTLD)[44], Neuropsychiatric Inventory Questionnaire (NPI-Q)[45], and the modified version of the Cambridge Behavior Inventory-Revised Version (CBI-M)[46] (Fig. 2i,j and Supplementary Table 9)). Similar results were observed for mEVs (Supplementary Fig. 7k,l and Supplementary Table 9).

Plasma EV tau ratios in pathology-confirmed cases

We stratified cases with known mutations ($n = 37$) or neuropathologically confirmed diagnoses ($n = 31$) into TDP-43, tau and non-TDP-43/non-tau pathology groups (number of individual cases $n = 63$, 5 of these had both genetic and neuropathological diagnosis) (Supplementary Tables 10 and 11). Most mutations were linked to TDP-43 pathology (18 *C9orf72*, 4 *GRN*, 4 *VCP* and 2 *TBK1*), with the exception of three *MAPT* mutations (*MAPT P301L*, *MAPT P364S* and *MAPT IVS10+16C>T*) in bvFTD.

Neuropathological diagnoses of nongenetic cases included 22 with TDP-43 (16 ALS-TDP, 6 FTLD-TDP) and 4 with tau pathology (3 PSP-type, 1 GGT-type). All genetic and neuropathologically confirmed cases with TDP-43 pathology were combined into a 'TDP-43 pathology'

https://doi.org/10.1038/s41591-024-02937-4

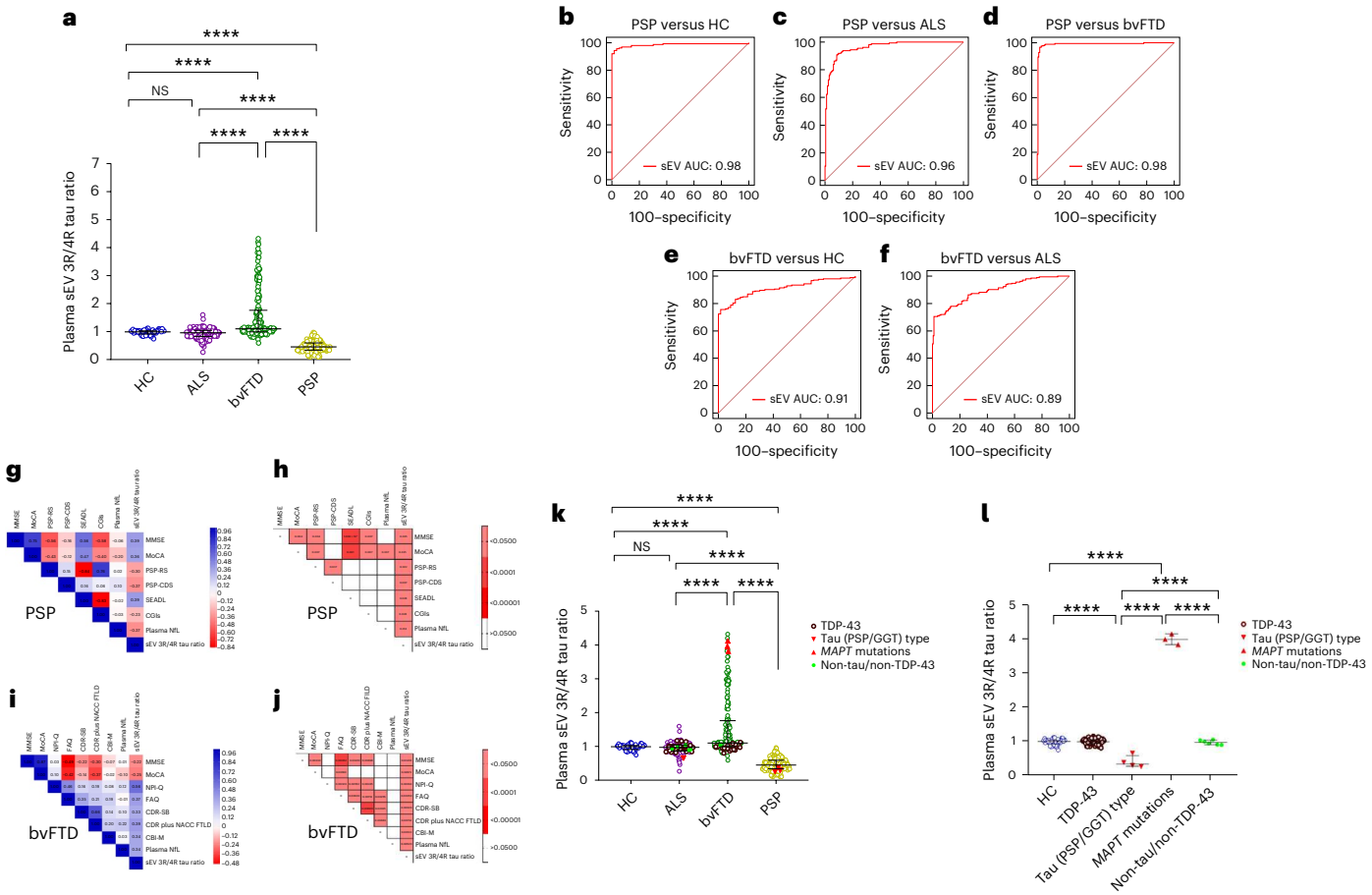

Fig. 2 | 3R/4R tau ratio in plasma sEV in DESCRIBE subcohort 2. a, Horizontal lines indicate median and IQR. Kruskal–Wallis test with Dunn's correction for multiple comparisons. HC versus bvFTD $P = 0.0000057$, HC versus PSP $P = 0.000009$, ALS versus bvFTD $P = 0.0000074$, ALS versus PSP $P = 0.0000023$, bvFTD versus PSP $P = 0.0000067$; ****$P < 0.00001$. Biologically independent samples: HC $n = 56$, ALS $n = 165$, bvFTD $n = 179$, PSP $n = 163$. **b**–**f**, ROC curve for plasma sEV 3R/4R tau ratio: PSP versus HC (**b**), PSP versus ALS (**c**), PSP versus bvFTD (**d**), bvFTD versus HC (**e**) and bvFTD versus ALS (**f**). **g**–**j**, Correlation matrix depicting the results of two-sided Spearman correlations, visualized by plotting strength of correlation (*r*) as a heat map along with *P* values (right): PSP (**g**,**h**) and bvFTD (**i**,**j**). **k**,**l**, 3R/4R tau ratio in plasma-derived sEV in genetically ($n = 37$) or autopsy-confirmed ($n = 31$) cases from DESCRIBE subcohort 2 (total number of individual cases $n = 63$, 5 of these cases had both genetic and neuropathological diagnosis). **k**, sEV 3R/4R tau ratios in the different pathology groups, stratified by clinical diagnosis. HC versus bvFTD $P = 0.0000052$, HC versus PSP $P = 0.0000012$, ALS versus bvFTD $P = 0.0000097$, ALS versus PSP $P = 0.0000056$, bvFTD versus PSP $P = 0.0000041$; ****$P < 0.00001$. **l**, sEV 3R/4R tau ratios of the different pathology groups, independent of clinical diagnostic group. The long horizontal line represents the median and the short horizontal lines represent the IQR. Kruskal–Wallis test with Dunn's correction for multiple comparisons. HC versus tau (PSP/GGT)-type $P = 0.000007$, HC versus *MAPT* mutations $P = 0.0000063$, tau(PSP/GGT)-type versus *MAPT* mutations $P = 0.000004$, tau(PSP/GGT)-type versus non-tau/non-TDP-43 $P = 0.0000078$, *MAPT* mutations versus non-tau/non-TDP-43 $P = 0.0000041$; ****$P < 0.00001$. TDP-43 pathology group: bvFTD (*C9orf72* ($n = 13$), *GRN* ($n = 4$), *VCP* ($n = 4$), *TBK-1* ($n = 2$)); ALS (*C9orf72* ($n = 5$)); neuropathological diagnosis (FTLD-TDP ($n = 1$)); ALS-TDP ($n = 17$), ALS-FTLD-TDP ($n = 6$)). PSP/GGT-type tau pathology group: neuropathological diagnosis ((PSP-tau ($n = 3$); FTLD-tau GGT-type ($n = 1$)). bvFTD *MAPT* mutations (*MAPT P301L* ($n = 1$), *MAPT P364S* ($n = 1$), *MAPT IVS10+16C>T* ($n = 1$)). Non-tau/non-TDP-43 pathology group: ALS (*SOD-1* ($n = 2$); *FUS* ($n = 2$); *CHCHD10* ($n = 1$)); bvFTD (*CHCHD10* ($n = 1$)).

group ($n = 50$) and all with tau pathology into the 'tau pathology' group ($n = 7$). Cases with neither TDP-43 nor tau pathology (2 *SOD1*, 2 *FUS* and 2 *CHCHD10* mutation carriers) were classified as 'non-TDP-43/non-tau pathology' ($n = 6$).

In the TDP-43 pathology group, and in the non-TDP-43/non-tau pathology group, sEV 3R/4R tau ratios were ~1 and did not differ from the HC group (HC: median sEV 0.99, IQR [0.91–1.03]; TDP-43 group: median sEV 0.95, IQR [0.92–0.97], versus HC $P > 0.05$; non-TDP-43/non-tau group: median sEV 0.96, IQR [0.90–1.03], versus HC $P > 0.05$) (Fig. 2k,l (mEV) and Supplementary Fig. 9a,b). Importantly, all bvFTD TDP-43 pathology cases were in the lower range, comparable with HC, and ALS PSP/GGT-type 4R tau pathology cases were characterized by decreased plasma EV 3R/4R tau levels (median sEV 0.42, IQR [0.35–0.60]) compared with HC (median sEV 0.99, IQR [0.91–1.03], $P < 0.00001$), with TDP-43 pathology (median sEV 0.95, IQR [0.92–0.97], $P < 0.00001$) and with non-TDP43/non-tau pathology groups (median sEV 0.96, IQR [0.90–1.03], $P < 0.00001$). By contrast, EV 3R/4R tau ratios in *MAPT* mutation carriers were approximately three to four times higher (median sEV 3.96, IQR [3.81–4.12]) compared with HC, TDP-43 and non-TDP-43/non-tau control groups ($P < 0.00001$). Thus, EV 3R/4R tau ratios may separate FTLD-tau pathology from FTLD-TDP and detect PSP/GGT-type tau pathology.

Plasma EVs contain TDP-43

Western blotting (Supplementary Fig. 10a) and single-molecule array (SIMOA) assay analysis confirmed the presence of TDP-43 in plasma EVs (for specificity and assay performance see Supplementary Data, Supplementary Fig. 10 and Supplementary Table 1). As illustrated in Supplementary Fig. 4, the majority of plasma EV TDP-43 stems from L1CAM-positive EVs.

https://doi.org/10.1038/s41591-024-02937-4

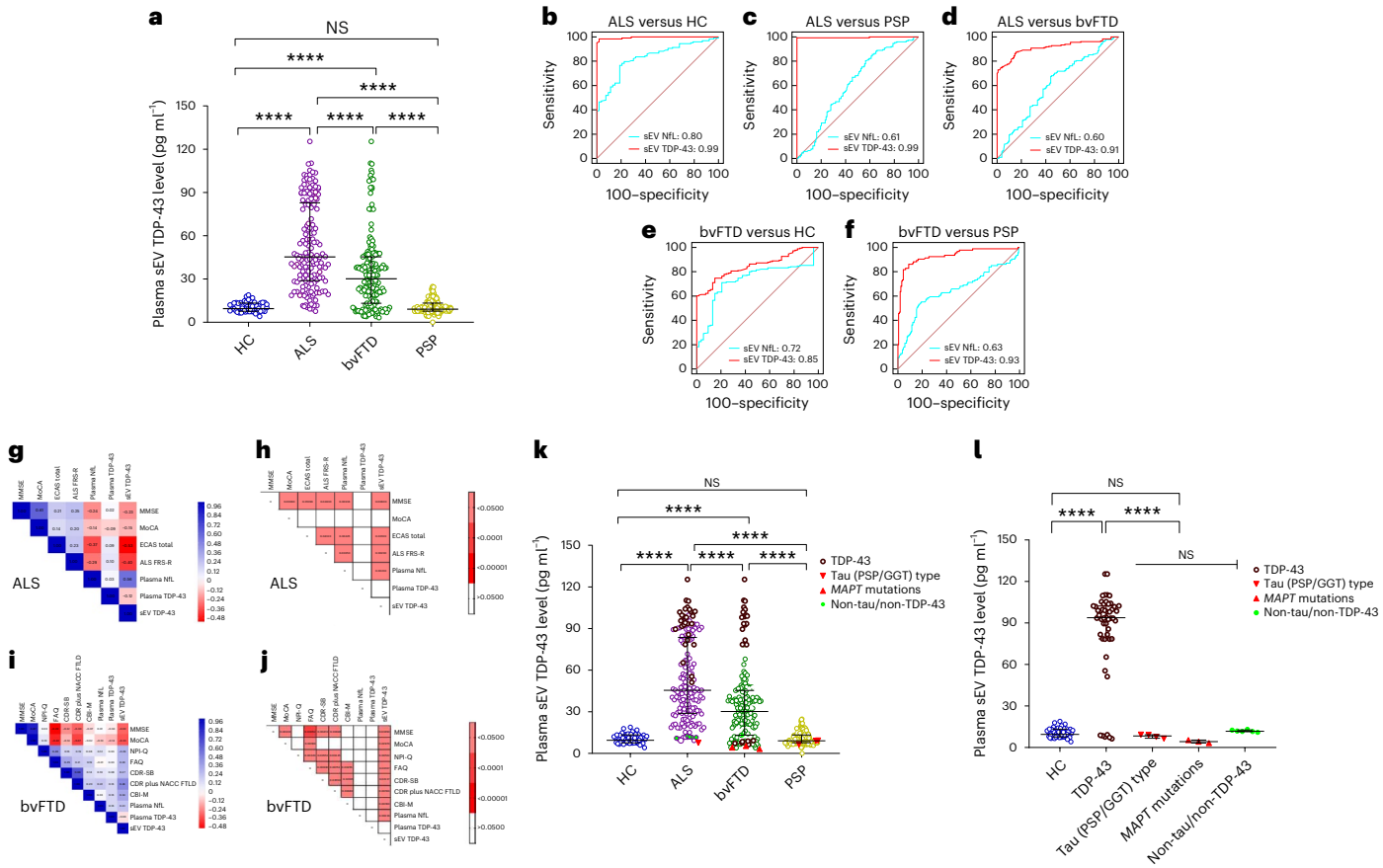

Fig. 3 | TDP-43 levels in plasma sEV in DESCRIBE subcohort 2. a, The long horizontal line represents the median and the short horizontal lines represent IQR. Kruskal–Wallis test with Dunn's correction for multiple comparisons. HC versus ALS $P = 0.000003$, HC versus bvFTD $P = 0.000006$, ALS versus bvFTD $P = 0.0000074$, ALS versus PSP $P = 0.0000028$, bvFTD versus PSP $P = 0.0000012$; ****$P < 0.00001$. Biologically independent samples: HC $n = 56$, ALS $n = 165$, bvFTD $n = 179$ and PSP $n = 163$. **b**–**f**, ROC curve for sEV TDP-43 (red) and plasma NfL (blue): ALS versus HC (**b**), ALS versus PSP (**c**), ALS versus bvFTD (**d**), bvFTD versus HC (**e**) and bvFTD versus PSP (**f**). **g**–**j**, Correlation matrix depicting results of two-sided Spearman correlations, visualized by plotting strength of correlation (r) as a heat map along with P values (right). ALS (**g**,**h**) and bvFTD (**i**,**j**). TDP-43 in plasma sEV in genetically ($n = 37$) or autopsy-confirmed ($n = 31$) cases from the DESCRIBE subcohort 2 (total number of individual cases: $n = 63$, 5 of which had both genetic and neuropathological diagnoses). **k**, sEV TDP-43 in the different pathology groups, stratified by clinical diagnosis. HC versus ALS $P = 0.000003$, HC versus bvFTD $P = 0.000006$, ALS versus bvFTD $P = 0.0000074$, ALS versus PSP $P = 0.0000028$, bvFTD versus PSP $P = 0.0000012$; ****$P < 0.00001$. **l**, sEV TDP-43 concentrations in the different pathology groups, independent of clinical diagnostic group. The long horizontal line represents the median and the short horizontal lines represent the IQR. Kruskal–Wallis test with Dunn's correction for multiple comparisons. HC versus TDP-43 $P = 0.000008$, TDP-43 versus tau (PSP/GGT)-type $P = 0.000006$, TDP-43 versus *MAPT* mutations $P = 0.0000035$, TDP-43 versus non-tau/non-TDP-43 $P = 0.0000039$; ****$P < 0.00001$. TDP-43 pathology group: bvFTD (*C9orf72* ($n = 13$), *GRN* ($n = 4$), *VCP* ($n = 4$), *TBK1* ($n = 2$)); ALS (*C9orf72* ($n = 5$)); neuropathological diagnosis (FTLD-TDP ($n = 1$); ALS-TDP ($n = 17$), ALS-FTLD-TDP ($n = 6$)). PSP/GGT-type tau pathology group: neuropathological diagnosis (PSP-tau ($n = 3$); FTLD-tau GGT-type ($n = 1$)). bvFTD *MAPT* mutations: *MAPT P301L* ($n = 1$), *MAPT P364S* ($n = 1$), *MAPT IVS10+16C>T* ($n = 1$). Non-tau/non-TDP-43 pathology group: ALS (*SOD-1* ($n = 2$); *FUS* ($n = 2$); *CHCHD10* ($n = 1$)); bvFTD (*CHCHD10* ($n = 1$)).

Plasma EV TDP-43 is increased in ALS and bvFTD

Plasma sEV TDP-43 levels were highest in ALS (median 45.45 pg ml^{-1}, IQR [28.88–83.21]) compared with HC (9.47 pg ml^{-1}, IQR [7.63–13.33], $P < 0.00001$), bvFTD (31.25 pg ml^{-1}, IQR [14.45–41.09]) and PSP (9.09 pg ml^{-1}, IQR [7.73–13.27], $P < 0.00001$) (Fig. 3a (sEV) and Supplementary Fig. 11a and Supplementary Table 3 (mEV)). Plasma sEV TDP-43 distinguished ALS from HC, PSP and bvFTD with AUC values of 0.99, CI [0.97–1.00]; 0.99, CI [0.98–1.00]; and 0.91, CI [0.88–0.94] (Fig. 3b–d). Similar results were obtained for plasma mEV TDP-43 concentrations and AUC values (Supplementary Fig. 11a–d). No correlation was observed with age, sex or disease duration (Supplementary Table 7). Of note, plasma TDP-43 levels did not differ between the diagnostic groups, highlighting the importance of EV analysis (Extended Data Fig. 3).

In bvFTD, plasma EV TDP-43 levels partially overlapped with HC and PSP (low levels) and the ALS group (high levels), suggesting that high levels could indicate TDP-43 pathology in bvFTD. Plasma sEV TDP-43 distinguished bvFTD from HC, PSP and ALS (AUC: bvFTD versus HC 0.85, CI [0.82–0.90]; versus PSP 0.93, CI [0.86–0.89]; versus ALS 0.91, CI [0.0.88–0.94]) (Fig. 3d–f (sEV) and Supplementary Fig. 11d–f (mEV)). Of note, plasma EV TDP-43-based AUC values exceeded plasma NfL-based AUC values (plasma NfL: ALS versus HC 0.83, CI [0.77–0.88]; versus PSP 0.62, CI [0.56–0.67]; versus bvFTD 0.61, CI [055–0.66]; bvFTD versus HC 0.73, CI [0.71–0.75]; versus PSP 0.63, CI [0.61–0.71]; $P < 0.0001$ for all comparisons) (Fig. 3b–f (sEV), Supplementary Fig. 11b–f and Supplementary Table 3 (mEV)).

Plasma EV TDP-43 correlates with disease severity

Plasma EV TDP-43 levels were highly correlated with plasma NfL concentrations in ALS and bvFTD (ALS sEV: $r = 0.67$, $P < 0.0001$; bvFTD sEV: $r = 0.42$, $P < 0.0001$; Extended Data Fig. 2c,d (sEV) and Supplementary Fig. 11g,h (mEV)). In ALS, higher plasma EV TDP-43 levels were associated with worse cognitive performance and disease severity (MMSE, Edinburgh Cognitive and Behavioral ALS Screen total

https://doi.org/10.1038/s41591-024-02937-4

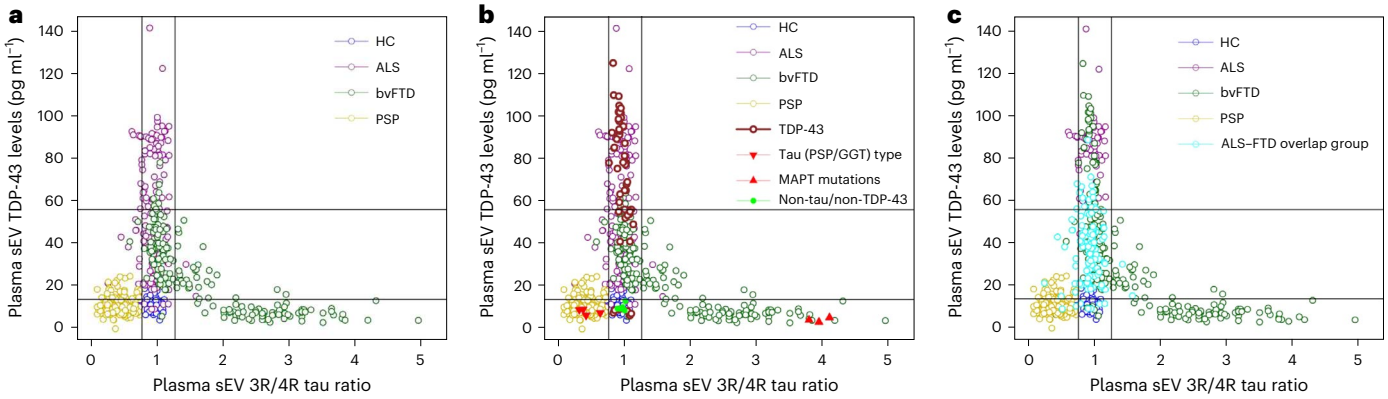

Fig. 4 | Distribution of plasma sEV 3R/4R tau ratio versus plasma EV TDP-43 levels stratified by diagnosis in DESCRIBE subcohort 2. a, Subcohort 2 without pathology-confirmed cases. Color codes indicate the different clinical diagnostic groups (ALS, bvFTD, PSP, HC). Cut-off values were determined by Gaussian mixture modeling. EV 3R/4R tau ratio cut-offs: 0.77 and 1.28; EV TDP-43 cut-offs: 13.87 pg ml^{-1} and 56.18 pg ml^{-1}. **b**, Genetically or neuropathologically confirmed cases were also plotted. **c**, The ALS–FTD overlap group (ALS with FTD (ALS–FTD), ALS patients with cognitive impairment and ALS patients with behavioral impairment) is indicated in light blue.

score, ALS Functional Rating Scale (ALS–FRS)) (Fig. 3g,h (sEV), Supplementary Fig. 11i,j (mEV) and Supplementary Table 12). In bvFTD, plasma EV TDP-43 concentrations correlated with cognitive impairment, impaired functional activities, increased symptom severity, more severe psychiatric and behavior symptoms (MMSE, MoCA, FAQ, CDR-SB, CDR plus NACC FTLD, NPI-Q, CBI-M) (Fig. 3i,j (sEV), Supplementary Fig. 11k,l (mEV) and Supplementary Table 9). Plasma EV TDP-43 levels correlated with CSF EV TDP-43 in the ALS group (Supplementary Fig. 12).

Plasma EV TDP-43 levels in pathology-confirmed cases

We next compared plasma EV TDP-43 levels of confirmed TDP-43, tau or non-TDP-43/non-tau pathology cases stratified by clinical diagnosis (Fig. 3k) and independent of clinical diagnosis (Fig. 3l). In the TDP pathology cases, EV TDP-43 was increased compared with HC (median sEV: 63.95 pg ml^{-1}, IQR [42.89–86.63], $P < 0.0001$), PSP/GGT-type tau (median sEV: 2.85 pg ml^{-1}, IQR [2.10–3.52], $P < 0.00001$), genetic *MAPT* (median sEV: 2.86 pg ml^{-1}, IQR [2.53–3.02], $P < 0.00001$) and the non-TDP-43/non-tau pathology group (median sEV: 11.35 pg ml^{-1}, IQR [10.62–12.05], $P < 0.00001$) (Fig. 3i; see Supplementary Fig. 13a,b for mEV data). In bvFTD with confirmed TDP-43 pathology, plasma EV TDP-43 levels were higher compared with bvFTD with *MAPT* mutations (bvFTD with TDP-43 pathology median sEV TDP-43: 36.15 pg ml^{-1}, IQR [4.52–52.65]; bvFTD with *MAPT* mutations median sEV TDP-43: 2.86 pg ml^{-1}, IQR [2.53–3.02], $P < 0.0001$). EV TDP-43 levels in PSP/GGT-type tau pathology were comparable with non-TDP-43/non-tau and HC groups ($P > 0.05$) (Fig. 3l and Supplementary Fig. 13b). Surprisingly, *VCP* and *TBK1* mutation carriers showed low levels of EV TDP-43, although both mutations had been linked to TDP-43 pathology before[47,48].

Plasma EV tau ratio and TDP-43 aid the diagnosis of FTD and ALS

In bvFTD, plasma EV TDP-43 concentrations were inversely correlated with EV 3R/4R tau ratios (sEV: $r = -0.496$, $P < 0.0001$; Supplementary Fig. 14a,b), indicating that high TDP-43 levels are associated with low tau ratios and vice versa. A plot of plasma sEV TDP-43 concentrations versus sEV 3R/4R tau ratios without genetically and neuropathologically confirmed cases revealed a clear separation of bvFTD cases into two subgroups (Fig. 4a). One of the two bvFTD subgroups, characterized by a low EV tau ratio and high EV TDP-43 levels, overlapped with ALS, whereas the other was characterized by high EV 3R/4R tau ratios but low TDP-43 levels (putative FTLD-TDP and FTLD-tau groups) (Fig. 4a (subcohort 2) and Extended Data Fig. 4 (bvFTD cases only)). PSP and HC groups formed separate clusters.

We next added pathology-confirmed cases to the graph (Fig. 4b). PSP/GGT-type tau pathology cases formed a cluster characterized by low TDP-43 and 3R/4R tau ratios. The HC group and all non-TDP-43/non-tau cases grouped together, consistent with the absence of TDP-43 and tau pathology. TDP-43-confirmed pathology cases were found in the cluster of ALS and TDP-43 high bvFTD cases. By contrast, bvFTD cases with confirmed *MAPT* pathology fell into the bvFTD group with high sEV tau ratios.

We applied a mixture modeling approach to sEV 3R/4R tau and sEV TDP-43 data to obtain cut-off values of 0.77 and 1.27 for 3R/4R tau, and 13.87 pg ml^{-1} and 56.18 pg ml^{-1} for TDP-43 (Fig. 4, Supplementary Data and Supplementary Fig. 15).

Low plasma sEV 3R/4R tau ratios (<0.77) discriminated clinical PSP cases form all other individuals in subcohort 2 (sensitivity: 93.25%, CI [88.25–96.58%]; specificity: 95.25%, CI [92.68–97.12%]) as well as PSP/GGT-type tau pathology cases from other pathology-confirmed cases (sensitivity: 100%, CI [39.76–100%]; specificity: 100%, CI [93.94–100%]). High plasma sEV 3R/4R tau ratios (>1.27) were found in 38.55% of clinical bvFTD cases. All *MAPT* mutation carriers, but no other patients with confirmed pathology, fell into the high plasma sEV tau ratio category (sensitivity: 100%, CI [29.24–100%]; specificity: 100%, CI [94.04–100%]). Importantly, all but one of the remaining clinical bvFTD patients (61.45%) showed tau ratios below the upper cut-off (<1.27) but elevated TDP-43 levels (>13.87 pg ml^{-1}), suggesting that sEV measurements can distinguish two separate subgroups among bvFTD patients.

TDP-43 pathology cases mapped to the TDP-43 high bvFTD (putative FTLD-TDP) and the ALS group, and were detected among all individuals with a genetically or neuropathologically proven diagnosis with a sensitivity of 88.00%, CI [76.13–95.67%] and a specificity of 100%, CI [75.29–100%] using the cut-off for at least mildly increased TDP-43 levels (>13.87 pg ml^{-1}) (Fig. 4b).

ALS cases with symptoms overlapping with bvFTD showed elevated plasma sEV TDP-43 levels (Fig. 4c).

Together, our data suggest that a combination of plasma EV TDP-43 and 3R/4R tau may distinguish FTLD-tau from FTLD-TDP.

Sant Pau validation cohort

We validated our findings in samples from the independent Sant Pau cohort[49] (ALS ($n = 65$), ALS–FTD ($n = 58$), bvFTD ($n = 50$), FTD mutation carriers ($n = 23$), PSP ($n = 41$) and HC ($n = 50$); see Extended Data Table 3 for patient demographics).

Plasma EV tau ratios are high in bvFTD and low in PSP

Similar to our findings from DESCRIBE, tau ratios were lowest in PSP (median sEV 3R/4R tau ratio 0.38, IQR [0.33–0.50]), compared with all other groups (median sEV HC 1.02, IQR [0.96–1.06], PSP versus HC $P < 0.00001$; ALS 1.02, IQR [0.92–1.11], PSP versus ALS $P < 0.00001$; ALS–FTD 0.95, IQR [0.84–1.00], PSP versus ALS–FTD $P < 0.00001$; bvFTD 1.34, IQR [1.17–2.34], PSP versus bvFTD $P < 0.00001$) and highest in bvFTD, median sEV bvFTD versus all other diagnostic groups $P < 0.00001$) (Fig. 5a and Extended Data Table 3 (sEV), and Supplementary Fig. 16a and Extended Data Table 3 (mEV)). No correlations of EV tau ratios with age, sex and disease duration were found (Supplementary Table 13). Approximately half of the bvFTD samples were characterized by high EV tau ratios, indicating tau pathology, whereas the other half were in the range observed for HC, ALS and ALS–FTD. We confirmed the feasibility of using plasma EV tau ratio as a diagnostic marker for different tauopathies by ROC analysis (sEV 3R/4R tau ratio: PSP versus HC (AUC 1.00, CI [0.960–1.000]), PSP versus ALS (AUC 0.99, CI [0.962–1.000]), PSP versus ALS–FTD (AUC 0.98, CI [0.960–1.000]) and PSP versus bvFTD (AUC 1.00, CI [0.969–1.000]); bvFTD versus HC (AUC 0.95, CI [0.905–0.985]) and bvFTD versus ALS (AUC 0.90, CI [0.845–0.948])) (Extended Data Fig. 5a–g and Supplementary Table 14 (sEV), and Supplementary Fig. 16b–h and Supplementary Table 14 (mEV)).

Sant Pau cohort samples included 34 genetically confirmed cases, 27 with TDP-43 (*GRN* $n = 6$, *C9orf72* $n = 16$, *TARDBP* $n = 1$, *VCP* $n = 1$ and *TBK1* $n = 3$) and 7 with neither TDP-43 nor tau pathology (*SOD1* $n = 4$ and FUS $n = 3$) (Supplementary Table 15). Consistent with the absence of tau pathology, plasma EV 3R/4R tau ratios of all genetically confirmed cases were in the range of HC, ALS and ALS–FTD (Fig. 5b,c and Supplementary Fig. 22a,b) (HC: median sEV 1.02, IQR [0.96–1.06]; TDP-43 pathology group: median sEV 1.15, IQR [1.07–1.23], versus HC $P > 0.9999$; non-TDP-43/non-tau group: median sEV 0.92, IQR [0.84–1.15], versus HC $P > 0.9999$).

Plasma EV tau ratios correlate with disease severity

Plasma EV 3R/4R tau ratios correlated with plasma NfL and clinical measures of disease severity in bvFTD and inversely in PSP (Fig. 5d–g (sEV), and Supplementary Fig. 16k,n and Supplementary Tables 16 and 17 (mEV)).

High plasma EV TDP-43 in ALS, ALS–FTD and a subset of bvFTD

As in DESCRIBE subcohort 2, plasma EV TDP-43 levels were increased in patients with ALS (median sEV TDP-43: 45.60 pg ml^{-1}, IQR [31.55–64.45]) compared with HC (median sEV TDP-43: 10.41 pg ml^{-1}, IQR [8.50–14.65], $P < 0.00001$), in ALS–FTD (median sEV TDP-43: 52.40 pg ml^{-1}, IQR [39.18–73.43], $P < 0.00001$ compared with HC) and in bvFTD (median sEV TDP-43: 24.15 pg ml^{-1}, IQR [11.13–40.55], $P < 0.00001$ compared with HC) (Fig. 5h (sEV), and Supplementary Fig. 19a and Extended Data Table 3 (mEV)). PSP EV TDP-43 levels were comparable with HC (median sEV TDP-43: 10.20 pg ml^{-1}, IQR [8.30–12.35], $P > 0.9999$). Plasma sEV TDP-43 distinguished ALS from HC, PSP and bvFTD with AUC values of 0.94, CI [0.892–0.981], 0.96, CI [0.910–0.991] and 0.76, CI [0.687–0.832] (Supplementary Table 14), and ALS–FTD from HC, PSP and bvFTD groups (AUC 0.98, CI [0.946–0.999], 0.99, CI [0.955–1.000] and 0.82, CI [0.745–0.881]) (Supplementary Fig. 19a–g (sEV), Supplementary Fig. 18b–h) (mEV) and Supplementary Table 14).

Genetic cases linked to TDP-43 pathology were characterized by high EV TDP-43 levels (median sEV TDP-43: 55.0 pg ml^{-1}, IQR [35.0–66.4]), with the exception of *VCP* and *TBK1* mutations similar to what we observed in the DESCRIBE cohort. Genetically confirmed cases, neither linked to TDP-43 nor tau, displayed low plasma EV TDP-43 levels (median sEV TDP-43: 12.7 pg ml^{-1}, IQR [11.3–15.7]), comparable to HC and PSP (HC median sEV TDP-43: 10.41 pg ml^{-1}, IQR [8.50–14.65]; PSP median sEV TDP-43: 10.20 pg ml^{-1}, IQR [8.30–12.35]) (Fig. 5i,j and Supplementary Fig. 19a,b).

Plasma EV TDP-43 discriminated bvFTD cases from HC, PSP, ALS and ALS–FTD (AUC sEV: bvFTD versus HC 0.87, CI [0.803–0.926]; versus PSP 0.91, CI [0.851–0.959]; versus ALS 0.76, CI [0.687–0.832]; versus ALS–FTD 0.82, CI [0.745–0.881]) (Extended Data Fig. 6i and Supplementary Table 14 (sEV), and Supplementary Fig. 18h–j and Supplementary Table 14 (mEV)). Comparable with our results from DESCRIBE, plasma EV TDP-43-based AUCs performed superior to NfL for bvFTD versus HC and PSP (plasma NfL AUCs: bvFTD versus HC 0.78, CI [0.734–0.842];

Fig. 5 | 3R/4R tau ratio in plasma sEVs in the Sant Pau cohort. a, Stratified by clinical diagnosis. Horizontal lines indicate the median and IQR. Kruskal–Wallis test with Dunn's correction for multiple comparisons. HC versus bvFTD $P = 0.000009$, HC versus PSP $P = 0.000007$, ALS versus bvFTD $P = 0.0000091$, ALS versus PSP $P = 0.0000016$, ALS–FTD versus bvFTD $P = 0.0000074$, ALS–FTD versus PSP $P = 0.0000041$, bvFTD versus PSP $P = 0.000006$; ****$P < 0.00001$. Biologically independent samples: HC $n = 50$, ALS $n = 65$, ALS–FTD $n = 58$, bvFTD $n = 50$ (+23 mutation carriers), PSP $n = 41$. **b**,**c**, sEV 3R/4R tau ratios in plasma-derived sEV in genetic cases from Sant Pau cohort ($n = 34$ genetic cases) stratified by clinical diagnosis (**b**), HC versus bvFTD $P = 0.000009$, HC versus PSP $P = 0.000007$, ALS versus bvFTD $P = 0.0000091$, ALS versus PSP $P = 0.0000016$, ALS–FTD versus bvFTD $P = 0.0000074$, ALS–FTD versus PSP $P = 0.0000041$, bvFTD versus PSP $P = 0.000006$; ****$P < 0.00001$; and stratified by associated molecular pathology and independent from clinical diagnosis (**c**). The long horizontal line represents the median and the short horizontal lines represent the IQR. Kruskal–Wallis test with Dunn's correction for multiple comparisons. HC versus TDP-43 $P = 0.758$, HC versus non-tau/non-TDP-43 $P = 0.632$, TDP-43 versus non-tau/non-TDP-43 $P = 0.425$; NS, not significant. TDP-43 pathology group: bvFTD (*C9orf72* ($n = 12$), *GRN* ($n = 6$), *TARDP* ($n = 1$), *VCP* ($n = 1$), *TBK-1* ($n = 3$)); ALS (*C9orf72* ($n = 3$)); ALS–FTD (*C9orf72* (n = 1)). Non-tau/non-TDP-43 pathology group: ALS (*SOD-1* ($n = 3$)); FUS ($n = 3$); ALS–FTD (SOD-1 ($n = 1$)). **d**,**e**, Correlation matrix depicting results of two-sided Spearman correlations in the PSP group, visualized by plotting strength of correlation (r) as a heat map (**d**) along with P values (**e**). **f**,**g**, Correlation matrix depicting results of two-sided Spearman correlations in the bvFTD group, visualized by plotting strength of correlation (r) as a heat map (**f**) along with P values (**g**). **h**, TDP-43 levels in plasma sEV of the Sant Pau cohort stratified by clinical diagnosis. The long horizontal line represents the median and the short horizontal lines represent the IQR. Kruskal–Wallis test with Dunn's correction for multiple comparisons. HC versus ALS $P = 0.0000075$, HC versus ALS–FTD $P = 0.0000046$, ALS versus bvFTD $P = 0.00074$, HC versus PSP $P = 0.578$, ALS versus bvFTD $P = 0.000009$, ALS versus PSP $P = 0.000007$, ALS–FTD versus bvFTD $P = 0.0000043$, ALS–FTD versus PSP $P = 0.0000055$, bvFTD versus PSP $P = 0.0005$; *$P < 0.05$, **$P < 0.001$, ***$P < 0.0001$, ****$P < 0.00001$. Biologically independent samples: HC $n = 50$, ALS $n = 65$, ALS–FTD $n = 58$, bvFTD $n = 50$ (+23 mutations), PSP $n = 41$. **i**,**j**, Plasma sEV TDP-43 concentrations in genetic cases of the Sant Pau cohort ($n = 34$ genetic cases) stratified by clinical diagnosis (**i**), HC versus ALS $P = 0.0000075$, HC versus ALS–FTD $P = 0.0000046$, ALS versus bvFTD $P = 0.00074$, HC versus PSP $P = 0.578$, ALS versus bvFTD $P = 0.000009$, ALS versus PSP $P = 0.000007$, ALS–FTD versus bvFTD $P = 0.0000043$, ALS–FTD versus PSP $P = 0.0000055$, bvFTD versus PSP $P = 0.0005$; and stratified by molecular pathology, independent of clinical diagnosis (**j**). The long horizontal line represents the median and the short horizontal lines represent the IQR. Kruskal–Wallis test with Dunn's correction for multiple comparisons. HC versus TDP-43 $P = 0.0000063$, HC versus non-tau/non-TDP-43 $P = 0.541$, TDP-43 versus non-tau/non-TDP-43 $P = 0.0000051$; ****$P < 0.00001$. TDP-43 pathology group: bvFTD (*C9orf72* ($n = 12$), *GRN* ($n = 6$), *TARDP* ($n = 1$), *VCP* ($n = 1$), *TBK-1* ($n = 3$)); ALS (*C9orf72* ($n = 3$)); ALS–FTD *C9orf72* ($n = 1$). Non-tau/non-TDP-43 pathology group: ALS (*SOD-1* ($n = 3$); FUS ($n = 3$)); ALS–FTD (SOD-1 ($n = 1$)). **k**,**i**, Correlation matrix depicting results of two-sided Spearman correlations in the ALS group, visualized by plotting strength of correlation (r) as a heat map (**k**) along with P values (**i**). ALS-FRS (sEV: $r = -0.212$), $P = 0.015$ and time since diagnosis/disease duration (sEV: $r = 0.514$, $P = 0.0004$). **n**,**m**, Correlation matrix depicting results of two-sided Spearman correlations in the ALS–FTD group, visualized by plotting strength of correlation (r) as a heat map (**m**) along with P values (**n**). ALS-FRS (sEV: $r = -0.702$), $P = 0.0002$ and time since diagnosis/disease duration (sEV: $r = 0.445$, $P = 0.0005$); MMSE (sEV: $r = -0.535$, $P = 0.018$).

https://doi.org/10.1038/s41591-024-02937-4

versus PSP 0.71, CI [0.689–0.789]; $P < 0.0001$ for all AUC comparisons) (Extended Data Fig. 7a,b (sEV), and Supplementary Fig. 23i,j and Supplementary Table 14 (mEV)). NfL measurements were not available for ALS and ALS–FTD in the Sant Pau cohort.

Plasma EV TDP-43 correlates with disease severity

Plasma EV TDP-43 levels correlated highly with plasma NfL concentrations in bvFTD (sEV: $r = 0.513$, $P < 0.0001$; mEV: $r = 0.465$, $P < 0.0001$) (Extended Data Fig. 2e–g (sEV) and Supplementary Fig. 20k (mEV)).

In ALS and ALS–FTD, higher plasma EV TDP-43 levels were associated with increased disease severity (ALS-FRS, time since diagnosis, MMSE; Fig. 5k–n (sEV), Supplementary Fig. 18l–o and Supplementary Tables 18 and 19a (mEV)).

In bvFTD, plasma EV TDP-43 concentrations correlated with cognitive impairment, increased symptom severity and more severe psychiatric symptoms (Fig. 5f,g (sEV), Supplementary Fig. 23p,r (mEV) and Supplementary Table 17).

Determination of cut-off levels

Plasma EV TDP-43 concentrations in bvFTD were inversely correlated to EV 3R/4R tau ratios (sEV: $r = -0.714$, $P < 0.0001$; mEV: $r = -0.617$, $P < 0.0001$; Supplementary Fig. 20a,b). A plot of plasma sEV TDP-43 concentrations versus sEV 3R/4R tau ratios without genetic cases showed a

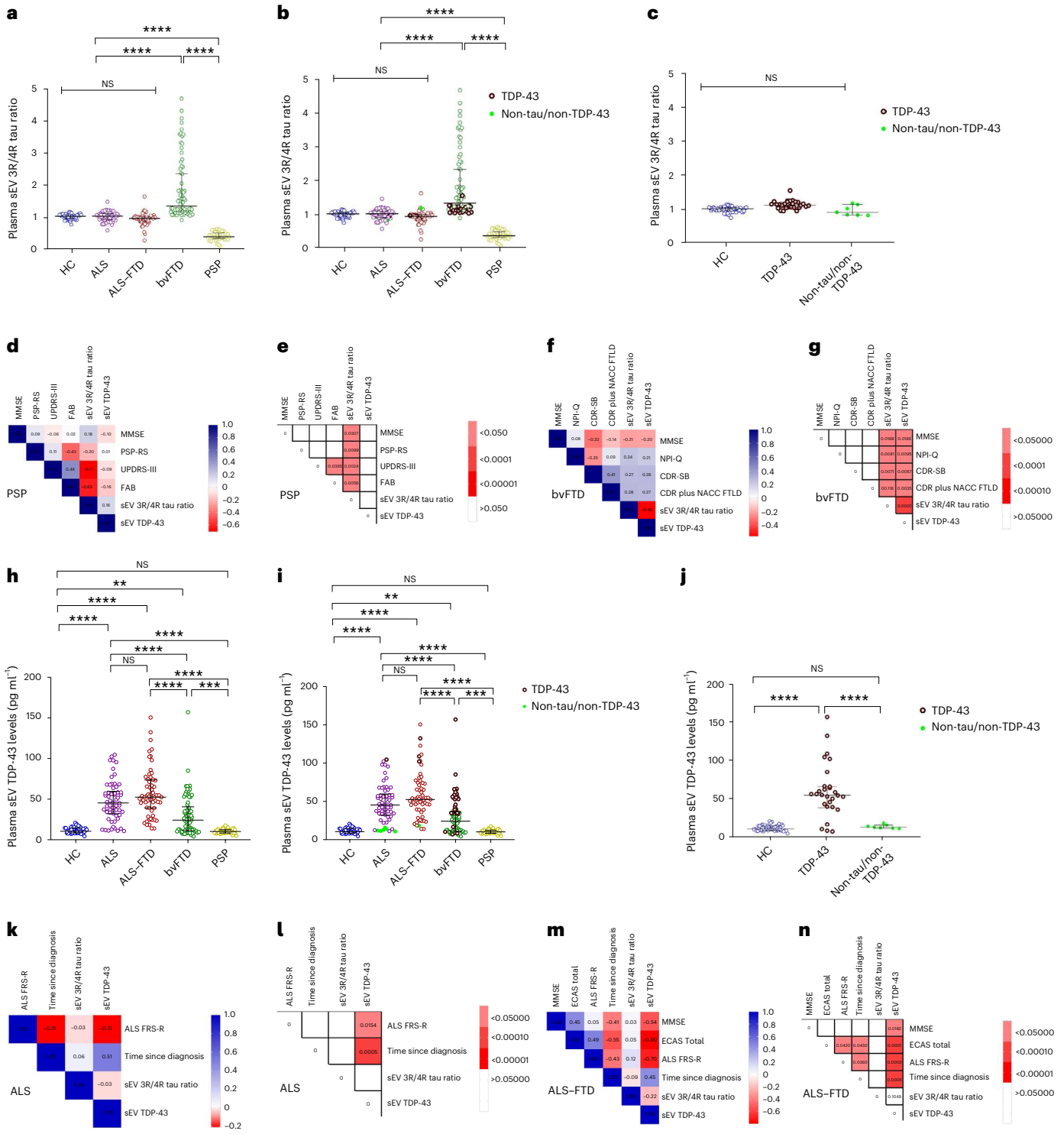

https://doi.org/10.1038/s41591-024-02937-4

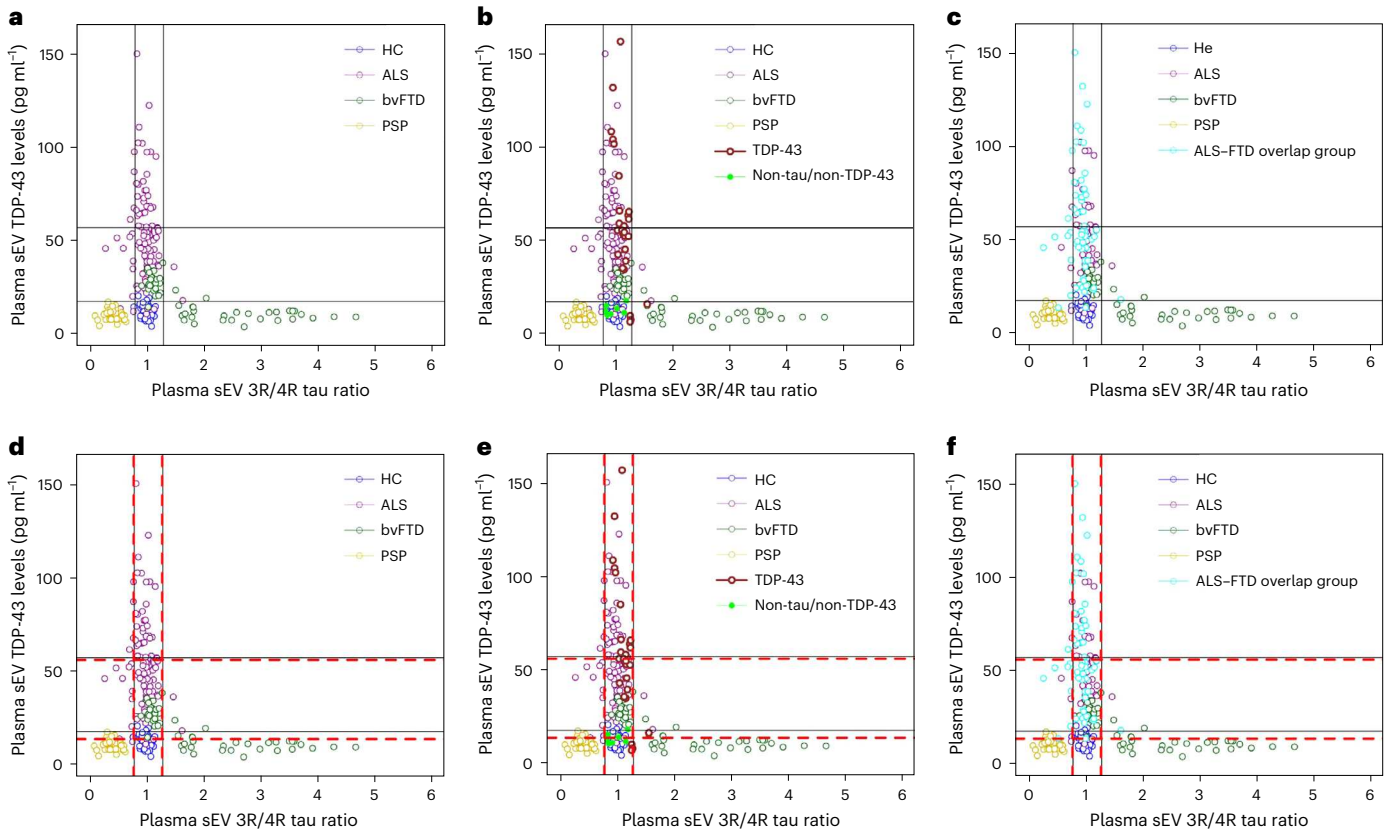

Fig. 6 | Distribution of plasma sEV 3R/4R tau ratio versus plasma EV TDP-43 levels stratified by diagnosis in the Sant Pau cohort. a, Sant Pau cohort without pathology-confirmed cases. Color codes indicate the different clinical diagnostic groups (ALS, bvFTD, PSP, HC). Cut-off values as determined by Gaussian mixture modeling. EV 3R/4R tau ratio cut-offs: 0.78 and 1.28; EV TDP-43 cut-offs: 17.85 pg ml^{-1} and 57.34 pg ml^{-1}. **b**, Genetically confirmed cases were also plotted in the graph. **c**, The ALS–FTD overlap group is indicated in light blue. **d**–**f**, Sant Pau cohort without pathology-confirmed cases (**d**), Sant Pau cohort including pathology-confirmed cases (**e**) and Sant Pau cohort, ALS–FTD group indicated in light blue (**f**). Similar to **a**–**c** but superimposed with Sant Pau and DESCRIBE cut-offs. The black solid line indicates Sant Pau cut-offs (EV 3R/4R tau ratio cut-offs: 0.78 and 1.28; EV TDP-43 cut-offs: 17.85 pg ml^{-1} and 57.34 pg ml^{-1}). The red dashed line indicates DESCIRBE subcohort 2 cut-offs (EV 3R/4R tau ratio cut-offs: 0.77 and 1.28; EV TDP-43 cut-offs: 13.87 pg ml^{-1} and 56.18 pg ml^{-1}).

similar distribution of the diagnostic groups as observed for DESCRIBE subcohort 2 and a separation of putative bvFTD TDP and tau subgroups (Fig. 6a). The TDP-43 high bvFTD subgroup overlapped with the ALS group (Fig. 6a), cases with confirmed TDP-43 pathology (Fig. 6b) and the ALS–FTD group (Fig. 6c). Cases with confirmed non-tau/non-TDP-43 pathology overlapped with the HC group (Fig. 6b).

Cut-offs were defined by mixture modeling (Supplementary Fig. 21), excluding genetically confirmed cases for subsequent testing of cut-offs (sEV 3R/4R tau ratio: 0.78 and 1.28; sEV TDP-43: 17.85 pg ml^{-1} and 57.34 pg ml^{-1}; Fig. 6d–f, black lines). Cut-offs were very close to those in DESCRIBE subcohort 2. sEV 3R/4R tau ratio: 0.77 and 1.28; sEV TDP-43 cut-offs: 13.87 pg ml^{-1} and 56.18 pg ml^{-1}.

The Sant Pau TDP-43 cut-off (>17.85 pg ml^{-1}) detected confirmed TDP-43 pathology cases among all individuals with a genetically proven diagnosis with a sensitivity of 88.89%, CI [70.84–97.65%] and a specificity of 85.71%, CI [42.13–99.64%].

Low plasma sEV 3R/4R tau ratios (<0.78, Sant Pau cohort cut-off) discriminated PSP cases form all other diagnoses (sensitivity: 100%, CI [91.40–100%]; specificity: 94.00%, CI [90.30–96.60%]). Similar results were obtained when applying the DESCRIBE cohort cut-off to Sant Pau data (sensitivity: 100%, CI [91.40–100%]; specificity: 94.94%, CI [91.77–97.50%]).

Fifty-eight percent of sporadic bvFTD patients in the Sant Pau cohort showed high plasma sEV 3R/4R tau ratios (>1.28), indicative of tau pathology. Of those with tau ratios below this cut-off (42%), all but one showed EV TDP-43 levels above the TDP cut-off, further supporting that sEV tau ratio and TDP-43 measurements can distinguish two separate bvFTD subgroups.

The Sant Pau EV TDP-43 cut-off identified patients with sporadic ALS and ALS–FTD with high sensitivity and specificity versus HC and PSP (ALS sensitivity: 86.15%, CI [75.34–93.47%]; specificity: 100%, CI [96.03–100%]; ALS–FTD sensitivity: 96.55%, CI [88.90–99.58%]; specificity: 100%, CI [96.03–100%]). Applying the DESCRIBE subcohort 2 cut-off values to Sant Pau resulted in a sensitivity of 89.23% (CI [79.06–95.56%]) and a specificity of 90.11% (CI [82.05–95.38%]) for ALS, and a sensitivity of 100% (CI [93.84–100%]) and specificity of 90.11% (CI [82.05–95.38%]) for ALS–FTD.

Together, these data indicate that cut-offs are nearly interchangeable between the two cohorts.

Discussion

Currently, there are no biomarkers available for ALS, FTD and FTD spectrum disorders that define the underlying proteinopathies. A low-invasive fluid biomarker for the identification of molecular pathology would allow pathology-based stratification of patients to clinical trials and strongly advance the development of new disease-modifying therapies. In light of novel therapeutic approaches in ALS and FTD, such biomarkers are strongly desired.

Our study in a large cohort of 704 patients, including 37 genetically and 31 pathologically confirmed samples as well as in an independent validation cohort of 287 patients with 34 genetically confirmed cases, shows that plasma EVs inform about tau and TDP-43 pathology

in bvFTD, and can additionally discriminate patients with ALS and PSP from healthy and neurodegenerative disease controls with high diagnostic accuracy (AUC > 0.91).

High plasma EV 3R/4R tau ratios in bvFTD were characterized by low EV TDP-43 levels and both markers separated bvFTD into two distinct groups, which can be discriminated based on cut-off values derived from mixture modeling. Plasma EV 3R/4R tau ratios in confirmed cases with TDP-43 pathology displayed low 3R/4R tau ratios, comparable with values in the HC group, but high TDP-43 levels. By contrast, *MAPT* mutation carriers showed high EV 3R/4R tau ratios and mapped to the bvFTD tau subgroup. Clinically diagnosed PSP, including neuropathologically proven cases of PSP-type tauopathy, segregated into a third group, characterized by a decreased EV 3R/4R tau ratio and EV TDP-43 levels in the range of HC.

It is unclear why the EV 3R/4R tau ratio is low in PSP but high in bvFTD cases with FTLD-tau. 4R tau predominance may explain low 3R/4R tau ratios in PSP; however, all three *MAPT* mutation carriers in DESCRIBE showed high 3R/4R tau ratios, despite being associated with 4R tau pathology. It is possible that different 'strains', posttranslational modifications or regional and cellular distribution of pathology may result in differential sorting of 3R and 4R tau isoforms to EVs in different tauopathies[50].

Plasma EV TDP-43 levels distinguished ALS from all other groups with high diagnostic accuracy (AUC ≥ 0.91 versus HC, PSP, bvFTD in DESCRIBE; AUC ≥ 0.94 versus HC, PSP; and AUC ≥ 0.76 versus bvFTD in the Sant Pau cohort). Cases with confirmed TDP-43 pathology were characterized by high EV TDP-43 levels, whereas ALS cases with mutations that are not linked to TDP-43 pathology displayed low EV TDP-43 concentrations, comparable with HC.

Unexpectedly, cases with *VCP* and *TBK1* mutations failed to show increased EV TDP-43 levels, although mutations in both genes have been linked to TDP-43 pathology[47,48]. One potential explanation could be the predominance of intranuclear lentiform inclusions and impaired endolysosomal protein sorting described in *VCP* mutation carriers, which may prevent release of TDP-43 with EVs[51]. Overactivation of TBK-1 can increase neuronal EV release[52]. Thus, *TBK-1* loss-of-function mutations may impair EV secretion. Indeed, plasma EV concentrations in *TBK-1* mutation carriers were approximately three times lower than the cohorts' mean plasma EV concentration (Supplementary Fig. 22).

In PSP and bvFTD, plasma EV tau ratios correlated with NfL, clinical, cognitive and behavior scales reflecting disease pathology, similar to plasma EV TDP-43 in ALS and bvFTD, including trial-relevant scales such as ALS-FRS-revised and CDR-SB. Plasma EV 3R/4R tau and TDP-43 may have the potential to mirror disease progression and could, after positive evaluation in longitudinal cohort samples and therapeutic intervention trials, potentially be used as a progression and surrogate marker for clinical studies.

We focused on plasma EV measurements due to several reasons:

(1) Plasma albumin and immunoglobulins can interfere with antibody binding[53] but are largely absent in plasma EV preparations[26], which may facilitate TDP-43 detection.

(2) Full-length tau concentrations in blood are extremely low because of tau fragmentation. By contrast, EV cargo is protected from degradation[54], which allows reliable quantification of 3R and 4R tau isoforms in plasma EVs.

(3) Increased EV levels of tau or TDP-43 in extracellular fluids may reflect disease pathology. Both tau and TDP-43 can be transported by EVs to other cells where they can induce protein aggregation. Cytoplasmic (mis)localization of TDP-43 is likely required for its secretion with EVs, and its release with EVs may mirror the nuclear to cytoplasmatic shift of TDP-43 observed in ALS and FTD.

Although our cohort included a high number of confirmed TDP-43 cases, future studies with additional confirmed FTLD-tau cases are needed, as well as measurements from preclinical disease stages, to determine how early these biomarkers increase before symptom onset. Cross-sectional and longitudinal samples need to be analyzed in additional, independent and ethnically more diverse cohorts (imbalanced group sizes in DESCRIBE subcohort 2: Supplementary Data).

EVs can pass the blood–brain barrier[55] but it is not known to what extent plasma EV TDP-43 or tau stem from the CNS because both are expressed in peripheral tissue[27,56,57]. The correlation of CSF with plasma EV TDP-43 in ALS supports the notion that plasma EV TDP-43 may reflect CNS pathology. Plasma EV tau and TDP-43 are almost exclusively found in L1CAM-positive EVs, which could further support a potential brain origin, although the neuronal specificity of L1CAM and its association with EVs are controversially discussed[30].

Strengths of our study are the large numbers of patient samples, 991 in total, and the independent validation in another cohort, containing altogether 97 genetically and/or neuropathologically confirmed samples. Our work is the first study, to our knowledge, demonstrating a blood-based, and therefore low invasive and easily accessible, fluid biomarker, which has great potential as a diagnostic marker to distinguish FTLD-TDP from FTLD-tau, and to detect ALS and PSP. Cut-off values determined by Gaussian mixture modeling were remarkably transferable between the different cohorts, particularly tau ratio cut-offs. Plasma mEVs may even offer faster and easier preparation than sEVs, although in our study, sEVs performed slightly better.

Our work may also have important implications for AD, where limbic predominant TDP-43 co-pathology has been described in up to 55% of cases[58,59] and is associated with a more aggressive clinical course[60]. A combination of 'classical' AD biomarkers with plasma EV TDP-43 may help to stratify AD cases with and without limbic predominant TDP-43 co-pathology pathology.

In summary, with EV 3R/4R tau and EV TDP-43 we describe the first marker that specifically detects underlying molecular pathology in patients with ALS, FTD and FTD spectrum disorders, whereas previously suggested biomarkers reflect downstream effects such as neurodegeneration (NfL)[61,62] or inflammation (glial fibrillary acidic protein)[63,64].

Online content

Any methods, additional references, Nature Portfolio reporting summaries, source data, extended data, supplementary information, acknowledgements, peer review information; details of author contributions and competing interests; and statements of data and code availability are available at https://doi.org/10.1038/s41591-024-02937-4.

References

1. Abramzon, Y. A., Fratta, P., Traynor, B. J. & Chia, R. The overlapping genetics of amyotrophic lateral sclerosis and frontotemporal dementia.*Front. Neurosci.* **14**, 42 (2020).
2. Chare, L. et al. New criteria for frontotemporal dementia syndromes: clinical and pathological diagnostic implications. *J. Neurol. Neurosurg. Psychiatry* **85**, 865–870 (2014).
3. Mann, D. M. A. & Snowden, J. S. Frontotemporal lobar degeneration: pathogenesis, pathology and pathways to phenotype. *Brain Pathol.* **27**, 723–736 (2017).
4. Mandelkow, E. & Mandelkow, E. M. Microtubules and microtubule-associated proteins. *Curr. Opin. Cell Biol.* **7**, 72–81 (1995).
5. Mackenzie, I. R. & Neumann, M. Molecular neuropathology of frontotemporal dementia: insights into disease mechanisms from postmortem studies. *J. Neurochem.* **138**, 54–70 (2016).
6. Richards, D., Morren, J. A. & Pioro, E. P. Time to diagnosis and factors affecting diagnostic delay in amyotrophic lateral sclerosis. *J. Neurol. Sci.* **417**, 117054 (2020).
7. Mamarabadi, M., Razjouyan, H. & Golbe, L. I. Is the latency from progressive supranuclear palsy onset to diagnosis improving? *Mov. Disord. Clin. Pract.* **5**, 603–606 (2018).

8. Tsoukra, P. et al. The diagnostic challenge of young-onset dementia syndromes and primary psychiatric diseases: results from a retrospective 20-year cross-sectional study. *J. Neuropsychiatry Clin. Neurosci.* **34**, 44–52 (2022).
9. Cousins, K. A. Q. et al. Distinguishing frontotemporal lobar degeneration tau from TDP-43 using plasma biomarkers. *JAMA Neurol.* **79**, 1155–1164 (2022).
10. Suarez-Calvet, M. et al. Plasma phosphorylated TDP-43 levels are elevated in patients with frontotemporal dementia carrying a C9orf72 repeat expansion or a GRN mutation. *J. Neurol. Neurosurg. Psychiatry* **85**, 684–691 (2014).
11. Ren, Y. et al. TDP-43 and phosphorylated TDP-43 levels in paired plasma and CSF samples in amyotrophic lateral sclerosis. *Front. Neurol.* **12**, 663637 (2021).
12. Katisko, K. et al. Serum total TDP-43 levels are decreased in frontotemporal dementia patients with C9orf72 repeat expansion or concomitant motoneuron disease phenotype. *Alzheimers Res. Ther.* **14**, 151 (2022).
13. Scialo, C. et al. TDP-43 real-time quaking induced conversion reaction optimization and detection of seeding activity in CSF of amyotrophic lateral sclerosis and frontotemporal dementia patients. *Brain Commun.* **2**, fcaa142 (2020).
14. Beyer, L. et al. TDP-43 as structure-based biomarker in amyotrophic lateral sclerosis. *Ann. Clin. Transl. Neurol.* **8**, 271–277 (2021).
15. Hu, W. T. et al. Reduced CSF p-Tau181 to Tau ratio is a biomarker for FTLD-TDP. *Neurology* **81**, 1945–1952 (2013).
16. Irwin, K.E. et al. A fluid biomarker reveals loss of TDP-43 splicing repression in presymptomatic ALS-FTD. *Nat. Med.* **30**, 382–393 (2024).
17. Luk, C. et al. Development and assessment of sensitive immuno-PCR assays for the quantification of cerebrospinal fluid three- and four-repeat tau isoforms in tauopathies. *J. Neurochem.* **123**, 396–405 (2012).
18. Meredith, J. E. Jr et al. Characterization of novel CSF Tau and ptau biomarkers for Alzheimer's disease. *PLoS ONE* **8**, e76523 (2013).
19. Horie, K. et al. CSF tau microtubule-binding region identifies pathological changes in primary tauopathies. *Nat. Med.* **28**, 2547–2554 (2022).
20. van Niel, G., D'Angelo, G. & Raposo, G. Shedding light on the cell biology of extracellular vesicles. *Nat. Rev. Mol. Cell Biol.* **19**, 213–228 (2018).
21. Perez, M., Avila, J. & Hernandez, F. Propagation of tau via extracellular vesicles. *Front. Neurosci.* **13**, 698 (2019).
22. Leroux, E. et al. Extracellular vesicles: major actors of heterogeneity in tau spreading among human tauopathies. *Mol. Ther.* **30**, 782–797 (2022).
23. Wang, Y. et al. The release and trans-synaptic transmission of Tau via exosomes. *Mol. Neurodegener.* **12**, 5 (2017).
24. Asai, H. et al. Depletion of microglia and inhibition of exosome synthesis halt tau propagation. *Nat. Neurosci.* **18**, 1584–1593 (2015).
25. Iguchi, Y. et al. Exosome secretion is a key pathway for clearance of pathological TDP-43. *Brain* **139**, 3187–3201 (2016).
26. Stuendl, A. et al. Alpha-synuclein in plasma-derived extracellular vesicles is a potential biomarker of Parkinson's disease. *Mov. Disord.* **36**, 2508–2518 (2021).
27. Lionnet, A. et al. Characterisation of tau in the human and rodent enteric nervous system under physiological conditions and in tauopathy. *Acta Neuropathol. Commun.* **6**, 65 (2018).
28. Mukaetova-Ladinska, E. B. et al. Platelet Tau protein as a potential peripheral biomarker in Alzheimer's disease: an explorative study. *Curr. Alzheimer Res.* **15**, 800–808 (2018).
29. Kvetnoy, I. M. et al. Tau-protein expression in human blood lymphocytes: a promising marker and suitable sample for life-time diagnosis of Alzheimer's disease. *Neuro. Endocrinol. Lett.* **21**, 313–318 (2000).
30. Norman, M. et al. L1CAM is not associated with extracellular vesicles in human cerebrospinal fluid or plasma. *Nat. Methods* **18**, 631–634 (2021).
31. Boyarko, B. & Hook, V. Human tau isoforms and proteolysis for production of toxic tau fragments in neurodegeneration. *Front. Neurosci.* **15**, 702788 (2021).
32. Neumann, M. et al. Ubiquitinated TDP-43 in frontotemporal lobar degeneration and amyotrophic lateral sclerosis. *Science* **314**, 130–133 (2006).
33. Folstein, M. F., Folstein, S. E. & McHugh, P. R. 'Mini-Mental State'. A practical method for grading the cognitive state of patients for the clinician. *J. Psychiatr. Res.* **12**, 189–198 (1975).
34. Nasreddine, Z. S. et al. The Montreal Cognitive Assessment, MoCA: a brief screening tool for mild cognitive impairment. *J. Am. Geriatr. Soc.* **53**, 695–699 (2005).
35. Golbe, L. I. & Ohman-Strickland, P. A. A clinical rating scale for progressive supranuclear palsy. *Brain* **130**, 1552–1565 (2007).
36. Piot, I. et al. The Progressive Supranuclear Palsy Clinical Deficits Scale. *Mov. Disord.* **35**, 650–661 (2020).
37. Schwab R. S. & England, A. Projection technique for evaluating surgery in Parkinson's disease. in *Third Symposium on Parkinson's Disease* (eds Billingham, F. H. & Donaldson, M. C.) 152–157 (Churchill, 1969).
38. Guy, W. in *ECDEU Assessment Manual for Psychopharmacology—Revised.* DHEW Publ No ADM 76-338. (U.S. Dept. of Health, Education, and Welfare, Public Health Service, Alcohol, Drug Abuse, and Mental Health Administration, National Institute of Mental Health, Psychopharmacology Research Branch, Division of Extramural Research Programs, 1976).
39. Goetz, C. G. et al. Movement Disorder Society-sponsored revision of the Unified Parkinson's Disease Rating Scale (MDS-UPDRS): process, format, and clinimetric testing plan. *Mov. Disord.* **22**, 41–47 (2007).
40. Starkstein, S. E. et al. Reliability, validity, and clinical correlates of apathy in Parkinson's disease. *J. Neuropsychiatry Clin. Neurosci.* **4**, 134–139 (1992).
41. Schrag, A. et al. Measuring quality of life in PSP: the PSP-QoL. *Neurology* **67**, 39–44 (2006).
42. Pfeffer, R. I., Kurosaki, T. T., Harrah, C. H. Jr., Chance, J. M. & Filos, S. Measurement of functional activities in older adults in the community. *J. Gerontol.* **37**, 323–329 (1982).
43. Hughes, C. P., Berg, L., Danziger, W. L., Coben, L. A. & Martin, R. L. A new clinical scale for the staging of dementia. *Br. J. Psychiatry* **140**, 566–572 (1982).
44. Knopman, D. S., Weintraub, S. & Pankratz, V. S. Language and behavior domains enhance the value of the Clinical Dementia Rating Scale. *Alzheimers Dement.* **7**, 293–299 (2011).
45. Cummings, J. L. et al. The Neuropsychiatric Inventory: comprehensive assessment of psychopathology in dementia. *Neurology* **44**, 2308–2314 (1994).
46. Wear, H. J. et al. The Cambridge Behavioural Inventory revised. *Dement. Neuropsychol.* **2**, 102–107 (2008).
47. Neumann, M. et al. TDP-43 in the ubiquitin pathology of frontotemporal dementia with VCP gene mutations. *J. Neuropathol. Exp. Neurol.* **66**, 152–157 (2007).
48. Gijselinck, I. et al. Loss of TBK1 is a frequent cause of frontotemporal dementia in a Belgian cohort. *Neurology* **85**, 2116–2125 (2015).
49. Alcolea, D. et al. The Sant Pau Initiative on Neurodegeneration (SPIN) cohort: a data set for biomarker discovery and validation in neurodegenerative disorders. *Alzheimers Dement. (N Y)* **5**, 597–609 (2019).
50. Vaquer-Alicea, J., Diamond, M. I. & Joachimiak, L. A. Tau strains shape disease. *Acta Neuropathol.* **142**, 57–71 (2021).
51. Ritz, D. et al. Endolysosomal sorting of ubiquitylated caveolin-1 is regulated by VCP and UBXD1 and impaired by VCP disease mutations. *Nat. Cell Biol.* **13**, 1116–1123 (2011).

52. Zhang, Y. et al. Cerebellar Kv3.3 potassium channels activate TANK-binding kinase 1 to regulate trafficking of the cell survival protein Hax-1. *Nat. Commun.* **12**, 1731 (2021).
53. Schwickart, M., Vainshtein, I., Lee, R., Schneider, A. & Liang, M. Interference in immunoassays to support therapeutic antibody development in preclinical and clinical studies. *Bioanalysis* **6**, 1939–1951 (2014).
54. O'Brien, K., Ughetto, S., Mahjoum, S., Nair, A. V. & Breakefield, X. O. Uptake, functionality, and re-release of extracellular vesicle-encapsulated cargo. *Cell Rep.* **39**, 110651 (2022).
55. Ramos-Zaldivar, H. M. et al. Extracellular vesicles through the blood–brain barrier: a review. *Fluids Barriers CNS* **19**, 60 (2022).
56. Riva, N. et al. Phosphorylated TDP-43 aggregates in peripheral motor nerves of patients with amyotrophic lateral sclerosis. *Brain* **145**, 276–284 (2022).
57. Wood, J. D. Enteric nervous system: neuropathic gastrointestinal motility. *Dig. Dis. Sci.* **61**, 1803–1816 (2016).
58. James, B. D. et al. TDP-43 stage, mixed pathologies, and clinical Alzheimer's-type dementia. *Brain* **139**, 2983–2993 (2016).
59. Nelson, P. T. et al. Frequency of LATE neuropathologic change across the spectrum of Alzheimer's disease neuropathology: combined data from 13 community-based or population-based autopsy cohorts. *Acta Neuropathol.* **144**, 27–44 (2022).
60. Nelson, P. T. et al. Limbic-predominant age-related TDP-43 encephalopathy (LATE): consensus working group report. *Brain* **142**, 1503–1527 (2019).
61. Rohrer, J. D. et al. Serum neurofilament light chain protein is a measure of disease intensity in frontotemporal dementia. *Neurology* **87**, 1329–1336 (2016).
62. Gendron, T. F. et al. Comprehensive cross-sectional and longitudinal analyses of plasma neurofilament light across FTD spectrum disorders. *Cell Rep. Med.* **3**, 100607 (2022).
63. Katisko, K. et al. GFAP as a biomarker in frontotemporal dementia and primary psychiatric disorders: diagnostic and prognostic performance. *J. Neurol. Neurosurg. Psychiatry* **92**, 1305–1312 (2021).
64. Zhu, N. et al. Plasma glial fibrillary acidic protein and neurofilament light chain for the diagnostic and prognostic evaluation of frontotemporal dementia. *Transl. Neurodegener.* **10**, 50 (2021).

Madhurima Chatterjee[1,56], Selcuk Özdemir[1,2,56], Christian Fritz[1], Wiebke Möbius[3,4], Luca Kleineidam[1,5], Eckhard Mandelkow[5], Jacek Biernat[5], Cem Doğdu[1], Oliver Peters[6,7], Nicoleta Carmen Cosma[6], Xiao Wang[6], Luisa-Sophia Schneider[6], Josef Priller[6,8,9,10], Eike Spruth[8], Andrea A. Kühn[6,11], Patricia Krause[11], Thomas Klockgether[1,12], Ina R. Vogt[1], Okka Kimmich[1], Annika Spottke[1,12], Daniel C. Hoffmann[1], Klaus Fliessbach[1,5], Carolin Miklitz[1,5], Cornelia McCormick[1,5], Patrick Weydt[1], Björn Falkenburger[13,14], Moritz Brandt[13,14], René Guenther[13,14], Elisabeth Dinter[13,14], Jens Wiltfang[15,16,17], Niels Hansen[15,16], Mathias Bähr[15,18,19], Inga Zerr[15,18], Agnes Flöel[20,21], Peter J. Nestor[22,23], Emrah Düzel[22,24,25], Wenzel Glanz[22,24,26], Enise Incesoy[22,24,27], Katharina Bürger[28,29], Daniel Janowitz[29], Robert Perneczky[28,30,31,32], Boris S. Rauchmann[30,33,34], Franziska Hopfner[35], Olivia Wagemann[28,35], Johannes Levin[28,31,35], Stefan Teipel[21,36], Ingo Kilimann[21,36], Doreen Goerss[21], Johannes Prudlo[21,37], Thomas Gasser[38,39], Kathrin Brockmann[38,39], David Mengel[38,39], Milan Zimmermann[38,39], Matthis Synofzik[38,39], Carlo Wilke[38,39], Judit Selma-González[40,41], Janina Turon-Sans[41,42], Miguel Angel Santos-Santos[40,43], Daniel Alcolea[40,43], Sara Rubio-Guerra[40,43], Juan Fortea[40,43], Álvaro Carbayo[41,42], Alberto Lleó[40,43], Ricardo Rojas-García[41,42], Ignacio Illán-Gala[40,43], Michael Wagner[1,5], Ingo Frommann[1,5], Sandra Roeske[1], Lucas Bertram[1], Michael T. Heneka[44,45], Frederic Brosseron[1], Alfredo Ramirez[1,5,46,47,48], Matthias Schmid[1,49], Rudi Beschorner[38,50], Annett Halle[1,51], Jochen Herms[28,31,52], Manuela Neumann[38,50], Nicolas R. Barthélemy[53,54], Randall J. Bateman[53,54], Patrizia Rizzu[38], Peter Heutink[38], Oriol Dols-Icardo[40,43], Günter Höglinger[28,31,35], Andreas Hermann[21,55] & Anja Schneider[1,5] ✉

[1]German Center for Neurodegenerative Diseases (DZNE), Bonn, Germany. [2]Department of Genetics, Atatürk University, Erzurum, Turkey. [3]Department of Neurogenetics, Max Planck Institute for Multidisciplinary Sciences, Göttingen, Germany. [4]Cluster of Excellence 'Multiscale Bioimaging: from Molecular Machines to Networks of Excitable Cells' (MBExC), University of Göttingen, Göttingen, Germany. [5]Department of Old Age Psychiatry and Cognitive Disorders, University Hospital Bonn, University of Bonn, Bonn, Germany. [6]German Center for Neurodegenerative Diseases (DZNE), Berlin, Germany. [7]Charité – Universitätsmedizin Berlin, corporate member of Freie Universität Berlin and Humboldt-Universität zu Berlin, Institute of Psychiatry and Psychotherapy, Berlin, Germany. [8]Department of Psychiatry and Psychotherapy, Charité – Universitätsmedizin Berlin, Berlin, Germany. [9]Department of Psychiatry and Psychotherapy, Technical University of Munich School of Medicine, Munich, Germany. [10]University of Edinburgh and UK DRI, Edinburgh, UK. [11]Movement Disorder and Neuromodulation Unit, Department of Neurology, Charité – Universitätsmedizin Berlin, Berlin, Germany. [12]Department of Neurology, University of Bonn, Bonn, Germany. [13]German Center for Neurodegenerative Diseases (DZNE), Dresden, Germany. [14]Department of Neurology, University Hospital Carl Gustav Carus, Technische Universität Dresden, Dresden, Germany. [15]German Center for Neurodegenerative Diseases (DZNE), Göttingen, Germany. [16]Department of Psychiatry and Psychotherapy, University Medical Center Göttingen, University of Göttingen, Göttingen, Germany.

[17]Neurosciences and Signaling Group, Institute of Biomedicine (iBiMED), Department of Medical Sciences, University of Aveiro, Aveiro, Portugal. [18]Department of Neurology, University Medical Center, Georg August University, Göttingen, Germany. [19]Cluster of Excellence Nanoscale Microscopy and Molecular Physiology of the Brain (CNMPB), University Medical Center Göttingen, Göttingen, Germany. [20]Department of Neurology, University Medicine Greifswald, Greifswald, Germany. [21]German Centre for Neurodegenerative Diseases (DZNE), Rostock/Greifswald, Germany. [22]German Center for Neurodegenerative Diseases (DZNE), Magdeburg, Germany. [23]Queensland Brain Institute, University of Queensland and Mater Public Hospital, Brisbane, Queensland, Australia. [24]Institute of Cognitive Neurology and Dementia Research, Otto-von-Guericke University, Magdeburg, Germany. [25]Institute of Cognitive Neuroscience, University College London, London, UK. [26]Clinic for Neurology, University Hospital Magdeburg, Magdeburg, Germany. [27]Department of Psychiatry and Psychotherapy, University Hospital Magdeburg, Magdeburg, Germany. [28]German Center for Neurodegenerative Diseases (DZNE), Munich, Germany. [29]Institute for Stroke and Dementia Research, University Hospital, LMU Munich, Munich, Germany. [30]Department of Psychiatry and Psychotherapy, University Hospital, LMU Munich, Munich, Germany. [31]Munich Cluster for Systems Neurology (SyNergy) Munich, Munich, Germany. [32]Ageing Epidemiology Research Unit, School of Public Health, Imperial College London, London, UK. [33]Department of Neuroradiology, University Hospital LMU, Munich, Germany. [34]Sheffield Institute for Translational Neuroscience (SITraN), University of Sheffield, Sheffield, UK. [35]Department of Neurology, University Hospital of Munich, Ludwig-Maximilians-Universität (LMU) Munich, Munich, Germany. [36]Department of Psychosomatic Medicine, Rostock University Medical Center, Rostock, Germany. [37]Department of Neurology, Rostock University Medical Centre, Rostock, Germany. [38]German Center for Neurodegenerative Diseases (DZNE), Tübingen, Germany. [39]Hertie Institute for Clinical Brain Research, Department of Neurodegenerative Diseases, University of Tübingen, Tübingen, Germany. [40]Sant Pau Memory Unit, Department of Neurology, Institut de Recerca Sant Pau, Hospital de la Santa Creu i Sant Pau, Universitat Autònoma de Barcelona, Barcelona, Spain. [41]Motor Neuron Disease Clinic, Neuromuscular Diseases Unit, Institut de Recerca Sant Pau, Hospital de la Santa Creu i Sant Pau, Universitat Autònoma de Barcelona, Barcelona, Spain. [42]Centro de Investigación Biomédica en Red de Enfermedades Raras (CIBERER), Madrid, Spain. [43]Centro de Investigación Biomédica en Red de Enfermedades Neurodegenerativas (CIBERNED), Madrid, Spain. [44]Luxembourg Centre for Systems Biomedicine (LCSB), University of Luxembourg, Belvaux, Luxembourg. [45]Department of Infectious Diseases and Immunology, University of Massachussetss Medical School, North Worcester, MA, USA. [46]Excellence Cluster on Cellular Stress Responses in Aging-Associated Diseases (CECAD), University of Cologne, Cologne, Germany. [47]Division of Neurogenetics and Molecular Psychiatry, Department of Psychiatry, University of Cologne, Cologne, Germany. [48]Department of Psychiatry, Glenn Biggs Institute for Alzheimer's & Neurodegenerative Diseases, UT Health San Antonio, San Antonio, TX, USA. [49]Institute for Medical Biometry, Informatics and Epidemiology, University Hospital Bonn, Bonn, Germany. [50]Department of Neuropathology, University of Tübingen, Tübingen, Germany. [51]Department of Neuropathology, University Hospital Bonn, Bonn, Germany. [52]Center for Neuropathology and Prion Research, LMU Munich, Munich, Germany. [53]Department of Neurology, Washington University School of Medicine, St. Louis, MO, USA. [54]Tracy Family SILQ Center for Neurodegenerative Biology, St. Louis, MO, USA. [55]Translational Neurodegeneration Section 'Albrecht Kossel' and Center for Transdisciplinary Neurosciences, University Medical Center Rostock, Rostock, Germany. [56]These authors contributed equally: Madhurima Chatterjee, Selcuk Özdemir. ✉e-mail: anja.schneider@dzne.de

Methods

Patient samples

The DZNE Clinical Registry Study of Neurodegenerative Diseases (DESCRIBE) cohort is a multicentric, longitudinal observational study conducted by the German Center for Neurodegenerative Diseases (DZNE) and its clinical sites. It recruits patients with different neurodegenerative conditions, including ALS, bvFTD and PSP. Recruitment of these patients is described in more detail below. The multicenter, longitudinal Degeneration Controls and Relatives cohort (DANCER) serves to provide HCs for all DESCRIBE subcohorts. After written informed consent (University of Bonn Ethics Board statement 311/14) all participants undergo baseline and annual follow-up visits with clinical and neurological examination, cognitive assessments, 3T magnetic resonance imaging (MRI), blood and CSF sampling following identical standard operating procedures. Patients with AD dementia were recruited as part of the DESCRIBE cohort, following the National Institutes of Aging–Alzheimer's Association diagnosis criteria[65] and confirmed by positive CSF amyloid-beta, total tau and p-tau181 status.

The DESCRIBE cohort

The DESCRIBE ALS cohort. ALS patients were diagnosed according to the revised El Escorial Criteria[66]. Different motor phenotypes of ALS were classified as classical ALS, progressive bulbar paresis, flail arm, flail leg, progressive muscular atrophy, primary lateral sclerosis or genetic ALS. Participants were clinically characterized using the Amyotrophic Lateral Sclerosis Functional Rating Scale-revised[67]. The Edinburgh Cognitive and Behavioral ALS Screen[68] served as an additional test to identify cognitive and behavioral impairment. ALS patients with cognitive impairment, ALS with behavioral impairment, ALS with cognitive and behavioral impairment, ALS–FTD following the Strong criteria[69] and genetic ALS with a pathogenic FTD mutation also underwent the assessments of the DESCRIBE FTD cohort.

The DESCRIBE FTD cohort. Patients with bvFTD were diagnosed according to the revised Rascovsky criteria[70] by an experienced multidisciplinary team of neurologists, psychiatrists and neuropsychologists, and under consideration of MRI and CSF data, when available. Neuropsychological assessments included MMSE, the MoCA[58], Free and Cued Selective Reminding Test[71], the Neuropsychological battery of the Consortium to Establish a Registry for Alzheimer's Disease Plus test[72] including Trail Making Tests A and B and the mini-Social cognition & Emotional Assessment test[73]. Psychiatric scales included Geriatric Depression Scale[74], the brief questionnaire of the NPI-Q[45], and the functional scales CDR-SB, CDR plus NACC FTLD, FAQ[42] and a modification of the revised Cambridge Behavior Inventory[46], the CBI-M.

Patients with svPPA were diagnosed according to Gordon-Tempini criteria[75]. Baseline assessment of patients with PPA additionally included a modified version of the Camel and Cactus test[76], the visual form of the Sentence Comprehension Test[77], the Sentence Repetition Test from the Aachen Aphasia Test[78], hierarchical word lists[79] and the Repeat and Point Test[80].

The DESCRIBE PSP cohort. The cohort design is summarized in ref. 81. Diagnosis of PSP was based on the National Institute of Neurological Disorders and Stroke and the Society for PSP criteria[82] for participants recruited before 2017, and on the Movement Disorder Society (MDS-PSP) diagnostic criteria[83] for participants recruited after 2017. Participants were clinically phenotyped by the PSP-RS[35], PSP-SS[35], PSP-QoL[41], PSP-CDS[36], SEADL[37], MDS-UPDRS Part III[39], SAS[40], CGI-s[38], Geriatric Depression Scale[74] and MoCA[34].

The healthy control cohort DANCER. HC samples were obtained from DANCER and included 71 participants who, based on neuropsychological testing, neurological and psychiatric examination, do not suffer from a neurodegenerative disease. Participants additionally underwent MRI. The neuropsychological test battery follows the same protocol and includes all assessments as the one used for participants of the DESCRIBE FTD cohort. Participants undergo an annual follow-up as well as genetic testing at baseline (see below). Relatives with a known pathogenic FTD–ALS mutation were excluded as controls.

Genetics. All patients with a diagnosis of bvFTD, FTD–ALS, ALS with cognitive and or behavior impairment, and all control subjects were tested for pathogenic *C9orf72* hexanucleotide repeat expansions, for insertions or deletions in *MAPT* and *GRN* genes by multiplex ligation-dependent probe amplification and for other protein-coding variants by whole-exome sequencing. Specifically, expansions of the *C9orf72* GGGGCC hexanucleotide repeat were detected by the AmplideX PCR/CE C9orf72 kit (Asuragen) with a cut-off value of 30 repeats defining pathologically expanded repeats. For detection of deletions or duplications in *GRN* and *MAPT* genes we employed the SALSA multiplex ligation-dependent probe amplification kit (MRC-Holland). Participants with ALS and PSP were not systematically screened for mutations as part of the DESCRIBE study protocol. Our study sample contained 37 mutation carriers, including 18 *C9orf*, 4 *GRN*, 3 *MAPT*, 4 *VCP*, 2 *TBK1*, 2 *CHCHD10*, 2 *FUS* and 2 *SOD-1* cases (Supplementary Table 10).

DZNE Brain Bank postmortem cohort and neuropathological diagnosis. In the DZNE Brain Bank, autopsies and sampling of tissues for diagnostics and research is performed after written informed consent in accordance with local ethics review boards. Brain autopsies and neuropathological diagnosis were available for 31 participants from subcohort 2, consisting of 24 cases with a TDP-43 proteinopathy (ALS-TDP and FTLD-TDP, including 2 cases with *TBK1* mutation), 5 cases with a tau proteinopathy (PSP and FTLD-tau including 1 case with *MAPT* mutation), as well as 1 ALS with a mutation in *SOD-1* and 1 ALS case with a *CHCHD10* mutation (Supplementary Table 11).

Neuropathological evaluation was performed for all cases on formalin-fixed paraffin-embedded tissue sections from 20 standardized neuroanatomical regions following guidelines for the assessment and diagnosis of neurodegenerative diseases including immunohistochemistry with antibodies against phosphorylated TDP-43 (clone 1D3)[84], phosphorylated tau (clone AT8, Thermo Fisher), α-synuclein (clone 4D6, Origene) and beta-amyloid (clone 4G8, Covance). For all cases, assessment included reporting of AD neuropathological changes[85] and presence/regional distribution of Lewy pathology[86]. Cases with FTLD-TDP were subclassified according to current criteria[87].

The Sant Pau cohort

Patients with ALS were prospectively recruited from the Motor Neuron Disease Clinic at Hospital de la Santa Creu i Sant Pau. We included patients categorized as probable laboratory-supported or definite ALS according to El Escorial revised criteria[88]. ALSFRS-R in its Spanish version[89] was systematically assessed at the time of sample acquisition. Unimpaired HCs, bvFTD and PSP patients were recruited at the Sant Pau Memory Unit and include individuals from the Sant Pau Initiative on Neurodegeneration multimodal biomarker cohort. ALS–FTD patients were recruited by Sant Apu Memory Unit and Motor Neuron Disease Clinic. Information about clinical and neuropsychological assessments and sample processing have been previously described in detail[49]. Plasma samples were obtained using the same standard operating procedure. All patient samples (ALS, ALS–FTD, bvFTD and PSP) were screened for the presence of a pathogenic repeat expansion mutation in *C9orf72*. In addition, patients with ALS were tested for mutations in genes causing ALS, FTD and AD using a gene panel. bvFTD and PSP patients underwent whole-exome sequencing. In total, pathogenic mutations were found in *C9orf72* ($n = 16$), *GRN* ($n = 6$), *SOD1* ($n = 4$), *TBK1* ($n = 3$), *FUS* ($n = 3$), *TARDBP* ($n = 1$) and *VCP* ($n = 1$). This study was approved by the Hospital de la Santa Creu i Sant Pau Ethics Committee. Written informed consent was obtained from all participants.

EV isolation from plasma and CSF

EVs were prepared from EDTA plasma as described in ref. 26 by a blinded experimentator. Briefly, 500 µl of plasma was thawed on ice and subjected to serial centrifugation to isolate sEVs and mEVs. To remove cellular debris, plasma was centrifuged for 10 min at 4 °C and 3,500*g*, and twice at 4,500*g*. The supernatant was subsequently centrifuged for 30 min at 10,000*g* and 4 °C. The resulting pellet (mEV fraction) was resuspended in 100 µl of PBS, 1% CHAPS, whereas the supernatant was applied to size-exclusion columns equilibrated with 10 ml of 20 mM HEPES buffer (pH 7.4) to isolate sEVs (qEVoriginal, 70 nm+; Izon Science Limited). Using the Izon Automatic Fraction Collector and by adding 20 mM HEPES buffer (pH 7.4), we eluted 24 fractions with a volume of 500 µl. As shown previously[26], fractions 7–10 contain the highest EV concentrations without contamination by nonvesicular plasma proteins. We therefore pooled fractions 7–10 as the sEV fraction and subjected them to 4,000g centrifugation at 4 °C in an Amicon Ultra centrifugal filter with a 3-kDa cut-off (Merck Millipore) for 40 min at 20 °C to concentrate the sample. Subsequently, the volume was filled up with 10% CHAPS in a 20-mM HEPES to a final concentration of 1% CHAPS (300 µl). Samples were divided in three, stored at −20 °C until further analysis of tau and TDP-43 content. CSF EV for correlation analysis of CSF and plasma EV tau levels were prepared from all DESCRIBE subcohort 1 cases, following the same protocol as for plasma EVs, with a starting volume of 1.5 ml of CSF. We prepared CSF EV for correlation analysis with corresponding plasma EV TDP-43 levels for all ALS cases in DESCRIBE subcohort 2 for which CSF was available ($n = 41$). A starting volume of 1 ml of CSF was used. Of note, in all cases CSF was drawn at the same visit as plasma samples.

In all cohorts, we aimed for sex-balanced and age-balanced diagnostic groups. The sex of participants was determined based on self-report.

L1CAM immunocapture assay

Plasma (500 µl) was thawed on ice and subjected to serial centrifugation to isolate mEVs and sEVs as described above. mEVs were resuspended in 300 µl of PBS. sEV preparations were concentrated to a final volume of 300 µl, which was divided into three aliquots of 100 µl each. L1CAM immunoisolation from EV preparations was performed as described previously[90]. In brief, 100 µl of sEVs were diluted in 400 µl of double-distilled H_2O supplemented with protease and phosphatase inhibitors and 3% bovine serum albumin. Dilutions were incubated for 60 min with 2.7 µg of biotinylated mouse anti-human CD171 (L1CAM neural adhesion protein) antibody (clone 5G3; eBiosciences) at room temperature and under constant shaking at 800 rpm. For the IgG control condition, 2.7 µg of biotinylated mouse immunoglobulin G2 (IgG2) antibody (clone eBM2a; cat. no. 13-4724-85, Thermo Fisher Scientific) was added instead of anti-human CD171 antibody. Subsequently, 26 µl of streptavidin agarose Ultralink resin (Thermo Fisher Scientific) was added followed by 60 min of incubation at room temperature and shaking at 800 rpm. Solutions were centrifuged for 10 min at 800*g* at 4 °C and pellets were resuspended for 10 s in 50 µl of cold 0.1 M glycine–HCl (pH 3.0) followed by centrifugation at 4 °C and 4,500*g* for 5 min. The supernatant was transferred to tubes containing 50 µl of 3% bovine serum albumin in 1 M Tris–HCl (pH 8.0). Aliquots of 5, 15 and 80 µl were used for nanoparticle tracking analyzer (NTA), western blot and TDP-43 or tau analysis by SIMOA or electrochemiluminescence/Meso Scale discovery (MSD)/ELISA, respectively. Before TDP-43 and tau analysis, CHAPS was added at a final concentration of 1%.

Western blotting

Western blotting was performed according to standard protocols using 10% or 12% sodium dodecyl sulfate polyacrylamide gels, followed by transfer to polyvinylidene fluoride (PVDF) membranes (Millipore). PVDF membranes were blocked for 30 min in 4% w/v nonfat dried milk in TBS-Tween 0.5% v/v (TBS-T). Primary antibodies were incubated with the PVDF membrane overnight at 4 °C, and secondary antibodies for 1 h at room temperature. Protein bands were visualized using an ECL western blotting detection kit (GE Healthcare). The following antibodies were used. (1) Primary antibodies: anti-Calnexin (1:2,000 dilution; cat. no. C4731, Sigma-Aldrich), anti-Flotillin-2 (1:500 dilution; cat. no. 610384, BD Biosciences); anti-3R tau (RD3 anti 3R tau antibody; 1:500 dilution; cat. no. 05-803, Merck), anti-4R tau (anti-4R tau antibody; dilution 1:500; cat. no. ab218314, Abcam), and anti-TDP-43 antibody (dilution 1:500; cat. no. ab305694, Abcam). (2) Secondary antibodies: HRP antimouse IgG (1:5,000 dilution; Dako), HRP antirabbit IgG (1:5,000 dilution; Dako).

Nanoparticle tracking analyzer

NTA was performed with a NanoSight LM10 instrument and a LM14 viewing unit equipped with a 532 nm laser (NanoSight, Malvern Instruments) by a blinded experimentator. Samples were recorded in quadruplicates for 30 s and analyzed with the NTA 2.3 software.

Development of 3R and 4R isoform-specific tau immunoassays

We developed two sandwich immunoassays for the specific detection of 3R and 4R tau isoforms, using antibody pairs of isoform-specific tau antibodies with HT7, an antibody raised against an N-terminal, isoform-independent epitope (amino acids 159–163).

Detection of 3R and 4R tau in plasma EVs and the specificity of the antibodies was demonstrated by western blot analysis with recombinant 3R and 4R tau proteins (Supplementary Fig. 3a–e).

Optimal dilutions of capture and detection antibodies were standardized, using the checkerboard method with serially increasing dilutions of capture and detection antibodies, different dilution buffers, incubation times, temperatures and EV lysis methods. The reproducibility of each assay was tested by performing them at least three times with technical replicates. Immunoassay performance parameters such as precision, intra-assay and interassay variability, matrix effect, linearity and parallelism were determined for both 3R and 4R tau assays in plasma-derived sEVs and mEVs using three biological replicates (Supplementary Table 1).

3R tau immunoassay

Plasma sEV and mEV 3R tau were measured in duplicate, 50 µl per well, by a blinded experimentator. Briefly, 96-well multiarray plates (Meso Scale Discovery) were coated with RD3 anti-3R tau antibody (cat. no. 05-803, Merck) after 1:600 dilution in Dulbecco´s Phosphate Buffered Saline overnight at 4 °C. After washing three times with 0.05% Tween-20 in Dulbecco´s Phosphate Buffered Saline (PBST), plates were blocked at room temperature with 150 µl of blocking buffer per well for 1 h under shaking at 350 rpm. Protein standards were prepared from 3R recombinant tau (htau23) by serial 2× dilution in blocking buffer (7,000 pg ml^{-1} highest standard to 109.38 pg ml^{-1} lowest standard). Standards and samples were incubated at room temperature under shaking at 350 rpm for 2 h, followed by washing three times with PBST. Plates were then incubated for 1 h at room temperature with the detection antibody, biotinylated anti-total tau HT7 (product no. MN1000B, Thermo Fisher Scientific, epitope residues 159–163), at a 1:300 dilution in blocking buffer and under shaking at 350 rpm. After washing three times in PBST, 50 µl of sulfo-tagged streptavidin (Meso Scale Discovery) was added in a 1:300 dilution per well and incubated for 1 h at room temperature in the dark and under shaking at 350 rpm. Plates were then washed three times and each well was incubated with 150 µl of 2× MSD Reading Buffer T (Meso Scale Discovery). Plates were then measured using a Sector Imager 6000 and the MSD Discovery Workbench 3.0 Data Analysis Toolbox (Meso Scale Discovery).

4R tau immunoassay

Plasma sEV and mEV 4R tau were measured in duplicate, 50 µl per well, by a blinded experimentator. Plates (cat. no. DY008, Biotechne) were

incubated with capture antibody directed against 4R tau (Abcam 4R antibody; [EPR21725], cat. no. ab218314) in 100 µl of a 1:300 dilution in plate-coating buffer (R&D DY008 kit) for 18 hours at room temperature and under constant shaking at 150 rpm. After washing three times washing in 1× washing buffer (R&D DY008 kit), blocking buffer (10× diluted in dPBS, R&D blocking buffer, containing 0.1× HAMA blocker (cat. no. ab193969, Abcam)) was added to each well and the mixture was incubated at room temperature for 1 h under shaking at 350 rpm. Wells were subsequently washed three times in washing buffer. 4R tau standard was prepared from recombinant 4R tau (htau40) by serial dilution in blocking buffer (standard 1 (7,000 pg ml^{-1}) to standard 7 (109.48 pg ml^{-1})). Standard and samples were incubated for 2 h 20 min at room temperature under shaking at 350 rpm. After washing three times, wells were incubated under shaking at 350 rpm for 2 h at room temperature with detection antibody (biotinylated total tau HT7, 1:300 dilution in blocking buffer; product no. MN1000B, Thermo Fisher Scientific), followed by washing three times and incubation with streptavidin HRP (R&D Systems) for 30 min at room temperature in the dark with shaking at 350 rpm. Next, wells were washed three times and incubated for 15 min with substrate solution (R&D DY008 kit) and subsequently with stop solution. The plates were subsequently measured immediately using a BMG Fluostar ELISA reader.

TDP-43 SIMOA assay

TDP-43 levels were determined from plasma, plasma sEV and mEV fractions using the human TDP-43 Advantage kit on a SIMOA HD-X analyzer, software v.3.1 (Quanterix) by a blinded experimentator following the manufacturer's instructions. As per the product information, the assay was developed against TDP-43 amino acids 203–209 and the C-terminal region. Samples were thawed on ice and randomized on plates. Plasma samples were measured in duplicate, and sEV and mEV samples as singlets, 50 µl per well.

Plasma EV TDP-43 levels were sometimes low in the HC and PSP groups, with 28 sample measurements below the lower limit of quantification, most likely reflecting the absence of TDP-43 alterations in these groups. Such floor effects could be a limiting factor; however, they can be easily overcome by using larger plasma volumes (>500 µl) for sample preparation, if necessary.

Plasma NfL SIMOA assay

Plasma NfL concentrations were determined in duplicate, as previously described[91], using the SIMOA NF-light Advantage kit on a Quanterix HD1 analyzer (Quanterix) by a blinded experimenter according to the manufacturer's instructions.

Statistical analysis

Statistical analysis and data visualization were performed using Prism 7 (GraphPad Software), SPSS Statistics 21 (IBM) and R (R Foundation for Statistical Computing) software programs. The statistical tests were two-tailed and values with $P < 0.05$ were considered significant.

Comparisons of marker levels were performed using Kruskal–Wallis tests followed by Dunn's correction for multiple comparisons because of non-Gaussian distributions. Normal distribution assumption was assessed based on visual inspection of histograms and Kolmogorov–Smirnov tests.

To assess the link between EV marker and clinical scales as well as plasma NfL, Spearman correlations were used. To illustrate associations between plasma NfL and plasma EV 3R/4R tau ratio, plasma NfL and plasma EV /TDP-43, as well as plasma EV 3R/4R tau and plasma EV TDP-43 (Figs. 1, 2 and 4 and Supplementary Figs. 5, 7, 11 and 14), monotonic regression splines (using the 'cgam' function from R package 'splines') were modeled. Notably, potential confounders (age, sex and disease duration) showed no influence on plasma biomarker levels (Supplementary Tables 3 and 7). We therefore used the nonparametric tests described above with covariate adjustment to account for violations of normal distribution assumptions and nonlinear relationships.

MedCalc software was used for computation and comparison of ROC curves, using the method of Hanley and McNeil[92] (standard error, 95% CI for the difference and *P* value), as well as for calculation of sensitivity and specificity. Precision recall curves, area under the precision recall curve and CIs were calculated using the R code from ref. 93 and published prevalence estimates for the different diagnoses (PSP[94], ALS[95], bvFTD[96]).

The cut-off values of 3R/4R tau ratio and TDP-43 levels were defined with Gaussian mixture modeling using the R statistical software program v.3.2.1 mix tools package as previously described in ref. 42. First, the R boot.comp function was used to determine the number of distributions that fitted best to the data. Next, we defined data-driven cut-offs as the point at which the lines of fitted normal distributions crossed each other. Specifically, we derived three normal distributions (as suggested by bootstrapping) and determined the intersection of the middle normal distribution with the two more extreme distributions. We computed sensitivity and specificity based on the cut-offs of plasma sEV 3R/4R tau ratio and TDP-43 levels as determined by mixture modeling.

A description of the CBI-M, transmission electron microscopy, cell culture and small interfering RNA transfection, immunoprecipitation–mass spectrometry of tau, preparation of recombinant tau protein and assay validation are given in the Supplementary Methods.

Reporting summary

Further information on research design is available in the Nature Portfolio Reporting Summary linked to this article.

Data availability

The data that support the findings of this study are available from the authors but restrictions apply to the availability of these data, and so they are not publicly available. Data are, however, available from the authors upon reasonable request and with permission from the cohorts' steering committees (contact for and information on data access: anja.schneider@dzne.de). Expected turnover times for data applications is 3 months.

Code availability

The code used to conduct analyses is described in Methods.

References

65. Jack, C. R. Jr et al. NIA-AA research framework: toward a biological definition of Alzheimer's disease. *Alzheimers Dement.* **14**, 535–562 (2018).
66. Ludolph, A. et al. A revision of the El Escorial criteria - 2015. *Amyotroph. Lateral Scler. Frontotemporal Degener.* **16**, 291–292 (2015).
67. Cedarbaum, J. M. et al. The ALSFRS-R: a revised ALS functional rating scale that incorporates assessments of respiratory function. BDNF ALS Study Group (Phase III). *J. Neurol. Sci.* **169**, 13–21 (1999).
68. Abrahams, S., Newton, J., Niven, E., Foley, J. & Bak, T. H. Screening for cognition and behaviour changes in ALS. *Amyotroph. Lateral Scler. Frontotemporal Degener.* **15**, 9–14 (2014).
69. Strong, M. J. et al. Amyotrophic lateral sclerosis–frontotemporal spectrum disorder (ALS–FTSD): revised diagnostic criteria. *Amyotroph. Lateral Scler. Frontotemporal Degener.* **18**, 153–174 (2017).
70. Rascovsky, K. et al. Sensitivity of revised diagnostic criteria for the behavioural variant of frontotemporal dementia. *Brain* **134**, 2456–2477 (2011).
71. Lemos, R., Duro, D., Simoes, M. R. & Santana, I. The free and cued selective reminding test distinguishes frontotemporal dementia from Alzheimer's disease. *Arch. Clin. Neuropsychol.* **29**, 670–679 (2014).

72. Welsh, K. A. et al. The Consortium to Establish a Registry for Alzheimer's Disease (CERAD). Part V. A normative study of the neuropsychological battery. *Neurology* **44**, 609–614 (1994).
73. Bertoux, M. et al. Social cognition and emotional assessment differentiates frontotemporal dementia from depression. *J. Neurol. Neurosurg. Psychiatry* **83**, 411–416 (2012).
74. Scogin, F., Rohen, N. & Bailey, E. in *Handbook of Psychological Assessment in Primary Care Settings* (ed. Maruish M. E.) 491–508 (Erlbaum, 2000).
75. Gorno-Tempini, M. L. et al. Classification of primary progressive aphasia and its variants. *Neurology* **76**, 1006–1014 (2011).
76. Bozeat, S., Lambon Ralph, M. A., Patterson, K., Garrard, P. & Hodges, J. R. Non-verbal semantic impairment in semantic dementia. *Neuropsychologia* **38**, 1207–1215 (2000).
77. Billette, O. V., Sajjadi, S. A., Patterson, K. & Nestor, P. J. SECT and MAST: new tests to assess grammatical abilities in primary progressive aphasia. *Aphasiology* **29**, 1135–1151 (2015).
78. Huber, W., Poeck, K., Weniger, D. & Willmes, K. *Der Aachener Aphasie Test (AAT)* (Hogrefe, 1983).
79. Ziegler, W., Aichert, I., Staiger, A. & Schimeczek, M. HWL-kompakt. https://neurophonetik.de/sprechapraxie-wortlisten (2019).
80. Hodges, J. R., Martinos, M., Woollams, A. M., Patterson, K. & Adlam, A. L. Repeat and point: differentiating semantic dementia from progressive non-fluent aphasia. *Cortex* **44**, 1265–1270 (2008).
81. Respondek, G. & Hoglinger, G. U. *DescribePSP* and *ProPSP*: German multicenter networks for standardized prospective collection of clinical data, imaging data, and biomaterials of patients with progressive supranuclear palsy. *Front. Neurol.* **12**, 644064 (2021).
82. Litvan, I. et al. Clinical research criteria for the diagnosis of progressive supranuclear palsy (Steele–Richardson–Olszewski syndrome): report of the NINDS-SPSP international workshop. *Neurology* **47**, 1–9 (1996).
83. Hoglinger, G. U. et al. Clinical diagnosis of progressive supranuclear palsy: The movement disorder society criteria. *Mov. Disord.* **32**, 853–864 (2017).
84. Neumann, M. et al. Phosphorylation of S409/410 of TDP-43 is a consistent feature in all sporadic and familial forms of TDP-43 proteinopathies. *Acta Neuropathol.* **117**, 137–149 (2009).
85. Montine, T. J. et al. National Institute on Aging–Alzheimer's Association guidelines for the neuropathologic assessment of Alzheimer's disease: a practical approach. *Acta Neuropathol.* **123**, 1–11 (2012).
86. Attems, J. et al. Neuropathological consensus criteria for the evaluation of Lewy pathology in post-mortem brains: a multi-centre study. *Acta Neuropathol.* **141**, 159–172 (2021).
87. Mackenzie, I. R. et al. A harmonized classification system for FTLD-TDP pathology. *Acta Neuropathol.* **122**, 111–113 (2011).
88. Brooks, B. R., Miller, R. G., Swash, M., Munsat, T. L. & World Federation of Neurology Research Group on Motor Neuron Diseases El Escorial revisited: revised criteria for the diagnosis of amyotrophic lateral sclerosis. *Amyotroph. Lateral Scler. Other Motor Neuron Disord.* **1**, 293–299 (2000).
89. Campos, T. S. et al. Spanish adaptation of the revised Amyotrophic Lateral Sclerosis Functional Rating Scale (ALSFRS-R). *Amyotroph. Lateral Scler.* **11**, 475–477 (2010).
90. Eren, E. et al. Neuronal-derived EV biomarkers track cognitive decline in Alzheimer's disease cells. *Cells* **11**, 436 (2022).
91. Oender, D. et al. Evolution of clinical outcome measures and biomarkers in sporadic adult-onset degenerative ataxia. *Mov. Disord.* **38**, 654–664 (2023).
92. Hanley, J. A. & McNeil, B. J. A method of comparing the areas under receiver operating characteristic curves derived from the same cases. *Radiology* **148**, 839–843 (1983).
93. Boyd, K. et al. (eds) in *ECML PKDD 2013, Part III, LNAI 8190*, 451–466 (Springer, 2013).
94. Barer, Y. et al. Epidemiology of progressive supranuclear Palsy: Real world data from the second largest health plan in Israel.*Brain. Sci.* **12**, 1126 (2022).
95. Brown, C. A., Lally, C., Kupelian, V. & Flanders, W. D. Estimated Prevalence and Incidence of Amyotrophic Lateral Sclerosis and SOD1 and C9orf72 genetic variants. *Neuroepidemiology* **55**, 342–353 (2021).
96. Onyike, C. U. & Diehl-Schmid, J. The epidemiology of frontotemporal dementia. *Int Rev. Psychiatry* **25**, 130–137 (2013).

Acknowledgements

We thank the patients and their caregivers who participated in the study. This study was funded by a grant from the German Federal Ministry of Education and Research (BMBF), grant identifier 01KX2230, to A. Schneider. A. Schneider received funding from BMBF (DESCARTES consortium, grant identifier 01EK2102A, and PREPARE, grant identifier 01GP2213A), Verum Foundation and BMBF/NUM (UTN consortium). E.M. and A. Schneider received funding from Cure Alzheimer's Fund. C.D. and A. Schneider. received funding from Netzwerke NRW iBehave consortium. E.M. received funding from the Katharina Hardt Foundation. A. Schneider is member of the Deutsche Forschungsgemeinschaft (DFG)-funded Cluster of Excellence ImmunoSensation^2—EXC2151—390873048. A. Schneider and A.R. were supported by La Fundación Reina Sofía, proyecto 'MANOLO BARRÓS'. A. Schneider and A.H. received funding from the Target ALS Foundation. M.C. received funding from Deutsche Demenzhilfe German Center for Neurodegenerative Diseases (DZNE) Innovative Minds Program and the Manfred-Strohscheer Foundation. L.K. received funding from the Hertie Foundation, Hertie Network of Excellence in Clinical Neurosciences and from the EU Joint Programme—Neurodegenerative Disease Research (JPND), grant no. 01ED2007B (PreAdapt). M.W. and M. Schmid received funding from BMBF (DESCARTES consortium, grant identifier 01EK2102A). C. Miklitz received funding from the Neuro-aCSis clinician scientist program (DFG, project no. 493623632). N.H. has received funding support from the DFG (project no. 5302297989). F.H. was funded by the Else Kröner-Fresenius Foundation and the CurePSP Foundation. M. Synofzik was supported by the JPND GENFI-PROX grant (DLR/DFG 01ED2008B). D.M. and M. Synofzik were supported by the Clinician Scientist program 'PRECISE.net' funded by the Else Kröner-Fresenius-Stiftung. D.M. and M.Z. were supported by the Clinician Scientist Program of the Medical Faculty Tübingen (D.M., 459-0-0; M.Z., 481-0-0). D.M. was also supported by the Elite Program for Postdoctoral Researchers of the Baden Württemberg Foundation (1.16101.21). K. Brockmann has received research funding from the Michael J. Fox Foundation for Parkinson's Research (MJFF-022343, MJFF-023275, MJFF-023365), the German Society for Parkinson (DPG), the Health Forum Baden Wuerttemberg, the Else Kröner-Fresenius Stiftung (ClinbrAIn), the University of Tuebingen, and from the DFG (BR-655671-1). J.W. received funding from the BMBF (grant identifier 13GW0479B). R.P. is supported by the DFG (1007) under Germany's Excellence Strategy within the framework of 1008 the Munich Cluster for Systems Neurology (EXC 2145 SyNergy—ID 390857198), the Davos Alzheimer's Collaborative, the VERUM Foundation, the Robert Vogel Memorial Foundation, the National Institutes for Health and Care Research (NIHR) Sheffield Biomedical Research Centre (NIHR203321), the University of Cambridge–Ludwig-Maximilians-University Munich Strategic Partnership within the framework of the German Excellence Initiative and Excellence Strategy and the European Commission under the Innovative Health Initiative program (project no. 101132356) R.R.-G. has been funded by Instituto de Salud Carlos III (ISCIII) through project no. PI23/00845, co-funded by European Regional Development Fund/European Social Fund (ERDF/ESF), 'A way to make Europe'/'Investing

in your future'. M.A.S.-S. is supported by funding from the ISCIII (Juan Rodés research grant no. JR18-00018; Fondo de investigación sanitaria grant no. PI19/00882), the Alzheimer's Association clinician scientist fellowship (AACSF-22-972945), and the National Institutes of Health (R01AG080470). D.A. received research grants from ISCIII, Spain PI18/00435, PI22/00611, INT19/00016, INT23/00048, and from the Department of Health Generalitat de Catalunya PERIS program SLT006/17/12. I.I.-G. is a senior Atlantic Fellow for Equity in Brain Health at the Global Brain Health Institute (GBHI), and receives funding from the GBHI, the Alzheimer's Association and the Alzheimer's Society (GBHI ALZ UK-21-720973 and AACSF-21-850193). I.I.-G. was also supported by the Juan Rodés Contract (JR20/0018) and PI21/00791 from ISCIII. O.D.-I. is funded by The Association for Frontotemporal Degeneration (Clinical Research Postdoctoral Fellowship, AFTD 2019–2021). This work was supported by research grants from FUNDELA ('Por un mundo sin ELA') and ISCIII, Spain PI18/00326 and PI21/01395 to O.D.-I. S.R.-G. received funding from Alzheimer's Association (grant no. AACSF-21-850193). G.H. was funded by the DFG under Germany's Excellence Strategy within the framework of the Munich Cluster for Systems Neurology (EXC 2145 SyNergy—ID 390857198), DFG (HO2402/18-1 MSAomics). A. Hermann is supported by the Hermann und Lilly Schilling Stiftung für medizinische Forschung im Stifterverband.

Author contributions

A. Schneider initiated this work and supervised the study. A.S., M.C. and S.Ö. drafted the paper. O.P., N.C.C., X.W., L.-S.S., J. Priller, E.S., A.K., P.K., T.K., I.R.V., A. Spottke, D.C.H., K.F., C. Miklitz, C. McCormick, P.W., B.F., M. Bähr, J.W., N.H., M. Brandt, I.Z., A.G., A.F., E. Dinter, W.G., K. Bürger, D.J., R.P., B.S.R., F.H., O.W., J.L., S.T., I.K., J. Prudlo, T.G., K. Brockmann, D.M., M.Z., M. Synofzik, C.W., O.K., R.G., E. Dübel, E.I., D.G., I.I.-G., R.R.-G., A.L., A.C., J.F., S.R.-G., D.A., M.A.S.-S., J.T.-S., J.S.-G., O.D.-I., G.H., A. Hermann and A. Schneider collected the blood samples and patient data. M.W., I.F., S.R. and L.B. collected the neuropsychological data. M. Schmid contributed to CSF biomarker cut-off data. M.T.H. and F.B. analyzed CSF biomarker data. C.F., S.Ö., M. Chatterjee, C.D., M. Schmid and L.K. analyzed the biomarker and clinical data. M.N., A. Halle, J.H. and R.B. performed neuropathological diagnosis and provided data. A.R., P.R. and P.H. collected and analyzed the genetic data in DESCRIBE. O.D.-I. collected and analyzed the genetic data in the Sant Pau cohort. C.F., S.Ö. and M. Chatterjee conducted and analyzed the laboratory, cell culture and biochemistry work. W.M. performed electron microscopy analysis. E.M. and J.B. contributed recombinant tau protein. N.R.B. and R.J.B. performed immunoprecipitation–mass spectrometry on CSF and blood EV tau. S.Ö. and M. Chatterjee are equal contributors listed as first coauthors. A. Schneider is the senior and corresponding author.

Funding

Open access funding provided by Deutsches Zentrum für Neurodegenerative Erkrankungen e.V. (DZNE) in der Helmholtz-Gemeinschaft.

Competing interests

All authors had access to the data in the study and accepted responsibility for submitting the paper for publication. A. Schneider serves in a scientific advisory board for and receives honoraria from Biogen. She additionally received funding for a scientific collaboration from Eisai and honoraria for presentations from Eisai. M.C. is currently an employee of uniQure Biopharma B.V. and recipient of employee stock options. F.H. receives author fees from Thieme medical publishers and W. Kohlhammer GmbH medical publishers. P.H. is an employee and owns stock in Alector LLC. K. Brockmann is a consultant for F. Hoffmann-La Roche Ltd, Vanqua Bio and the Michael J. Fox Foundation for Parkinson's Research and has received speaker honoraria from AbbVie, Lundbeck, UCB (Union Chimique Belge) and Zambon. N.H. has received travel support from Eli Lilly. A. Hermann has received honoraria for presentations and participation in advisory boards from Amylyx and IFT Pharma. He has received royalities from Elsevier Press and Kohlhammer. Washington University and R.J.B. have equity ownership interest in C2N Diagnostics and R.J.B. receives income from C2N Diagnostics for serving on the scientific advisory board. R.J.B. and N.R.B. may receive income based on technology (methods to detect microtubule binding region (MTBR) tau isoforms and use thereof) licensed by Washington University to C2N Diagnostics. R.J.B. has received research funding from Avid Radiopharmaceuticals, Janssen, Roche/Genentech, Eli Lilly, Eisai, Biogen, AbbVie, Bristol Myers Squibb and Novartis. R.J.B. serves on the Roche Gantenerumab Steering Committee as an unpaid member. R.G. received speaker fees and nonfinancial support from Biogen, Roche, Zambon and research support from Biogen, ITF Pharma and Zambon outside this work. D.A. participated in advisory boards from Fujirebio-Europe, Roche Diagnostics, Grifols S.A. and Lilly, and received speaker honoraria from Fujirebio-Europe, Roche Diagnostics, Nutricia, Krka Farmacéutica S.L., Zambon S.A.U. and Esteve Pharmaceuticals S.A. D.A. declares a filed patent application (WO2019175379 A1 Markers of synaptopathy in neurodegenerative disease). J.W. received lecture honoraria from Beeijing Yibai Science and Technology Ltd, Gloryren, Janssen Cilag, Pfizer, Med Update GmbH, Roche Pharma, Lilly and serves on advisory boards for Biogen, Abbott, Boehringer Ingelheim, Lilly, MSD Sharp & Dohme and Roche. M. Brandt received speaker honoraria from Idorsia, Eisai and Bristol Myers Squibb. All other authors state no competing interests.

Additional information

Extended data is available for this paper at https://doi.org/10.1038/s41591-024-02937-4.

Supplementary information The online version contains supplementary material available at https://doi.org/10.1038/s41591-024-02937-4.

Correspondence and requests for materials should be addressed to Anja Schneider.

Peer review information *Nature Medicine* thanks the anonymous reviewers for their contribution to the peer review of this work. Primary Handling Editor: Jerome Staal, in collaboration with the *Nature Medicine* team.

https://doi.org/10.1038/s41591-024-02937-4

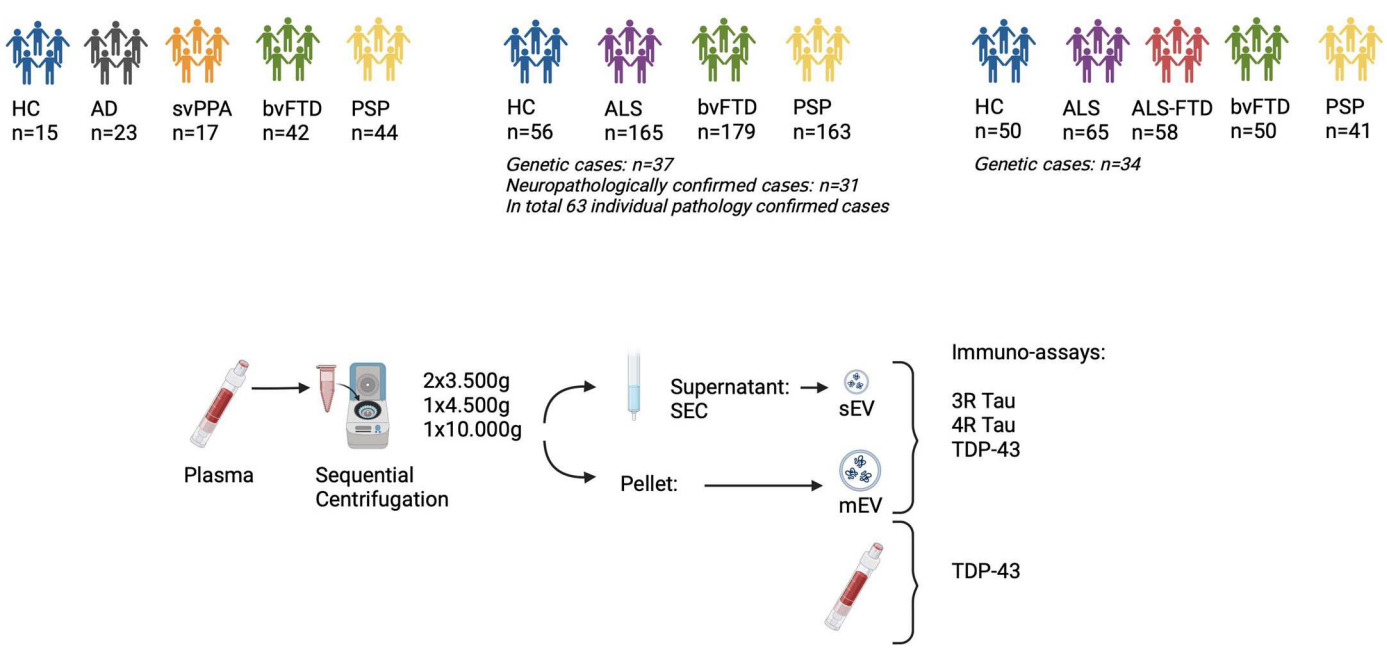

Extended Data Fig. 1 | Study Design. Pilot study with samples from the DESCRIBE cohort (subcohort 1): HC, AD, svPPA, bvFTD, PSP groups, based on clinical diagnosis and supported by CSF biomarkers in AD; detection of plasma EV 3R/4R Tau. Validation study in the larger DESCRIBE subcohort 2, comprising samples of the DESCRIBE cohort with HC, ALS, bvFTD and PSP groups and 63 pathology confirmed samples: detection of plasma EV 3R/4R Tau ratios, plasma EV TDP-43 levels, and plasma TDP-43 concentrations. Validation of plasma EV Tau ratios, and plasma EV TDP-43 levels in the independent Sant Pau cohort, including HC, ALS, ALS-FTD, bvFTD, and PSP as diagnostic groups with altogether 34 genetically confirmed samples. Lower panel: Experimental flow of sEV and mEV preparation. This figure was created using BioRender.com.

https://doi.org/10.1038/s41591-024-02937-4

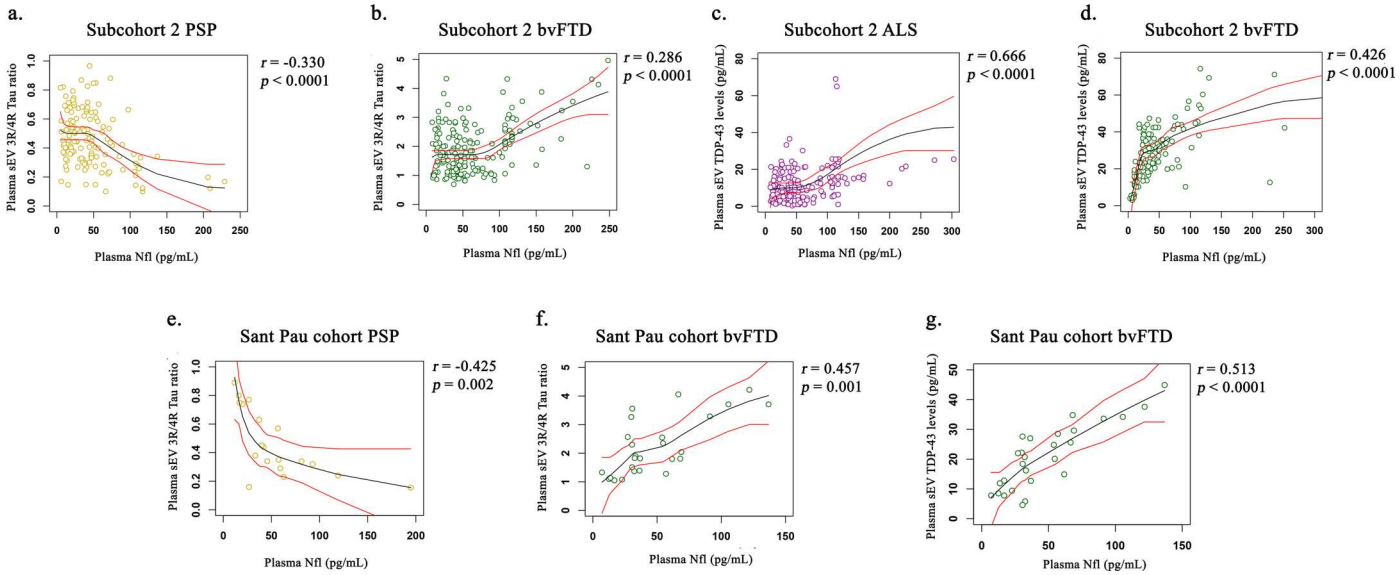

Extended Data Fig. 2 | Correlation of plasma EV Tau ratio with NfL in DESCRIBE cohort 2 and Sant Pau cohort. (**a**-**d**) Two-sided Spearman correlation analysis of associations and monotonic regression splines between plasma sEV 3R/4R Tau ratios and plasma Nfl levels in (**a**) PSP ($p = 0.000012$) and (**b**) bvFTD ($p = 0.000051$) diagnostic groups. Spearman correlation analysis of associations and monotonic regression splines between plasma sEV TDP-43 levels and plasma Nfl levels in (**c**) ALS ($p = 0.000046$) and (**d**) bvFTD ($p = 0.000063$). (**e**-**g**) **Sant Pau cohort:** Spearman correlation analysis of associations and monotonic regression splines between plasma sEV 3R/4R Tau ratio and plasma Nfl levels in (**e**) PSP and (**f**) bvFTD. Spearman correlation analysis of associations and monotonic regression splines between plasma sEV TDP-43 and plasma Nfl levels in (**g**) bvFTD ($p = 0.000085$). (NfL measurements were only available for a subset of Sant Pau cases).

https://doi.org/10.1038/s41591-024-02937-4

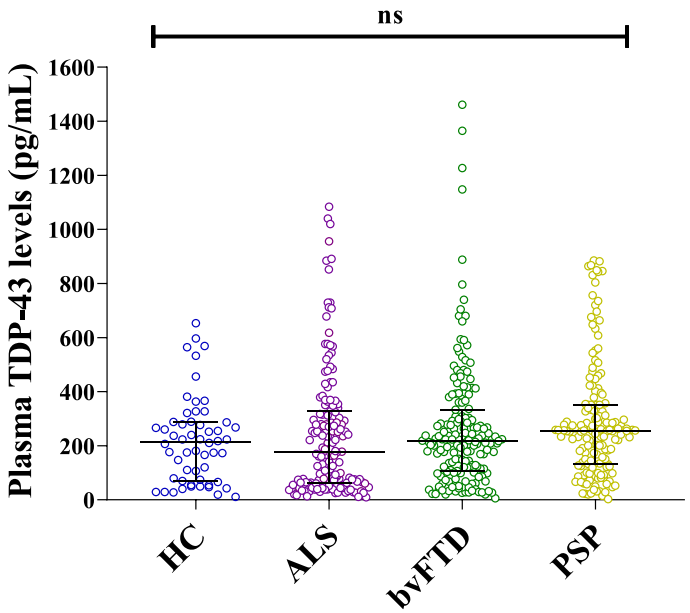

Extended Data Fig. 3 | Plasma TDP-43 levels in DESCRIBE subcohort 2. (biologically independent samples: HC n = 56, ALS n = 165, bvFTD n = 179, PSP n = 163). The long horizontal line represents the median and the short horizontal lines represent the inter-quartile range (IQR) Kruskal–Wallis test with Dunn's correction for multiple comparisons. ns: non-significant.

https://doi.org/10.1038/s41591-024-02937-4

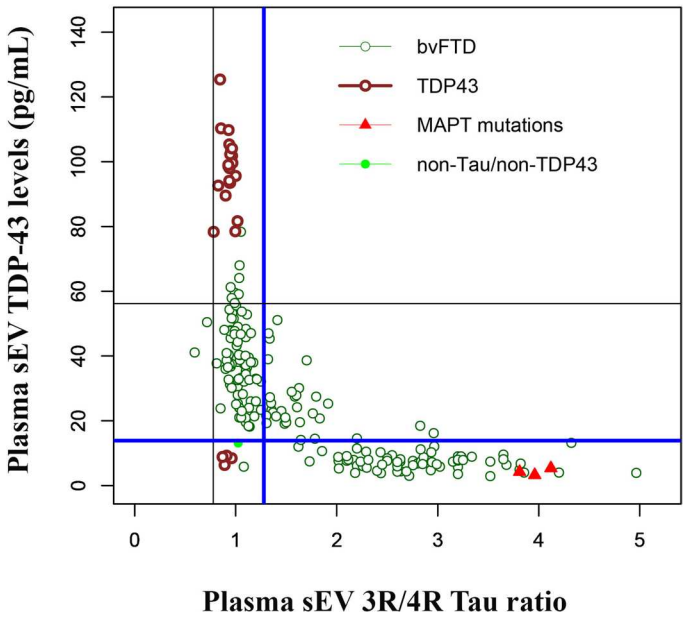

Extended Data Fig. 4 | Plasma sEV 3R/4R Tau ratio versus plasma EV TDP-43 levels in bvFTD cases of DESCRIBE subcohort 2. Genetically or neuropathologically defined bvFTD cases are indicated by the different color-codes. Cut-off values as determined by Gaussian mixture modeling for subcohort 2 (Fig. 4, Supplementary Fig. 15). The two cut-offs for separation of bvFTD into putative TDP-43 and Tau pathology groups are indicated by bold blue lines (sEV 3R/4R Tau ratio cut-off: 1.27; sEV TDP-43 cut-off: 13.87 pg/ml).

https://doi.org/10.1038/s41591-024-02937-4

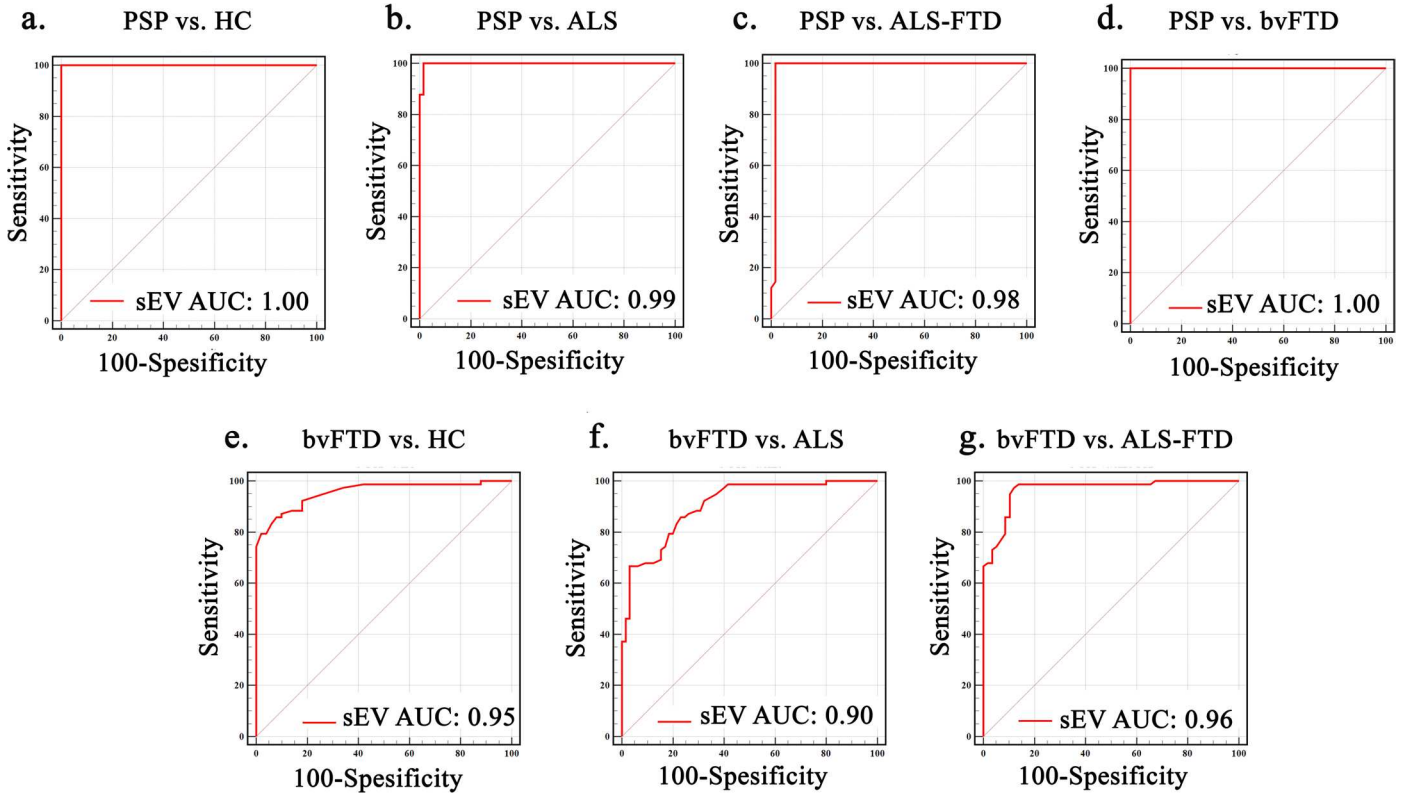

Extended Data Fig. 5 | Sant Pau cohort, Receiver Operating Characteristic (ROC) curves for plasma sEV 3R/4R Tau ratios. (**a**) PSP vs. HC (**b**) PSP vs. ALS (**c**) PSP vs. ALS-FTD (**d**) PSP vs. bvFTD (**e**) bvFTD vs. HC (**f**) bvFTD vs. ALS (**g**) bvFTD vs. ALS-FTD.

https://doi.org/10.1038/s41591-024-02937-4

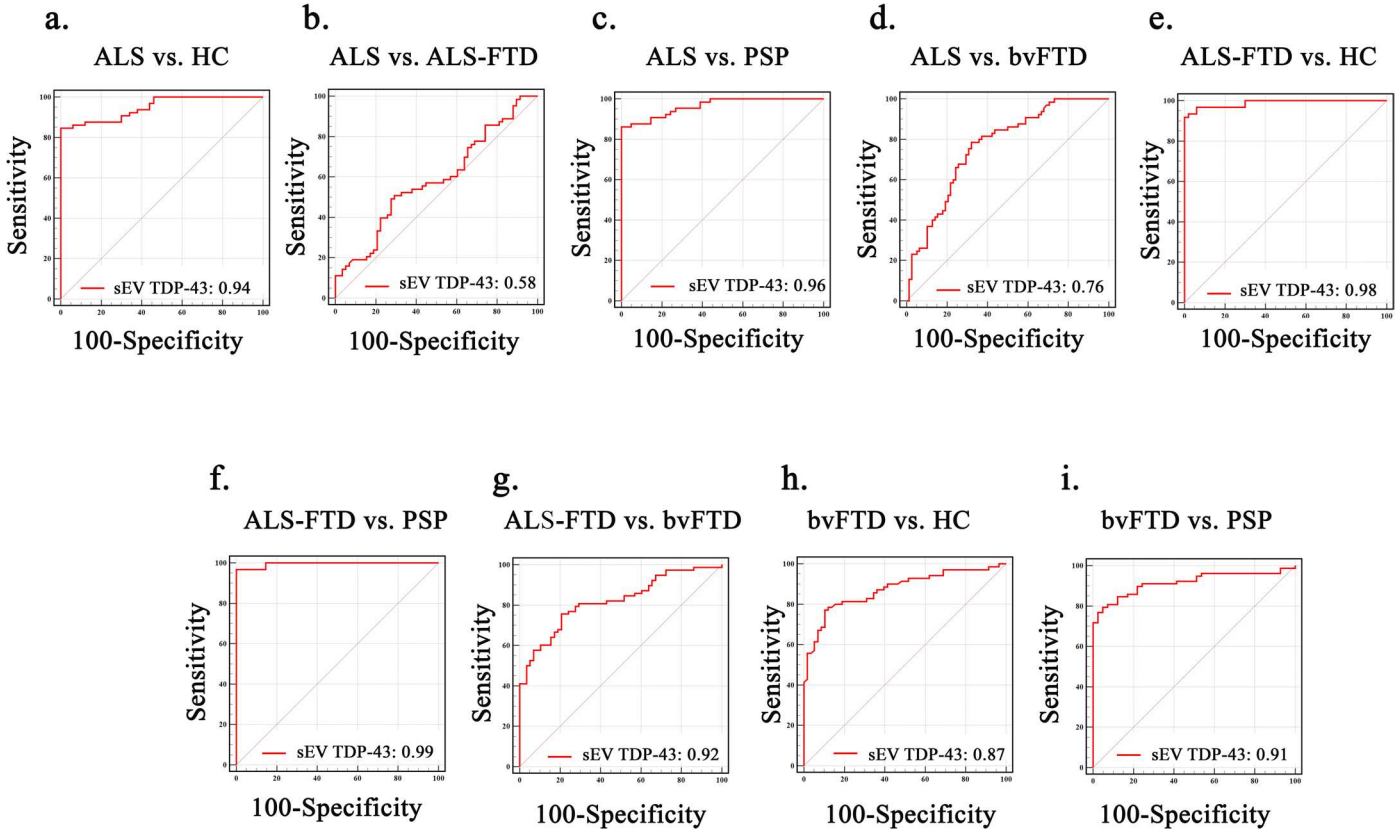

Extended Data Fig. 6 | Receiver Operating Characteristic (ROC) curve with AUC values for plasma sEV TDP-43 in Sant Pau cohort. (**a**) ALS vs. HC (**b**) ALS vs. ALS-FTD (**c**) ALS vs. PSP (**d**) ALS vs. bvFTD (**e**) ALS-FTD vs. HC (**f**) ALS-FTD vs. PSP (**g**) ALS-FTD vs. bvFTD (**h**) bvFTD vs. HC (**i**) bvFTD vs. PSP.

https://doi.org/10.1038/s41591-024-02937-4

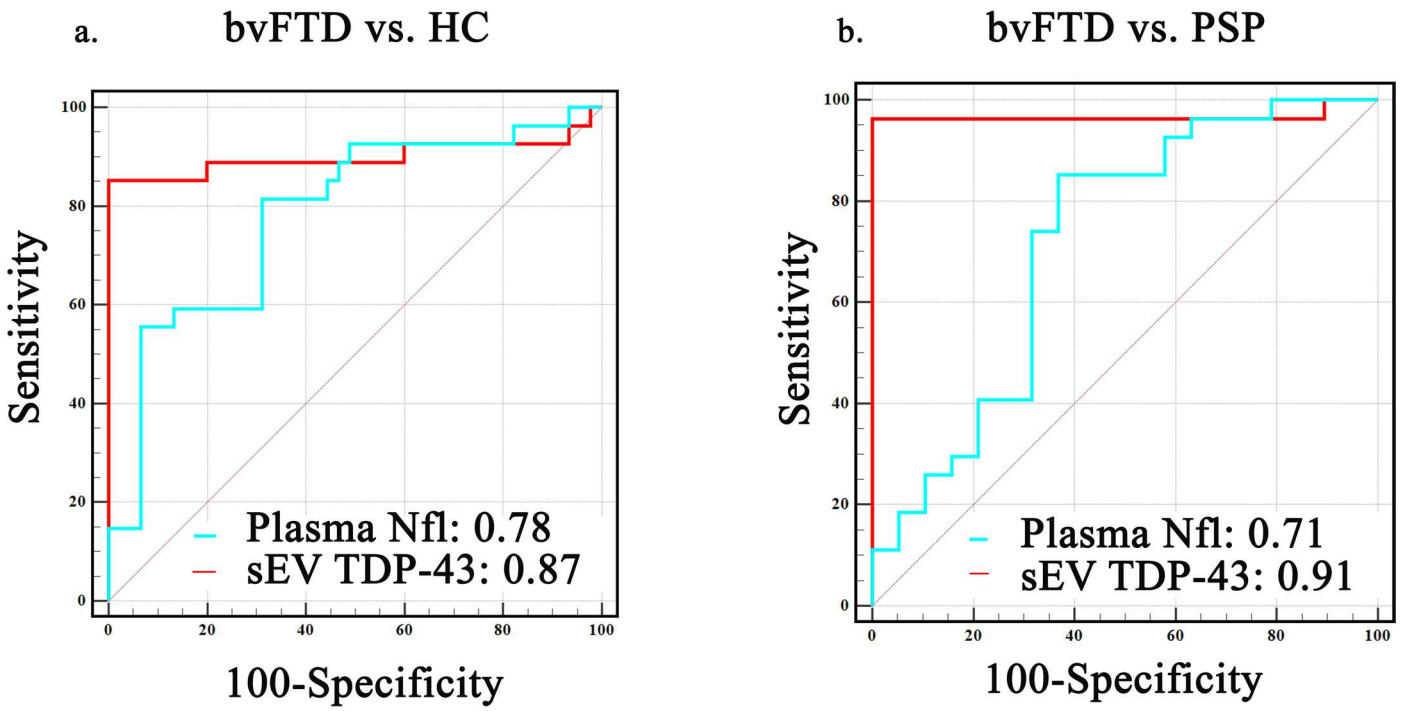

Extended Data Fig. 7 | Receiver Operating Characteristic (ROC) curve with AUC values for plasma sEV TDP-43 (red) and plasma NfL (blue) in the Sant Pau cohort. (**a**) bvFTD vs. HC and (**b**) bvFTD vs. PSP. Plasma NfL levels were not available for ALS and ALS-FTD groups.

https://doi.org/10.1038/s41591-024-02937-4

Extended Data Table 1 | Demographic and Clinical Characteristics of All Patients in DESCRIBE subcohort 1

Characteristic	DESCRIBE subcohort 1				
Groups	HC	AD	svPPA	bvFTD	PSP
n (total 704)	15	23	17	42	44
Sex	f=7 m=8	f=15 m=8	f=12 m=5	f=14 m=28	f=19 m=25
Age (mean ± SD)	65±7 [a]	72 ± 6	68±5	61 ± 10	66 ± 8
Disease duration (median [IQR])	NA	4.0[2.0-4.5] [g]	4.5 [3.0-5.0]	5.5[2.0-5.0]	2.0[1.0-3.0]
Aβ1-42 (pg/ml)(median[IQR])(n=494)	1268[863-1463] [a,b,c,d]	528[463-854] [e,f,g]	612[425-762]	665[416-789]	662[285-805]
Aβ42/40 (mean ± SD) (n=501)	0.15±0.23 [a]	0.042±0.1	0.1±0.2	0.096±0.12	0.11±1.3
tTau (pg/ml)(median[IQR]) (n=423)	165[147-209] [a,b,c,d]	385[263-412] [e,f,g]	309 [240-390]	312 [251-389]	306[157-365]
pTau (pg/ml)(median[IQR]) (n=354)	45[35-44] [a,b,c,d]	88[54-119) [e,f,g]	75[56-109]	65[46-115]	67[44-86]
MMSE (mean ± SD)(n=541)	28 ± 2 [a,c]	22 ± 2 [e,f,g]	25 ± 4	24 ± 5	25 ± 8
MoCA (mean ± SD) (n=114)	27±2 [a,c,d]	19±1 [e,f]	24±5	21±2	23±2
NPI-Q (mean ± SD) (n=203)	3±0.6 [a,b,c,d]	18±3 [f]	21±1	24.2±2	21±1
FAQ (mean ± SD) (n=612)	2±0.4 [a,b,c,d]	21±4	21±3	22±2	20±1
CDR-SB (mean ± SD) (n=259)	0.5±0.8 [a,b,c]	15±2 [e, f, g]	12±2	11.5±3	10.5±4
CDR plus NACC FTLD (mean ± SD) (n=134)	0.5±0.65 [c]	NA	NA	10.2±2.5	NA
CBI-M (mean ± SD) (n=189)	0.34±0.1 [c]	NA	NA	1.37±0.86	NA
PSP-RS (mean ± SD) (n=194)	NA	NA	NA	NA	29.45±14.8
PSP-SS (mean ± SD) (n=190)	NA	NA	NA	NA	2.61±1.18
PSP-CDS (mean ± SD) (n=77)	NA	NA	NA	NA	18.6±2.5
UPDRS III (mean ± SD) (n=195)	NA	NA	NA	NA	32.10±17.93
SAS (mean ± SD) (n=179)	NA	NA	NA	NA	21±8.52
SEADL (mean ± SD) (n=200)	NA	NA	NA	NA	55.58±27.97
CGIs (mean ± SD) (n=192)	NA	NA	NA	NA	3.61±1.59
FAB (mean ± SD) (n=175)	NA	NA	NA	NA	6.51±5.41
PSP-QoL (mean ± SD) (n=184)	NA	NA	NA	NA	38.52±18.46
Plasma Nfl (pg/mL)(median[IQR]) (n=755)	11.7[8.65-13.56] [a,b,c,d]	33.45[28.5-56.89]	27.15[12-39]	32.45[22-41]	29.48[18-41]
sEV 3R Tau (pg/mL)(median[IQR])	329.4 [293.1-379.4] [c,d]	328.4[239.4-384.8] [d,e]	312.0 [233.6-384.9]	684.1[591.9-888.8] [j]	91.20[61.34-150.2]
sEV 4R Tau (pg/mL)(median[IQR])	287.7[272.1-340.2] [c,d]	307.3[260.3-482.5] [e]	295.8[236.5-356.1]	270.2 [211.8-381.6] [j]	448.9[332.2-775.8]
sEV 3R/4R Tau ratio(median[IQR])	1.16[0.99-1.29] [c,d]	0.91[0.58-1.25] [f,g]	0.99[0.98-1.11] [h, i]	2.59 [2.02-3.87] [j]	0. 18[0.13-0.29]

[a] HC versus AD $p < 0.0001$
[b] HC versus svPPA $p < 0.0001$
[c] HC versus bvFTD $p < 0.0001$
[d] HC versus PSP $p < 0.0001$

[e] AD versus svPPA $p < 0.0001$
[f] AD versus bvFTD $p < 0.0001$
[g] AD versus PSP $p < 0.0001$
[h] svPPA versus bvFTD $p < 0.0001$
[i] svPPA versus PSP $p < 0.0001$
[j] bvFTD versus PSP $p < 0.0001$
Kruskal-Wallis test with Dunn's correction for multiple comparisons.

Abbreviations: AD (Alzheimer's disease); svPPA (semantic variant Primary Progressive Aphasia); ALS (amyotrophic lateral sclerosis); bvFTD (behavioral variant frontotemporal dementia); PSP (progressive supranuclear palsy); MMSE (Mini-Mental State Examination); MoCA (Montreal Cognitive Assessment); NPI-Q (The Neuropsychiatric Inventory–Questionnaire); FAQ (The Functional Activities Questionnaire); PSP-RS (Progressive Supranuclear Palsy Rating Scale), PSP-SS (Progressive Supranuclear Palsy Staging System Score); PSP-CDS (The Progressive Supranuclear Palsy Clinical Deficits Scale); UPDRS III (Unified Parkinson's Disease Rating Scale III); SEADL (The Schwab and England Activities of Daily Living); CGIs (Clinical Global Impression-Severity scale), FAB (Frontal Assessment Battery); PSP-QoL (Health-Related Quality of Life Questionnaire for Patients); CDR-SB (sum of the boxes score of the 6 domains of the Clinical Dementia Rating Scale); CDR plus NACC FTLD (Clinical Dementia Rating Scale plus behavior/comportment and language domains); CBI-M (The Cambridge Behavioural Inventory Modified Version); IQR (Inter-Quartile Range); NA (not applicable). Cut-off values for normal and abnormal concentrations of Aß42 (< 496 pg/ml), tTau (> 470 pg/ml), pTau (> 57 pg/ml), and Aβ42/40 ratio (< 0.09) (DELCODE/Bonn).

Demographic and Clinical Characteristics of All Patients in DESCRIBE subcohort 1.

https://doi.org/10.1038/s41591-024-02937-4

Extended Data Table 2 | Demographic and Clinical Characteristics of All Patients in DESCRIBE subcohort 2

Characteristic	DESCRIBE subcohort 2			
Groups	HC	ALS	bvFTD	PSP
n (total 704)	56	165	179	163
Sex	f=31 m=25	f=68 m=97	f=95 m=84	f=82 m=81
Age (mean ± SD)	68±7[a]	61 ± 3	65 ± 8	67 ± 9
Disease duration (median [IQR])	NA	2.0[1.0-3.5][d]	5.0[3.0-6.0]	3.0[3.0-5.0]
Aβ1-42 (pg/ml)(median[IQR])(n=494)	1021[797.8-1288] [a,b,c]	515.3[381.3-642.2]	658.6 [406.5-843.6]	657.9[239.9-832.7]
Aβ42/40 (mean ± SD) (n=501)	0.12±0.18	0.11±0.12	0.098±0.19	0.13±0.08
tTau (pg/ml)(median[IQR]) (n=423)	184[156-202] [a,b,c]	302[243-408]	358[245-366]	318[163-367]
pTau (pg/ml)(median[IQR]) (n=354)	48.6[26.1-41.2] [a,b,c]	61.3[52.4-96.1)	67.7 [45.7-112.8]	65.2[43.6-92.8]
MMSE (mean ± SD)(n=541)	28 ± 5 [a,b,c]	24 ± 4	24 ± 3	24 ± 6
MoCA (mean ± SD) (n=114)	26±4 [a,b]	21±2	20±1	24±1
NPI-Q (mean ± SD) (n=203)	2±2 [a,b,c]	20±2	23±1	20±2
FAQ (mean ± SD) (n=612)	4±1 [a,b,c]	22±2	23±3	22±4
CDR-SB (mean ± SD) (n=259)	0.5±0.2 [a,b,c]	8±1	13.5±2	11±4
CDR plus NACC FTLD (mean ± SD) (n=134)	0.5±0.3 [b]	NA	12.5±1	NA
CBI-M (mean ± SD) (n=189)	0.29±0.03 [b]	NA	1.49±0.5	NA
PSP-RS (mean ± SD) (n=194)	NA	NA	NA	35.47±14.4
PSP-SS (mean ± SD) (n=190)	NA	NA	NA	3.10±1.07
PSP-CDS (mean ± SD) (n=77)	NA	NA	NA	19.4±3
UPDRS III (mean ± SD) (n=195)	NA	NA	NA	42.78±17.12
SAS (mean ± SD) (n=179)	NA	NA	NA	20±5.3
SEADL (mean ± SD) (n=200)	NA	NA	NA	55.92±23.22
CGIs (mean ± SD) (n=192)	NA	NA	NA	4.26±1.07
FAB (mean ± SD) (n=175)	NA	NA	NA	6.81±4.23
PSP-QoL (mean ± SD) (n=184)	NA	NA	NA	35.05±21.28
Language (mean ± SD) (n=141)	NA	26.21±2.127	NA	NA
Verbal fluency (mean ± SD) (n=138)	NA	13.18±5.18	NA	NA
Executive (mean ± SD) (n=145)	NA	37.6±6.25	NA	NA
Memory (mean ± SD) (n=148)	NA	15.94±5.27	NA	NA
Visuospatial (mean ± SD) (n=143)	NA	11.51±1.08	NA	NA
ALS specific(mean ± SD) (n=141)	NA	77.24±10.86	NA	NA
ALS-nonspecific (mean ± SD) (n=145)	NA	27.47±5.75	NA	NA
ECAS Total (mean ± SD) (n=145)	NA	104.6±15.22	NA	NA
ALS FRS-R (mean ± SD) (n=132)	NA	18.63±4.3	NA	NA
Plasma Nfl (pg/mL)(median[IQR]) (n=755)	8.7 [5.23-7.52] [a,b,c]	38.56[28.5-46.89]	36.44[23.2-44]	30.28[18.2-40.55]
sEV 3R Tau (pg/mL)(median[IQR])	477. 2[420.4-552.8] [b,c]	430.9[380.8-484.4] [d,e]	518.0[418.4-663.9] [f]	237.3[172.7-320.0]
sEV 4R Tau (pg/mL)(median[IQR])	492.5[420.0-584.6] [b,c]	445.7[386.9-539.5] [d]	450.9[237.5-583.7] [f]	532.4[357.3-851.6]
mEV 3R Tau (pg/mL)(median[IQR])	460.2[359.3-582.1] [b]	566.6[438.1-720.0] [d,e]	517.6[363.9-687.0] [f]	205.6[182.2-254.4]
mEV 4R Tau (pg/mL)(median[IQR])	540.2[451.3-645.9] [b,c]	568.1[446.5-695.8] [d,e]	330.5[245.0-446.1] [f]	438.1[312.7-556.2]
sEV 3R/4R Tau ratio(median[IQR])	0.99[0.91-1.03] [b,c]	0.95[0.88-1.01] [d,e]	1.10[0.99-1.76] [f]	0.45[0.34-0.60]
mEV 3R/4R Tau ratio(median[IQR])	0.93 [0.75-1.06] [b,c]	1.00[0.91-1.09] [d,e]	1.42[1.10-2.06] [f]	0. 50[0.39-0.63]
Plasma TDP-43 (pg/mL)(median[IQR])	213.9 [70.80-287.40] [c]	178.0 [60.90-330.0]	213.9 [103.20-333.0]	256.6 [132.6-351.0]
sEV TDP-43 (pg/mL)(median[IQR])	9.47[7.63-13.33] [a,b]	45.45[28.88-83.21] [d,e]	31.25[14.45-41.09] [f]	9.09[7.73-13.27]
mEV TDP-43 (pg/mL)(median[IQR])	10.67[8.54-15.10][a,b]	41.60 [31.35-53.56][d,e]	19.30[9.79-35.00][f]	9.70[8.43-15.00]
EV particles (10^{12}/mL) (mean ± SD)	38.5±15.1	36.2±5.3	33.6±6.2	34.7±4.2

[a] HC versus ALS $p < 0.0001$
[b] HC versus bvFTD $p < 0.0001$
[c] HC versus PSP $p < 0.0001$
[d] ALS versus bvFTD $p < 0.0001$
[e] ALS versus PSP $p < 0.0001$
[f] bvFTD versus PSP $p < 0.0001$
Kruskal-Wallis test with Dunn's correction for multiple comparisons.

Abbreviations: AD (Alzheimer's disease); svPPA (semantic variant Primary Progressive Aphasia); ALS (amyotrophic lateral sclerosis); bvFTD (behavioral variant frontotemporal dementia); PSP (progressive supranuclear palsy); MMSE (Mini-Mental State Examination); MoCA (Montreal Cognitive Assessment); NPI-Q (The Neuropsychiatric Inventory–Questionnaire); FAQ (The Functional Activities Questionnaire); PSP-RS (Progressive Supranuclear Palsy Rating Scale), PSP-SS (Progressive Supranuclear Palsy Staging System Score); PSP-CDS (The Progressive Supranuclear Palsy Clinical Deficits Scale); UPDRS III (Unified Parkinson's Disease Rating Scale III); SEADL (The Schwab and England Activities of Daily Living); CGIs (Clinical Global Impression-Severity scale), FAB (Frontal Assessment Battery); PSP-QoL (Health-Related Quality of Life Questionnaire for Patients); ECAS (Edinburgh Cognitive and Behavioural ALS Screen); FRS-R (Functional Rating Scale-Revised); CDR-SB (sum of the boxes score of the 6 domains of the Clinical Dementia Rating Scale); CDR plus NACC FTLD (Clinical Dementia Rating Scale plus behavior/compartment and language domains); CBI-M (The Cambridge Behavioural Inventory Modified Version); IQR (Inter-Quartile Range); NA (not applicable). Cut-off values for normal and abnormal concentrations of Aß42 (< 496 pg/ml), tTau (> 470 pg/ml), pTau (> 57 pg/ml), and Aβ42/40 ratio (< 0.09) (DELCODE/Bonn).

Demographic and Clinical Characteristics of All Patients in DESCRIBE subcohort 2.

https://doi.org/10.1038/s41591-024-02937-4

Extended Data Table 3 | Demographic and Clinical Characteristics of All Patients in Sant Pau cohort

Characteristic	Sant Pau cohort				
Groups	HC	ALS	ALS-FTD	bvFTD	PSP
n (total 292)	50	65	58	50	41
Sex	f=31 m=19	f=29 m=36	f=29 m=39	f=17 m=33	f=22 m=19
Age (mean ± SD)	58 ± 4[a]	63 ± 14[g]	67±9	67 ± 10	72 ± 7
MMSE (mean ± SD)(n=115)	29.3 ± 0.97 [b, c, d]	NA	25.84 ± 4	21.9 ± 7.7	23.28 ± 6.9
Aβ1-42(pg/ml)(median[IQR])(n=89)	1069[659-1971] [c]	NA	NA	837[411-1981]	841[384-1733]
Aβ42/40 (mean ± SD) (n=89)	0.1±0.01 [c]	NA	NA	0.09±0.02	0.08±0.03
tTau (pg/ml)(median[IQR]) (n=88)	239[132-391] [c, d]	NA	NA	366[128-1015]	418[155-786]
pTau (pg/ml)(median[IQR]) (n=87)	31.65[15.4-55.8]	NA	NA	37.9[18.8-122.3]	42.15[25.5-112.1]
NPI-Q (mean ± SD) (n=65)	NA	NA	4.76±6.7[h]	8.42±5.6	6.5±4.5
CDR-SB (mean ± SD) (n=41)	NA	NA	1.29±1.5	4±3.99	NA
CDR plus NACC FTLD (mean ± SD) (n=41)	NA	NA	2.96 ± 2.2[h]	6.1 ± 3.1	NA
PSP-RS (mean ± SD) (n=9)	NA	NA	NA	NA	5.5±5
UPDRS III (mean ± SD) (n=14)	NA	NA	NA	NA	34.21±15
FAB (mean ± SD) (n=14)	NA	NA	NA	NA	10±3.69
ALS specific(mean ± SD) (n=30)	NA	NA	55.93 ± 18	NA	NA
ALS-nonspecific (mean ± SD) (n=30)	NA	NA	25.53 ± 5.6	NA	NA
ECAS Total (mean ± SD) (n=30)	NA	NA	81.47 ± 21.02	NA	NA
ALS FRS-R (mean ± SD) (n=121)	NA	32.83 ± 9.64	31.81 ± 9.09	NA	NA
Disease duration (months) (median [IQR])	NA	16.5[1-347]	23 [4-361]	NA	NA
Plasma Nfl (pg/mL)(median[IQR]) (n=91)	8.25[3.12-27.22] [c, d]	NA	NA	33.11[7-136]	41.86[11.76-194.9]
sEV 3R Tau (pg/mL)(median[IQR])	417.6[369.9-481.1] [d]	429.2[309.6-465.5][g]	396.3[354.1-448.2][i]	507.9[241.6-637.2] [j]	320.5[249.8-385.8]
sEV 4R Tau (pg/mL)(median[IQR])	415.2[326.7-495.0] [c,d]	422.9[348.6-508.3][e]	416.9[375.0-511.5]	325.3[120.5-536.1] [j]	773.7[523.3-1130.0]
mEV 3R Tau (pg/mL)(median[IQR])	460.1[407.6-530.1] [c,d]	473.0[407.3-512.9]	437[390.1-493.8]	503.8[266.2-698.9]	355.9[267.8-441.6]
mEV 4R Tau (pg/mL)(median[IQR])	495.7[433.0-591.0] [c,d]	504.9[416.2-606.8]	497.7[447.7-610.6]	405.8[143.8-658.2]	831.6[566.7-1172.0]
sEV 3R/4R Tau ratio(median[IQR])	1.02[0.96-1.06] [c,d]	1.025[0.92-1.11] [f,g]	0.95[0.84-1.00] [h, I]	1.34[1.17-2.34] [j]	0.38[0.33-0.50]
mEV 3R/4R Tau ratio(median[IQR])	0.94[0.88-0.98] [c,d]	0.94[0.85-1.02] [f,g]	0.88[0.78-0.92] [h, I]	1.26[1.06-2.16]	0.37[0.33-0.53]
sEV TDP-43 (pg/mL)(median[IQR])	10.41[8.50-14.65] [a,b,c]	45.60 [31.55-64.45] [f,g]	52.354[11.13-40.55] [h, I]	24.15[11.13-40.55] [j]	10.2[8.30-12.35]
mEV TDP-43 (pg/mL)(median[IQR])	13.89[11.33-19.53]	60.80[42.10-85.95]	69.80[52.28-97.90]	20.35[12.80-43.55]	12.70[11.15-16.20]
EV particles (10^7/mL) (mean ± SD)	21.6±10.62	29.71±22	29.4±13.4	39.4±35.9	21.2±12.5

[a] HC versus ALS $p < 0.0001$
[b] HC versus ALS-FTD $p < 0.0001$
[c] HC versus bvFTD $p < 0.0001$
[d] HC versus PSP $p < 0.0001$
[e] ALS versus ALS-FTD $p < 0.0001$
[f] ALS versus bvFTD $p < 0.0001$
[g] ALS versus PSP $p < 0.0001$
[h] ALS-FTD versus bvFTD $p < 0.0001$
[I] ALS-FTD versus PSP $p < 0.0001$
[j] bvFTD versus PSP $p < 0.0001$
Kruskal-Wallis test with Dunn's correction for multiple comparisons.

Abbreviations: AD (Alzheimer's disease); svPPA (semantic variant Primary Progressive Aphasia); ALS (amyotrophic lateral sclerosis); bvFTD (behavioral variant frontotemporal dementia); PSP (progressive supranuclear palsy); MMSE (Mini-Mental State Examination); MoCA (Montreal Cognitive Assessment); NPI-Q (The Neuropsychiatric Inventory–Questionnaire); FAQ (The Functional Activities Questionnaire); PSP-RS (Progressive Supranuclear Palsy Rating Scale), PSP-SS (Progressive Supranuclear Palsy Staging System Score); PSP-CDS (The Progressive Supranuclear Palsy Clinical Deficits Scale); UPDRS III (Unified Parkinson's Disease Rating Scale III); SEADL (The Schwab and England Activities of Daily Living); CGIs (Clinical Global Impression-Severity scale), FAB (Frontal Assessment Battery); PSP-QoL (Health-Related Quality of Life Questionnaire for Patients); ECAS (Edinburgh Cognitive and Behavioural ALS Screen); FRS-R (Functional Rating Scale-Revised); CDR-SB (sum of the boxes score of the 6 domains of the Clinical Dementia Rating Scale); CDR plus NACC FTLD (Clinical Dementia Rating Scale plus behavior/comportment and language domains); CBI-M (The Cambridge Behavioural Inventory Modified Version); IQR (Inter-Quartile Range); NA (not applicable).

Demographic and Clinical Characteristics of All Patients in Sant Pau cohort.

nature portfolio

Corresponding author(s): Anja Schneider

Last updated by author(s): 14.03.2024

Reporting Summary

Nature Portfolio wishes to improve the reproducibility of the work that we publish. This form provides structure for consistency and transparency in reporting. For further information on Nature Portfolio policies, see our Editorial Policies and the Editorial Policy Checklist.

Statistics

For all statistical analyses, confirm that the following items are present in the figure legend, table legend, main text, or Methods section.

n/a	Confirmed
☐	☒ The exact sample size (*n*) for each experimental group/condition, given as a discrete number and unit of measurement
☐	☒ A statement on whether measurements were taken from distinct samples or whether the same sample was measured repeatedly
☐	☒ The statistical test(s) used AND whether they are one- or two-sided *Only common tests should be described solely by name; describe more complex techniques in the Methods section.*
☐	☒ A description of all covariates tested
☐	☒ A description of any assumptions or corrections, such as tests of normality and adjustment for multiple comparisons
☐	☒ A full description of the statistical parameters including central tendency (e.g. means) or other basic estimates (e.g. regression coefficient) AND variation (e.g. standard deviation) or associated estimates of uncertainty (e.g. confidence intervals)
☐	☒ For null hypothesis testing, the test statistic (e.g. *F*, *t*, *r*) with confidence intervals, effect sizes, degrees of freedom and *P* value noted *Give P values as exact values whenever suitable.*
☒	☐ For Bayesian analysis, information on the choice of priors and Markov chain Monte Carlo settings
☒	☐ For hierarchical and complex designs, identification of the appropriate level for tests and full reporting of outcomes
☐	☒ Estimates of effect sizes (e.g. Cohen's *d*, Pearson's *r*), indicating how they were calculated

Our web collection on statistics for biologists contains articles on many of the points above.

Software and code

Policy information about availability of computer code

Data collection: No code involved in data collection

Data analysis:

No unpublished software.

Statistical analysis
Statistical analysis and data visualization were performed using Prism 7 (GraphPad Software Inc., La Jolla, CA, USA), IBM SPSS Statistics 21 (IBM Corporation, Armonk, NY, USA), R studio 3.2.1 (R Foundation for Statistical Computing, Institute for Statistics and Mathematics, Wirtschaftsuniversität Wien, Vienna, Austria), MedCalc software version 22.021 and HD-X analyzer, software version 3.1 (Quanterix, Billerica, MA, USA). The statistical tests were two-tailed and values with $p < 0.05$ were considered significant. Comparisons of marker levels were performed using Kruskal-Wallis tests followed by Dunn's correction for multiple comparisons due to non- Gaussian distributions. Normal distribution assumption was assessed based on visual inspection of histograms and Kolmogorov-Smirnov tests. To assess the link between EV marker and clinical scales as well as plasma NfL, Spearman correlations were used. To illustrate associations between plasma Nfl and plasma EV 3R/4R Tau ratio, plasma NfL and plasma EV /TDP-43, as well as plasma EV 3R/4R Tau and plasma EV TDP-43 (Fig. 1,2,4, Suppl. Fig.S,7,11,14), monotonic regression splines (using the "cgam" function from R package "splines") were modeled. Notably, potential confounders (i.e. age, sex and disease duration) showed no influence on plasma biomarker levels (Suppl. Tables 3, 7). We therefore used the non-parametric tests described above with covariate adjustment to account for violations of normal distribution assumptions and non-linear relationships.
MedCalc was used for computation and comparison of ROC curves (with the method of Hanley&McNeil[122])(standard error (SE), 95% confidence interval (CI) for the difference, and p-value) as well as for calculation of sensitivity and specificity. Precision recall curves, area under the precision recall curve (AUPRC) and confidence intervals were calculated using the R code from Boyd et al. (2013)[123] and published prevalence estimates for the different diagnoses (PSP[124], ALS[125], bvFTD[126]).

The cut-off values of 3R/4R Tau ratio and TDP-43 levels were defined with Gaussian mixture modeling using the R 3.2.1 mix tools package as previously described by Bertens et al. [61]. First, the R boot.comp function was used to determine the number of distributions that fitted best to the data. Next, we defined data-driven cut-offs as the point where the lines of fitted normal distributions crossed each other. Specifically, we derived three normal distributions (as suggested by bootstrapping) and determined the intersection of the middle normal distribution with the two more extreme distributions. We computed sensitivity and specificity based on the cut-offs of plasma sEV 3R/4R Tau ratio and TDP-43 levels as determined by mixture modelling.

For manuscripts utilizing custom algorithms or software that are central to the research but not yet described in published literature, software must be made available to editors and reviewers. We strongly encourage code deposition in a community repository (e.g. GitHub). See the Nature Portfolio guidelines for submitting code & software for further information.

Data

Policy information about availability of data

All manuscripts must include a data availability statement. This statement should provide the following information, where applicable:

- Accession codes, unique identifiers, or web links for publicly available datasets
- A description of any restrictions on data availability
- For clinical datasets or third party data, please ensure that the statement adheres to our policy

The data that support the findings of this study are available from the authors but restrictions apply, and hence not available publicly due to ethics approval regulations/data protection. Data are, however, available from the authors upon reasonable request and with permission from the cohorts' steering committees (contact for and information on data access: anja.schneider@dzne.de). Expected turnover times for data applications is 3 months.

Research involving human participants, their data, or biological material

Policy information about studies with human participants or human data. See also policy information about sex, gender (identity/presentation), and sexual orientation and race, ethnicity and racism.

Reporting on sex and gender	We report on sex in a demographics table. We tested for correlation of our data with sex and no correlation was found.
Reporting on race, ethnicity, or other socially relevant groupings	We do not report on race, ethnicity or socially relevant groupings. Information on sex was obtained by the study physicians (database entry). Study physicians obtained this information from patients, patients charts, name or in case of ambiguity by asking patients and or caregivers.
Population characteristics	Detailed information is found in Extended Data Tables 1&2
Recruitment	Patient samples The DZNE Clinical Registry Study of Neurodegenerative Diseases (DESCRIBE) cohort is a multicentric, longitudinal observational study conducted by the German Center for Neurodegenerative Diseases (DZNE) and its clinical sites. It recruits patients with different neurodegenerative conditions, including ALS, bvFTD and PSP. Recruitment of these patients is described in more detail below. The multicenter, longitudinal Degeneration Controls and Relatives cohort (DANCER) serves to provide healthy controls for all DESCRIBE subcohorts. After written informed consent (University of Bonn Ethics Board statement 311/14) all participants undergo baseline and annual follow-up visits with clinical and neurological examination, cognitive assessments, 3T magnetic resonance imaging (MRI), blood and CSF sampling following identical standard operating procedures (SOPs). Patients with Alzheimer's Disease (AD) dementia were recruited as part of the DESCRIBE cohort, following the National Institutes of Aging- Alzheimer's Association (NIA-AA) diagnosis criteria90 and confirmed by positive CSF amyloid-beta, total Tau and p-Tau181 status. Patients were recruited at the different DZNE clinical cooperation units from specialized outpatient clinics. Patients were referred to these clinics by general physicians, neurologists or psychiatrists. DANCER participants were recruited by advertisement (DZNE website, flyers) from the general population. Although we included patients at all disease stages at all levels of cognitive or motor impairment, there could be a selection bias since patients with more severe impairment or their caregivers may not be willing to participate. Thus, our cohort may underrepresent more progressed disease stages. Since the study focuses on early diagnostic markers and since we also correlated results with clinical scales of disease severity, this should not have affected our findings. The DESCRIBE ALS cohort ALS patients were diagnosed according to the revised El-Escorial-Criteria91. Different motor phenotypes of ALS were classified as classical ALS, progressive bulbar paresis, flail arm, flail leg, progressive muscular atrophy (PMA), primary lateral sclerosis (PLS) or genetic ALS. Participants were clinically characterized using the Amyotrophic Lateral Sclerosis Functional Rating Scale-revised (ALS-FRS-R)92. The Edinburgh Cognitive and Behavioral ALS Screen (ECAS)93 served as an additional test to identify cognitive and behavioral impairment. ALS patients with cognitive impairment (ALSci), ALS with behavioral impairment (ALSbi), ALS with cognitive and behavioral impairment (ALScbi) and ALS with frontotemporal dementia (ALS-FTD) following the Strong criteria94 and genetic ALS with a pathogenic FTD mutation, additionally underwent the assessments of the DESCRIBE FTD cohort (see below). The DESCRIBE FTD cohort Patients with bvFTD were diagnosed according to the revised Rascovsky criteria9S by an experienced multidisciplinary team of neurologists, psychiatrists and neuropsychologists and under consideration of MRI images and CSF data, when available. Neuropsychological assessments included Mini Mental State Examination Test (MMSE), the Montreal Cognitive Assessment

(MoCA)41, Free and Cued Selective Reminding Test (FCSRT)96, the Neuropsychological battery of the Consortium to Establish a Registry for Alzheimer's Disease (CERAD) Plus test97 including Trail Making Tests A and B and the mini-Social cognition & Emotional Assessment (Mini-SEA)98 test. Psychiatric scales included Geriatric Depression Scale (GDS)99, the brief questionnaire of the Neuropsychiatric Interview (NPI-Q)S3, and the functional scales CDR-SB, CDR plus NACC FTLD, Functional Activities Questionnaire (FAQ)S0, and a modification of the revised Cambridge Behavior Inventory (CBI-R)54, the CBI-M.
Patients with semantic variant PPA (svPPA) were diagnosed according to Gordon-Tempini criteria100. Baseline assessment of patients with PPA additionally included a modified version of the Camel and Cactus test101, the visual form of the Sentence Comprehension Test (SECT-V)102, the Sentence Repetition Test from the Aachen Aphasia Test103, hierarchical word lists104 and the Repeat and Point Test105.

The DESCRIBE PSP cohort
The cohort design is summarized in106. Diagnosis of PSP was based on the National Institute of Neurological Disorders and Stroke and the Society for PSP (NIND-SPSP) criteria107 for participants recruited before 2017, and on the Movement Disorder Society (MDS-PSP) diagnostic criteria108 for participants recruited after 2017. Participants were clinically phenotyped by PSP rating scale (PSP-RS)42, PSP staging system (PSP-SS)109, PSP quality of life scale (PSP-QoL)48, PSP-clinical deficits scale (PSP-CDS)43, Schwab and England disability scale (SEADL)44, MDS-Unified Parkinson's Disability Rating Scale (MDS-UPDRS) Part III46, Starkstein Apathy Scale (SAS)47, Clinical Global Impression Severity Scale (CGI-s)45, GDS99, and MoCA41.

The Healthy Control cohort DANCER
Healthy controls samples were obtained from the Degeneration Controls and Relatives cohort (DANCER) and included 71 participants who, based on neuropsychological testing, neurological and psychiatric examination, do not suffer from a neurodegenerative disease. Participants additionally underwent MR imaging. The neuropsychological test battery follows the same protocol and includes all assessments as the one used for participants of the DESCRIBE FTD cohort. Participants undergo an annual follow-up as well as genetic testing at baseline (see below). Relatives with a known pathogenic FTD-ALS mutation were excluded as controls.

The Sant Pau cohort
Patients with ALS were prospectively recruited from the Motor Neuron Disease Clinic at Hospital de la Santa Creu i Sant Pau. We included patients categorized as probable laboratory-supported, or definite ALS according to El Escorial revised criteria119. ALSFRS-R in its Spanish version120 was systematically assessed at the time of sample acquisition. Unimpaired healthy controls, bvFTD and PSP patients were recruited at the Sant Pau Memory Unit and include individuals from the Sant Pau Initiative on Neurodegeneration multimodal biomarker cohort. ALS-FTD patients were recruited by Sant Apu Memory Unit and Motor Neuron Disease Clinic. Information about clinical and neuropsychological assessments and sample processing have been previously described in detail64. Plasma samples were obtained using the same SOP. All patient samples (ALS, ALS-FTD, bvFTD and PSP) were screened for the presence of a pathogenic repeat expansion mutation in C9orf72. In addition, patients with ALS were tested for mutations in ALS, FTD and AD causing genes using a gene panel. bvFTD and PSP patients underwent whole exome sequencing. In total, pathogenic mutations were found in C9orf72 (n=16), GRN (n=6), SOD1 (n=4), TBK1 (n=3), FUS (n=3), TARDBP (n=1), VCP (n=1). This study was approved by the Hospital de la Santa Creu i Sant Pau Ethics Committee).

Ethics oversight

University of Bonn Ethics Board statement 311/14
Sant Pau Ethics Committee
The DESCRIBE and DANCER cohort studies were approved by University of Bonn Ethics Board, statement 311/14. The Sant Pau cohort was approved by the Sant Pau Ethics Committee.

Note that full information on the approval of the study protocol must also be provided in the manuscript.

Field-specific reporting

Please select the one below that is the best fit for your research. If you are not sure, read the appropriate sections before making your selection.

☒ Life sciences ☐ Behavioural & social sciences ☐ Ecological, evolutionary & environmental sciences

For a reference copy of the document with all sections, see nature.com/documents/nr-reporting-summary-flat.pdf

Life sciences study design

All studies must disclose on these points even when the disclosure is negative.

Sample size

DESCRIBE: subcohort 1 was a pilot study. Subcohort 2: we asked for all available samples and received the given numbers, resulting in unequal group sizes. No power calculation was performed. Sant Pau: sample sizes were chosen based on available sample numbers and with the aim of similar numbers per diagostic groups.

DESCRIBE: We applied for all available samples from the DZNE DESCRIBE cohort with a diagnosis of bvFTD, for 100 samples with ALS and for 125 with PSP and 75 healthy controls. All bvFTD samples were asked for because of the scope of this study to detect TDP-43 and Tau pathology in this group. PSP was applied for as a 4R Tau control cohort, ALS as a TDP-43 control cohort. Sample numbers were determined by availability of samples.
Sant Pau: we applied for n=50 with diagnosis of ALS, ALS-FTD, bvFTD, PSP, healthy controls and as many as possible genetically confirmed cases.

Data exclusions	Modified version of the Cambridge Behavioural Inventory (CBI-M) In the DESCRIBE-FTD cohort, we used a modified 50-item version of the CBI-R. Before including this new version into the analyses, we conducted a principal component analysis (PCA) with varimax rotation to confirm the theoretical factor structure. Participants with over 20% missing rate over all items were removed. In addition, one item with over 20% missing rate across all participants was excluded. Four further items were excluded due to the low factor loadings and cross-loadings. Therefore, the modified version (CBI-M) resulted in 45 items with 12 new items and 33 items from the CBI-R. The total CBI-M score was calculated by the mean of all available item scores for each bvFTD participant. Plasma: 1 case was excluded from subcohort 1 as 4R Tau was not measurable. No other values/samples were excluded. CSF: Several cases had to be excluded from subcohort 1 CSF as 4R Tau was not measurable. The number of excluded cases is given in the manuscript.
Replication	We replicated our findings on Tau ratio in a second subset of the DZNE DESCRIBE cohort (subcohort 2). Measurements of the DESCRIBE cohort samples were done once (singletons) due to the limited availability of sample volume. Findings were reproduced in the independent Sant Pau cohort for both tau and TDP-43. For EV TDP-43 findings in subcohort 2, we determined cut-off values using mixture modelling and tested their sensitivity and specificity in a hold-out data set of confirmed pathology.
Randomization	Samples were randomized on the 96-well plates using sample randomization tool https://olink.com/faq/sample-randomization/
Blinding	Experimenters were blinded to diagnosis

Reporting for specific materials, systems and methods

We require information from authors about some types of materials, experimental systems and methods used in many studies. Here, indicate whether each material, system or method listed is relevant to your study. If you are not sure if a list item applies to your research, read the appropriate section before selecting a response.

Materials & experimental systems

n/a	Involved in the study
☐	☒ Antibodies
☐	☒ Eukaryotic cell lines
☒	☐ Palaeontology and archaeology
☒	☐ Animals and other organisms
☐	☒ Clinical data
☒	☐ Dual use research of concern
☒	☐ Plants

Methods

n/a	Involved in the study
☒	☐ ChIP-seq
☒	☐ Flow cytometry
☒	☐ MRI-based neuroimaging

Antibodies

Antibodies used	Pathology: Tau1 (provided by Drs. Nicholas Kanaan and Lester Binder) and HJ8.5 (provided by Dr. David Holtzman) antibodies against phosphorylated TDP-43 (clone 1D3110), phosphorylated tau (clone AT8, cat no. MN1020,Thermo Fisher), α-synuclein (clone 4D6, cat no. AM05094PU-N, Origene), and beta-Amyloid (clone 4G8, cat no. SIG-39220, Covance). Western Blotting (WB), ELISA and MSD: Primary antibodies: Anti-Calnexin (cat no. C4731, Sigma-Aldrich, Darmstadt, Germany, 1:2000 dilution for WB), anti-Flotillin-2 (cat no. 610384, BD Biosciences, San Jose, CA, USA, 1:500 for WB), anti-3R Tau (RD3, cat no. 05-803, Merck,1:600 for MSD, 1:500 for WB), anti-4R Tau (cat no. ab218314, Abcam, 1:300 for ELISA, 1:500 for WB), anti-TDP-43 antibody (cat no. ab305694, Abcam, 1:500 for WB), HT7 (cat no. MN1000B, Thermo Fisher Scientific, epitope residues 159 – 163, 1:300 for MSD/ELISA, 1:500 for WB), biotinylated mouse anti-human CD171 (L1CAM neural adhesion protein) antibody (clone 5G3, eBiosciences, San Diego, CA, USA, cat no. 13171982, Thermo Fisher Scientific,1:500 for WB and IP), biotinylated mouse IgG2 antibody (clone eBM2a, cat no.13472485, Thermo Fisher Scientific),1:500 for WB and IP. Secondary antibodies: HRP anti mouse IgG (Dako, cat number P044701-2, 1:5000), HRP anti rabbit IgG (Dako, cat number P044801-2, 1:5000). TDP-43 Simoa advantage kit, cat no. 103293, lot no.503756, Nfl Simoa Advantage kit cat no. 103186, lot no. 503546.
Validation	This validation statement below is provided for 3R tau, 4R tau and TDP-43. Suppl Table 1 and Sensitivity: For the determination of the lower limit of quantification (LLOQ) of each assay, 16 blank samples were measured on one plate. The calibration curves were calculated using a four-parameter logistic curve fit for all assays, which gave the optimal fit. LLOQ was calculated as the concentration corresponding to the 2.S signal standard deviation above the background (zero calibrator) following the guidelines in Andreasson et al.6. Precision: Intra-assay variation (repeatability) was determined by analysis of samples (n=5) in four replicates on one plate. Inter-assay variation (intermediate precision) was measured to determine the variation of analyses between 5 different days. Dilutional linearity: Three different EV samples were used in duplicates to perform the dilution linearity experiments. The dilutional linearity (dilutions 2x, 4x and 8x) was calculated as follows: %Linearity = [observed C *dilution

factor/ previous observed C"previous dilution factor] "100; C = concentration(pg/mL). Recovery: Three different plasma EV samples, measured in duplicates, were spiked with recombinant 3R Tau, 4R Tau, and TDP43 calibrator at three different concentrations (low: 3R and 4R Tau 1,750 pg/mL, TDP-43 1,250 pg/mL; medium: 3R and 4R Tau 3,500 pg/mL, TDP-43 2,500 pg/mL; high: 3R and 4R Tau 7,000 pg/mL, TDP-43 5,000 pg/mL). For neat samples, the buffer was spiked instead of the calibrator. Spike recoveries were calculated according to the formula: % Recovery = [C spike sample-C neat sample /theoretical C spike] *100; C = concentration (pg/mL). Parallelism: Three different EV samples with high endogenous protein concentrations were serially diluted (2x, 4x and 8x). Both reciprocal relative dilution factor and OD450 absorbance signals of the samples and calibrator were log-transformed and linear regression was performed to calculate the slopes of the sample and calibrator curves. The slope of the linear parts of the log—log transformed calibrator and sample dilution series were compared to determine the degree of parallelism by calculating the "in range %" using the following formula: in range% = [slope of sample dilution /series slope of calibration curve] *100.

Other antibodies:
-Anti-Calnexin (cat no. C4731, Sigma-Aldrich, Darmstadt, Germany)
This antibody has been validated with an 'Enhanced Validity (EV)' certificate by the manufacturer. Manufacturer has tested this antibody on Western blot (WB)-Cell Line/Tissue Extract Hela or HepG2 Cells, WB Titer 1:2000-1:4000 and immuno-precipitation (IP) on Cell /Tissue Lysate Hela Cells. On 'CiteAb' antibody database (www.citeab.com), this antibody has been cited in 233 publications where around 55% of the assays were performed on human origin samples followed by mouse.
-Anti-Flotillin-2 (cat no. 610384, BD Biosciences, San Jose, CA, USA)
According to the manufacturer, this antibody has been QC tested on human samples. On 'CiteAb' antibody database (www.citeab.com), this antibody has been cited in 17 publications where almost 75% of the assays were performed on human origin samples followed by mouse. Reported application is Western Blot (WB) at 1:1000 dilution.
-Biotinylated mouse anti-human CD171 (L1CAM neural adhesion protein) antibody (clone 5G3
eBiosciences, San Diego, CA, USA (Cat no. 13171982, Thermo Fisher Scientific))
On 'CiteAb' antibody database (www.citeab.com), this antibody has been cited in 37 publications all assays were performed on human origin samples. Reported applications are Western Blot (WB), ELISA and FC/FACS. This antibody has been used to capture extracellular vesicle (EVs) from serum in Winston et al. 'Evaluation of blood-based, extracellular vesicles as biomarkers for aging-related TDP-43 pathology.' Alzheimers Dement (Amst). 2022 Dec 15;14(1):e12365. doi: 10.1002/dad2.12365. PMID: 36540894; PMCID: PMC9753157.
-HT7 (cat no. MN1000B, Thermo Fisher Scientific, epitope residues 159 – 163)
According to the manufacturer, this antibody has been QC tested on human samples. On 'CiteAb' antibody database (www.citeab.com), this antibody has been cited in over 100 publications where almost 60% of the assays were performed on human origin samples followed by mouse and rat. Reported application is Western Blot (WB), ELISA, IHC and ICC. This antibody is also used in Tau ELISA from Fujirebio which is widely used in the clinic for diagnosis of Alzheimer disease (AD) patients.
Pathology: Tau1 (provided by Drs. Nicholas Kanaan and Lester Binder) and HJ8.5 (provided by Dr. David Holtzman) antibodies against phosphorylated TDP-43 (clone 1D3110), phosphorylated tau (clone AT8, cat no. MN1020,Thermo Fisher), α-synuclein (clone 4D6, cat no. AM05094PU-N, Origene), and beta-Amyloid (clone 4G8, cat no. SIG-39220, Covance).
These antibodies are widely used antibodies and regularly used in diagnosis confirmation post-mortem.

Eukaryotic cell lines

Policy information about cell lines and Sex and Gender in Research

Cell line source(s)	SH-SYSY cells
Authentication	SH-SY5Y cell line was purchased from ATCC (cat no. CRL-2266)
Mycoplasma contamination	cells were not tested for mycoplasma contamination
Commonly misidentified lines (See ICLAC register)	none

Clinical data

Policy information about clinical studies

All manuscripts should comply with the ICMJE guidelines for publication of clinical research and a completed CONSORT checklist must be included with all submissions.

Clinical trial registration	Cohort study, no clinical intervention trial.
Study protocol	available upon reasonable request
Data collection	Ongoing recruitment
Outcomes	No defined outcomes, since longitudinal cohort study

Plants

Seed stocks

Report on the source of all seed stocks or other plant material used. If applicable, state the seed stock centre and catalogue number. If plant specimens were collected from the field, describe the collection location, date and sampling procedures.

Novel plant genotypes

Describe the methods by which all novel plant genotypes were produced. This includes those generated by transgenic approaches, gene editing, chemical/radiation-based mutagenesis and hybridization. For transgenic lines, describe the transformation method, the number of independent lines analyzed and the generation upon which experiments were performed. For gene-edited lines, describe the editor used, the endogenous sequence targeted for editing, the targeting guide RNA sequence (if applicable) and how the editor was applied.

Authentication

Describe any authentication procedures for each seed stock used or novel genotype generated. Describe any experiments used to assess the effect of a mutation and, where applicable, how potential secondary effects (e.g. second site T-DNA insertions, mosiacism, off-target gene editing) were examined.